# 7. SITE 662[1]

Shipboard Scientific Party[2]

## HOLE 662A

**Date occupied:** 24 March 1986, 0300 UTC

**Date departed:** 25 March 1986, 0745 UTC

**Time on hole:** 28.75 hr

**Position:** 1°23.41'S, 11°44.35'W

**Water depth (sea level; corrected m, echo-sounding):** 3821.3

**Water depth (rig floor; corrected m, echo-sounding):** 3831.8

**Bottom felt (rig floor; m, drill pipe measurement):** 3824.3

**Distance between rig floor and sea level (m):** 10.5

**Total depth (rig floor, m):** 4034.8

**Penetration (m):** 200.0

**Number of cores (including cores with no recovery):** 22

**Total length of cored section (m):** 200

**Total core recovered (m):** 204.12

**Core recovery (%):** 102.06

**Oldest sediment cored:**
Depth (mbsf): 200.0
Nature: calcareous nannofossil ooze
Age: Pliocene, 3.6 Ma
Measured velocity (km/s): 1.52

## HOLE 662B

**Date occupied:** 25 March 1986, 0745 UTC

**Date departed:** 26 March 1986, 1215 UTC

**Time on hole:** 28.5 hr

**Position:** 1°23.41'S, 11°44.35'W

**Water depth (sea level; corrected m, echo-sounding):** 3821.3

**Water depth (rig floor; corrected m, echo-sounding):** 3831.8

**Bottom felt (rig floor; m, drill pipe measurement):** 3824.3

**Distance between rig floor and sea level (m):** 10.5

**Total depth (rig floor, m):** 4023.0

**Penetration (m):** 188.2

**Number of cores (including cores with no recovery):** 12

**Total length of cored section (m):** 114

**Total core recovered (m):** 114.66

**Core recovery (%):** 100.58

**Oldest sediment cored:**
Depth (mbsf): 188.2
Nature: calcareous nannofossil ooze
Age: Pliocene, 3.58 Ma
Measured velocity (km/s): 1.52

**Principal results:** Site 662 is located in the eastern equatorial Atlantic at 1°23.41'S, 11°44.35'W in a water depth of 3813.8 m on the upper eastern flank of the mid-Atlantic Ridge just south of the Romanche Fracture Zone (see "Background and Scientific Objectives" section, this chapter). This site is situated in a sediment pond with about 0.5 s of moderately reflective acoustic layering in a region characterized mostly by outcropping basement (see "Background and Scientific Objectives" section, this chapter). Our primary objective was to obtain late Neogene records of equatorial divergence, advection of the Benguela Current, and eolian sedimentation.

From Holes 662A and 662B, we recovered a total of 34 advanced-piston-corer (APC) cores to depths of 200.0 and 188.2 meters below the seafloor (mbsf), respectively. Hole 662A was cored continuously; Hole 662B was spot cored in the upper 120 mbsf (Table 1). Recovery averaged 102.06% in Hole 662A and 100.58% in Hole 662B.

The entire section cored (0–200 mbsf) is one lithologic unit composed of nannofossil and foraminifer-nannofossil oozes of late Pliocene through Holocene age. Secondary components include clay, diatoms, and radiolarians.

This unit is divided into four subunits, based on carbonate content (see "Organic Geochemistry" section, this chapter) and on deformation features (Fig. 1). Subunit IA (0–26.2 mbsf) is composed of Pleistocene (0 to 0.5 Ma) nannofossil and foraminifer-nannofossil oozes deposited by pelagic sedimentation, except for two turbidites. Subunit IB (26.2–96.2 mbsf) has the same lithology as Subunit IA, but was deposited mostly by mass-gravitational flows, such as slumps, debris flows, and turbidites. Two intervals of undisturbed, or little-disturbed, pelagic sediments also occur between three large slumps (Fig. 1). Subunit IC (96.2–154.6 mbsf) is upper Pliocene to early Pleistocene nannofossil ooze similar to Subunit IA. Subunit ID (154.6–200 mbsf) is made up of upper Pliocene nannofossil and foraminifer-nannofossil oozes, distinguished from the overlying subunits by their uniformly higher carbonate content (see "Organic Geochemistry" section, this chapter).

Although a useable paleomagnetic stratigraphy could not be obtained at Site 662, the nannofossil and planktonic-foraminifer biostratigraphy provided several well-dated datum levels to constrain the age-depth curve (see "Sediment-Accumulation Rates" section, this chapter). Depositional rates of pelagic sediments in Subunits IA, IC, and ID average 42 m/m.y. Preservation of calcareous fossils is good to moderate; preservation of diatoms is moderate to fair.

[1] Ruddiman, W., Sarnthein, M., Baldauf, J., et al., 1988. *Proc., Init. Repts. (Pt. A), ODP*, 108.

[2] William Ruddiman (Co-Chief Scientist), Lamont-Doherty Geological Observatory, Palisades, NY 10964; Michael Sarnthein (Co-Chief Scientist), Geologisch-Paläontologisches Institut, Universität Kiel, Olshausenstrasse 40, D-2300 Kiel, Federal Republic of Germany; Jack Baldauf, ODP Staff Scientist, Ocean Drilling Program, Texas A&M University, College Station, TX 77843; Jan Backman, Department of Geology, University of Stockholm, S-106 91 Stockholm, Sweden; Jan Bloemendal, Graduate School of Oceanography, University of Rhode Island, Narragansett, RI 02882-1197; William Curry, Woods Hole Oceanographic Institution, Woods Hole, MA 02543; Paul Farrimond, School of Chemistry, University of Bristol, Cantocks Close, Bristol BS8 1TS, United Kingdom; Jean Claude Faugeres, Laboratoire de Géologie-Océanographie, Université de Bordeaux I, Avenue des Facultés Talence 33405, France; Thomas Janacek, Lamont-Doherty Geological Observatory, Palisades, NY 10964; Yuzo Katsura, Institute of Geosciences, University of Tsukuba, Ibaraki 305, Japan; Hélène Manivit, Laboratoire de Stratigraphie des Continents et Océans, (UA 319) Université Paris VI, 4 Place Jussieu, 75230 Paris Cedex, France; James Mazzullo, Department of Geology, Texas A&M University, College Station, TX 77843; Jürgen Mienert, Geologisch-Paläontologisches Institut, Universität Kiel, Olshausenstrasse 40, D-2300 Kiel, Federal Republic of Germany, and Woods Hole Oceanographic Institution, Woods Hole, MA 02543; Edward Pokras, Lamont-Doherty Geological Observatory, Palisades, NY 10964; Maureen Raymo, Lamont-Doherty Geological Observatory, Palisades, NY 10964; Peter Schultheiss, Institute of Oceanographic Sciences, Brook Road, Wormley, Godalming, Surrey GU8 5UG, United Kingdom; Rüdiger Stein, Geologisch-Paläontologisches Institut, Universität Giessen, Senckenbergstrasse 3, 6300 Giessen, Federal Republic of Germany; Lisa Tauxe, Scripps Institution of Oceanography, La Jolla, CA 92093; Jean-Pierre Valet, Centre des Faibles Radioactivités, CNRS, Avenue de la Terrasse, 91190 Gif-sur-Yvette, France; Philip Weaver, Institute of Oceanographic Sciences, Brook Road, Wormley, Godalming, Surrey GU8 5UG, United Kingdom; Hisato Yasuda, Department of Geology, Kochi University, Kochi 780, Japan.

Table 1. Site 662 coring summary (drilling depths).

| Core no. | Date (March 1986) | Time (UTC) | Depths (mbsf) | Length cored (m) | Length recovered (m) | Recovery (%) |
|---|---|---|---|---|---|---|
| 108-662A-1H | 24 | 1355 | 0-3.2 | 3.2 | 3.2 | 100.0 |
| 108-662A-2H | 24 | 1445 | 3.2-12.7 | 9.5 | 9.9 | 104.0 |
| 108-662A-3H | 24 | 1534 | 12.7-22.2 | 9.5 | 9.5 | 99.6 |
| 108-662A-4H | 24 | 1622 | 22.2-31.7 | 9.5 | 9.6 | 100.0 |
| 108-662A-5H | 24 | 1714 | 31.7-41.2 | 9.5 | 9.4 | 98.5 |
| 108-662A-6H | 24 | 1807 | 41.2-50.7 | 9.5 | 9.5 | 100.0 |
| 108-662A-7H | 24 | 1854 | 50.7-60.2 | 9.5 | 9.6 | 101.0 |
| 108-662A-8H | 24 | 1944 | 60.2-69.7 | 9.5 | 9.6 | 101.0 |
| 108-662A-9H | 24 | 2034 | 69.7-79.2 | 9.5 | 8.8 | 92.9 |
| 108-662A-10H | 24 | 2123 | 79.2-88.7 | 9.5 | 9.6 | 101.0 |
| 108-662A-11H | 24 | 2212 | 88.7-98.2 | 9.5 | 9.7 | 102.0 |
| 108-662A-12H | 24 | 2259 | 98.2-107.7 | 9.5 | 9.8 | 103.0 |
| 108-662A-13H | 24 | 2346 | 107.7-117.2 | 9.5 | 9.7 | 102.0 |
| 108-662A-14H | 25 | 0038 | 117.2-126.7 | 9.5 | 9.4 | 98.4 |
| 108-662A-15H | 25 | 0118 | 126.7-136.2 | 9.5 | 9.7 | 102.0 |
| 108-662A-16H | 25 | 0154 | 136.2-145.7 | 9.5 | 9.8 | 103.0 |
| 108-662A-17H | 25 | 0245 | 145.7-155.2 | 9.5 | 9.0 | 94.9 |
| 108-662A-18H | 25 | 0320 | 155.2-164.7 | 9.5 | 9.7 | 102.0 |
| 108-662A-19H | 25 | 0408 | 164.7-174.2 | 9.5 | 9.5 | 100.0 |
| 108-662A-20H | 25 | 0505 | 174.2-183.7 | 9.5 | 9.6 | 100.0 |
| 108-662A-21H | 25 | 0600 | 183.7-193.2 | 9.5 | 9.6 | 101.0 |
| 108-662A-22H | 25 | 0645 | 193.2-200.0 | 6.8 | 9.8 | 145.0 |
| 108-662B-1H | 25 | 0918 | 0-9.5 | 9.5 | 9.5 | 100.0 |
| 108-662B-2H | 25 | 1005 | 9.5-19.0 | 9.5 | 9.6 | 101.0 |
| 108-662B-3H | 25 | 1140 | 36.2-45.7 | 9.5 | 9.3 | 97.5 |
| 108-662B-4H | 25 | 1420 | 64.7-74.2 | 9.5 | 9.4 | 99.3 |
| 108-662B-5H | 25 | 1710 | 93.2-102.7 | 9.5 | 9.4 | 98.6 |
| 108-662B-6H | 25 | 1948 | 121.7-131.2 | 9.5 | 9.7 | 102.0 |
| 108-662B-7H | 25 | 2035 | 131.2-140.7 | 9.5 | 9.7 | 102.0 |
| 108-662B-8H | 25 | 2136 | 140.7-150.2 | 9.5 | 9.7 | 102.0 |
| 108-662B-9H | 25 | 2227 | 150.2-159.7 | 9.5 | 9.6 | 101.0 |
| 108-662B-10H | 26 | 0300 | 159.7-169.2 | 9.5 | 9.6 | 101.0 |
| 108-662B-11H | 26 | 0445 | 169.2-178.7 | 9.5 | 9.7 | 102.0 |
| 108-662B-12H | 26 | 0545 | 178.7-188.2 | 9.5 | 9.6 | 101.0 |

Note: H = hydraulic piston. UTC = Universal Time Coordinated.

If the slumps and disturbed sediments in Subunit IB are removed, the undisturbed pelagic sediments in this subunit also appear to have been deposited at rates close to 42 m/m.y. As explained in the "Sediment-Accumulation Rates" section (this chapter), extrapolation of sedimentation rates from existing control points appears to indicate largely continuous sedimentation around the disturbed sections. Thus, it appears that these slumps were added to rapidly deposited pelagic sediment sections, with little loss to erosion.

Neither magnetic-susceptibility nor *P*-wave measurements were useful for between-hole correlations, except for some suggestion of *P*-wave correlations in Subunit ID. As a result, we used carbonate layering visible in core photographs to attempt these correlations. We succeeded in correlating measurements between the two holes only within Subunits IA, IC, and ID. This indicates that we have complete composite-depth sections of pelagic sedimentation from 0 to 0.5 Ma and from 1.3 to 3.6 Ma at Site 662.

One paleoclimatic result evident in this pelagic sequence from initial shipboard studies is the intensification of $CaCO_3$ variations toward higher-amplitude changes and lower $CaCO_3$ minima around 2.6 Ma (see "Organic Geochemistry" section, this chapter). This prominent change appears to precede slightly or to correlate with the initiation of significant-scale Northern Hemisphere glaciation at 2.5 Ma. This change may reflect (1) increased dilution of carbonate content by opaline silica, (2) increased dilution by eolian dust, (3) increased dissolution of $CaCO_3$, or (4) decreased productivity of $CaCO_3$. As the sedimentation rates do not change, it seems likely that explanations 3 and/or 4 must be balanced by explanations 1 and/or 2.

The relatively low levels of dissolution observed at Site 662 are not sufficient to have caused the observed $CaCO_3$ changes alone. Increased silica would require increased productivity, but this might contradict decreased $CaCO_3$ productivity. Increased dust input would indicate increased continental aridity or wind velocity. More detailed studies and accurate age-depth models will be required to choose among these possibilities.

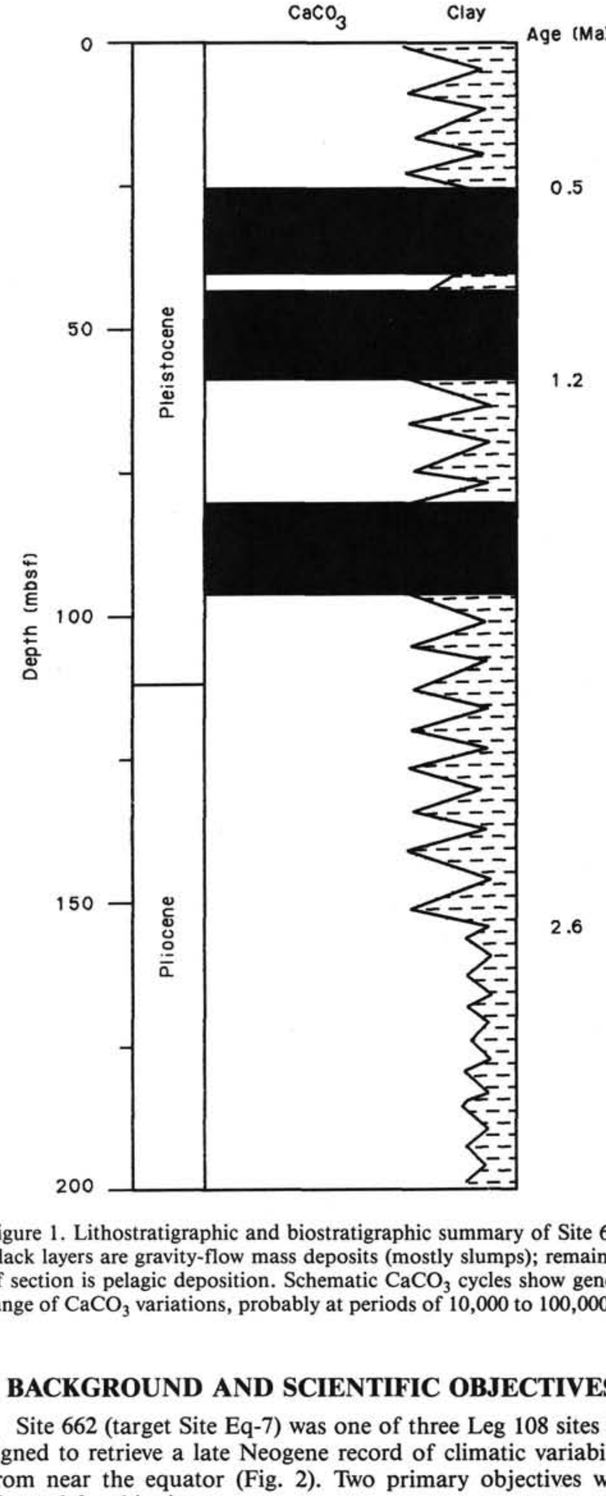


Figure 1. Lithostratigraphic and biostratigraphic summary of Site 662. Black layers are gravity-flow mass deposits (mostly slumps); remainder of section is pelagic deposition. Schematic $CaCO_3$ cycles show general range of $CaCO_3$ variations, probably at periods of 10,000 to 100,000 yr.

## BACKGROUND AND SCIENTIFIC OBJECTIVES

Site 662 (target Site Eq-7) was one of three Leg 108 sites designed to retrieve a late Neogene record of climatic variability from near the equator (Fig. 2). Two primary objectives were planned for this site:

1. To determine the late Neogene history of variations in surface-ocean circulation.

Reconstructions of sea-surface temperatures at the last glacial maximum 18,000 yr ago show that the surface ocean was chilled as much as 6° to 8°C in relation to the present in a band along and just south of the equator in the eastern half of the Atlantic Ocean (CLIMAP, 1981). Studies of the last 250,000 yr of the Pleistocene by McIntyre et al. (in press) show that the rel-

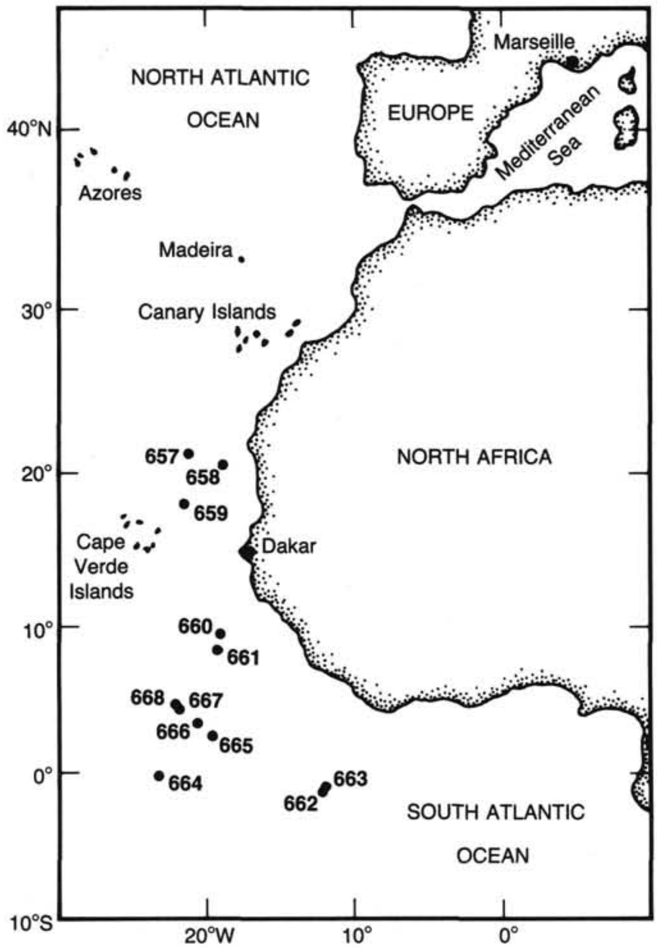


Figure 2. Locations of Sites 662 through 668.

ative abundance of planktonic foraminifers indicating cool water varied mostly with a 23,000-yr period of orbital precession. This signal requires extensive cooling of the sea surface or of the shallow subsurface layers, either by increased advection of colder waters from high southern latitudes, or by wind-driven changes in the subsurface isotherm structure caused by increased divergence or shallowing of the thermocline. Tracing several paleoceanographic signals back through the Neogene should help to distinguish among the above explanations. The critical indicator signals are (1) estimated sea-surface temperature and (2) the fluxes of opaline silica, $CaCO_3$, and organic carbon.

Site 662's position in the far southeastern part of the equatorial Atlantic enabled us to detect both the near-equatorial divergence signal as well as the advective Southern-Hemisphere contribution from the Benguela Current. Site 662 lies in the Southern-Hemisphere thermal regime (south of the thermal equator), and its long-term, sea-surface-temperature response probably reflects forcing from the Southern Hemisphere.

2. To monitor late Neogene variations in African aridity, as indicated by biogenic material and windblown terrigenous dust from the African continent.

Pokras and Mix (1985) proposed that the abundance of freshwater diatoms (genus *Melosira*) can be used in this region to monitor periodic drying out of lakes in north equatorial Africa during a 23,000-yr cycle. Because of the prominence of southern trade winds at this site, eolian deposition also may include a contribution from southern African source areas in or near the Namib and Kalahari deserts. Evaluating the relative importance of northern and southern sources was a primary objective at Site 662.

In addition to our two primary objectives, secondary objectives were as follows:

1. To obtain a continuous late-Neogene sequence for high-resolution paleomagnetic, biostratigraphic, and stable-isotopic analyses.
2. To obtain a calcareous sequence to monitor late-Neogene carbonate dissolution. Based on its location, Site 662 must be free of the fluvial input that may contribute to the record of several preceding Leg 108 sites, which indicates that productivity, dissolution, and dilution are the primary factors controlling the $CaCO_3$ record.

## Geologic and Topographic Setting

Site 662 is located in the southeastern equatorial Atlantic on the upper eastern flank of the mid-Atlantic Ridge just south of the Romanche Fracture Zone (Figs. 2 and 3). *Conrad* cruise air-gun records indicate small scattered ponds of sediment up to 5 nmi wide in an area of outcropping, or nearly outcropping, basement (Fig. 4). Site 662 lies in one of the larger ponds. A tendency toward focusing of thicker sediment accumulations into low terrain indicates some degree of sediment redistribution along the seafloor, including the possibility of turbidites and other gravity-controlled sediment deposition. Despite this risk, we chose to core in such a pond because sediment cover on the nearby topographic highs was thin, discontinuous, and, in some areas, faulted.

The basement age at Site 662 is late Miocene, based on regional magnetic lineations. The anticipated sedimentary section is cyclically alternating upper Miocene through Holocene nannofossil ooze and mud.

# OPERATIONS

After departing Site 661, we steamed at an average speed of 13.7 kt on a southeasterly course to a way point at 1°00′S, 11°59′W (Fig. 3), where the ship slowed to 5 kt at 2205 UTC on 23 March 1986, and we streamed out the geophysical gear (using 80-in.$^3$ water guns and a magnetometer). We then followed a course of 147° toward the eventual location of Site 662. We dropped a beacon at 0300 UTC on 24 March as we crossed the site (1°23.41′S, 11°44.35′W). The ship slowed, we retrieved the geophysical gear, and then returned to the beacon. (All times are UTC, Universal Time Coordinated, formerly GMT, Greenwich Mean Time.)

We began running drill pipe into Hole 662A at 0315 and finished coring by 0845 on 24 March. After three attempted mud-line cores came up empty, we discovered a 60-m miscount on the bottom-hole assembly. With this problem corrected, the first APC core came on deck at 1355. We continued APC coring to the complete penetration depth of Hole 662A (200.0 mbsf). The last APC core (108-662A-22H) came on deck at 0645 on 25 March. Total recovery for Hole 662A was 102%. We then began pulling out of Hole 662A at 0700 and cleared the mud line at 0745.

The drill string was offset 15 m south to Hole 662B, the hole spudded in, and we retrieved the first APC core at 0918 on 25 March. Based on frequent slumps and turbidites in Hole 662A above 120 mbsf, we decided to spot core in Hole 662B only those depth intervals in the upper 100 m equivalent to relatively undisturbed pelagic sections in Hole 662A. We retrieved Cores 108-662B-1H through -662B-5H within longer washed-down intervals, as indicated in Table 1. Beginning with Core 108-662B-6H, recovered from 121.7 to 131.2 mbsf and brought on board at 1948 on 25 March, we cored continuously to Core 108-

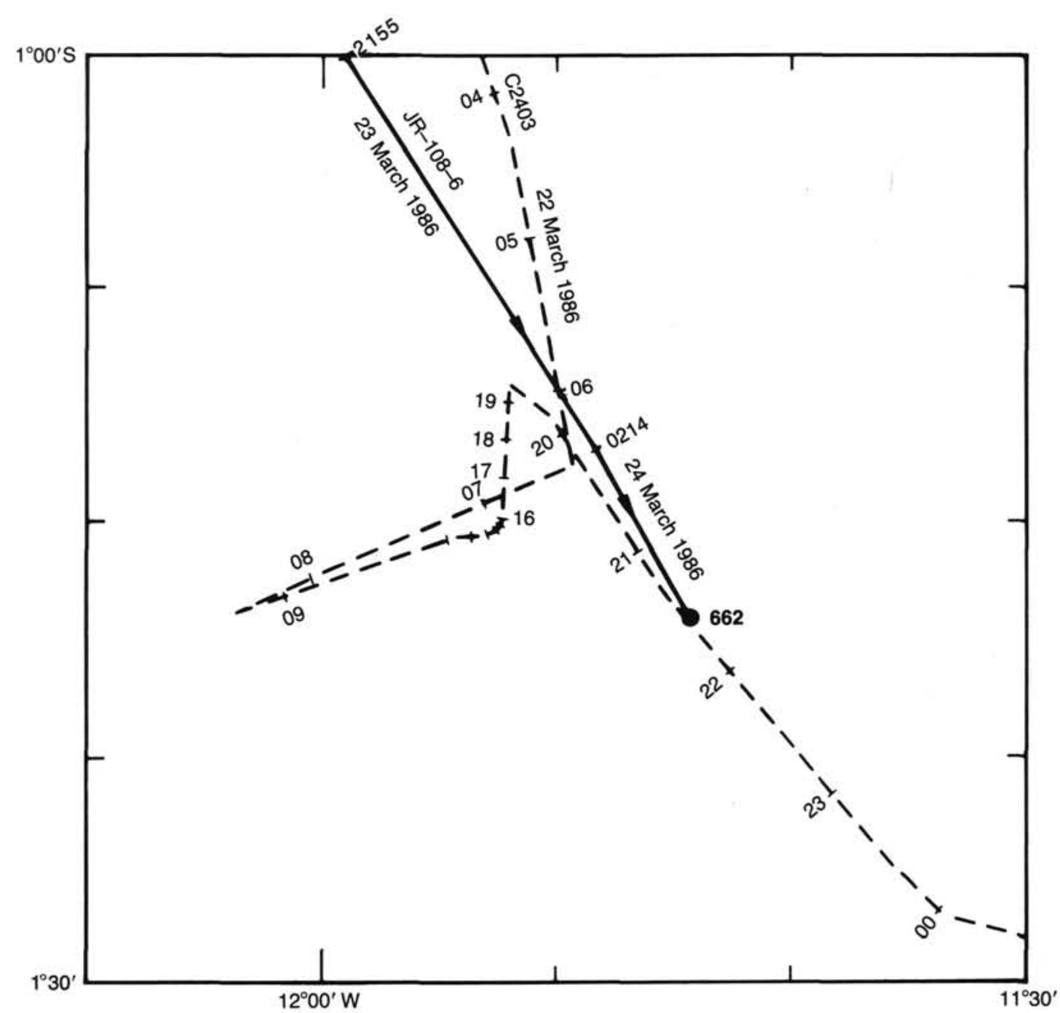


Figure 3. Seismic track lines near Site 662.

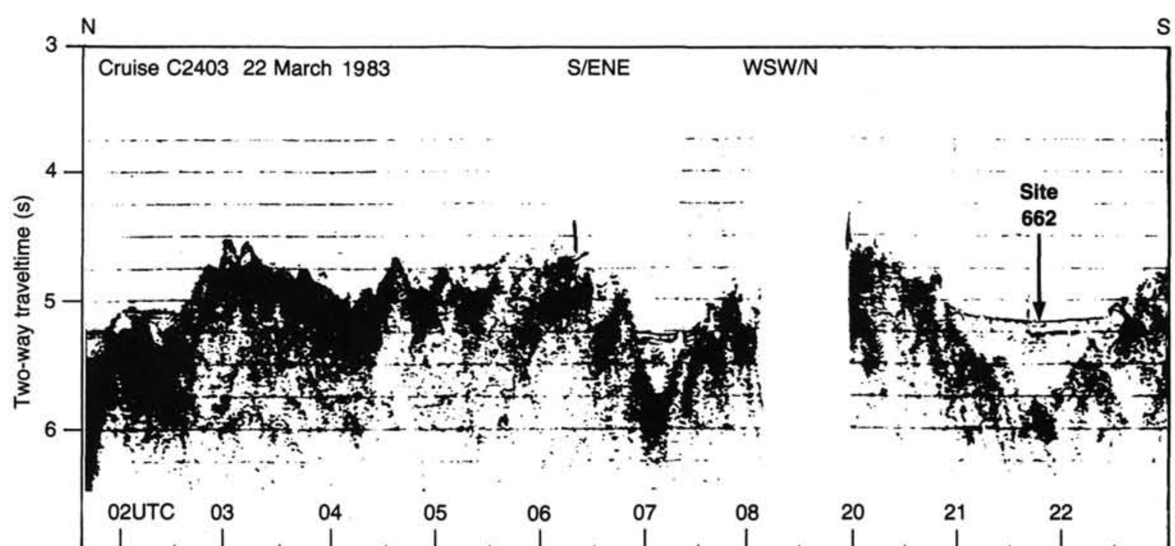


Figure 4. Seismic-reflection record from cruise C2403 near Site 662.

662B-12H, at a total penetration depth of 188.2 mbsf. About 2 hr of coring was lost between Cores 108-662B-9H and -662B-10H in the early hours of 26 March because of a broken strand in the No. 2 sand line. The final core (108-662B-12H) was brought on board at 0545 on 26 March. Total recovery for Hole 662B was 100.58%. We began pulling out of Hole 662B at 0600 and were under way from Site 662 by 1215. Weather was favorable throughout all operations, with weak winds and swell, but only variable currents of moderate strength.

## LITHOSTRATIGRAPHY AND SEDIMENTOLOGY

### Introduction

One major sedimentary unit was recognized at Site 662 (Fig. 5). This unit is composed primarily of interbedded nannofossil and foraminifer-nannofossil oozes and is Pliocene to Pleistocene in age. The unit can be subdivided further into four subunits, based on variations in carbonate content and deformation features. Each subunit is described in the following sections.

### Subunit IA

Cores 108-662A-1H through -662A-4H-3, 100 cm; depth, 0–26.2 mbsf; age, Pleistocene.
Cores 108-662B-1H through 662B-2H, CC, 19 cm; depth, 0–19.0, mbsf; age, Pleistocene.

Subunit IA is composed primarily of interbedded foraminifer-nannofossil and nannofossil oozes with minor (10% to 25%) amounts of clay, diatoms, radiolarians, and sponge spicules. In addition, Cores 108-662A-2H and -662A-3H contain a siliceous

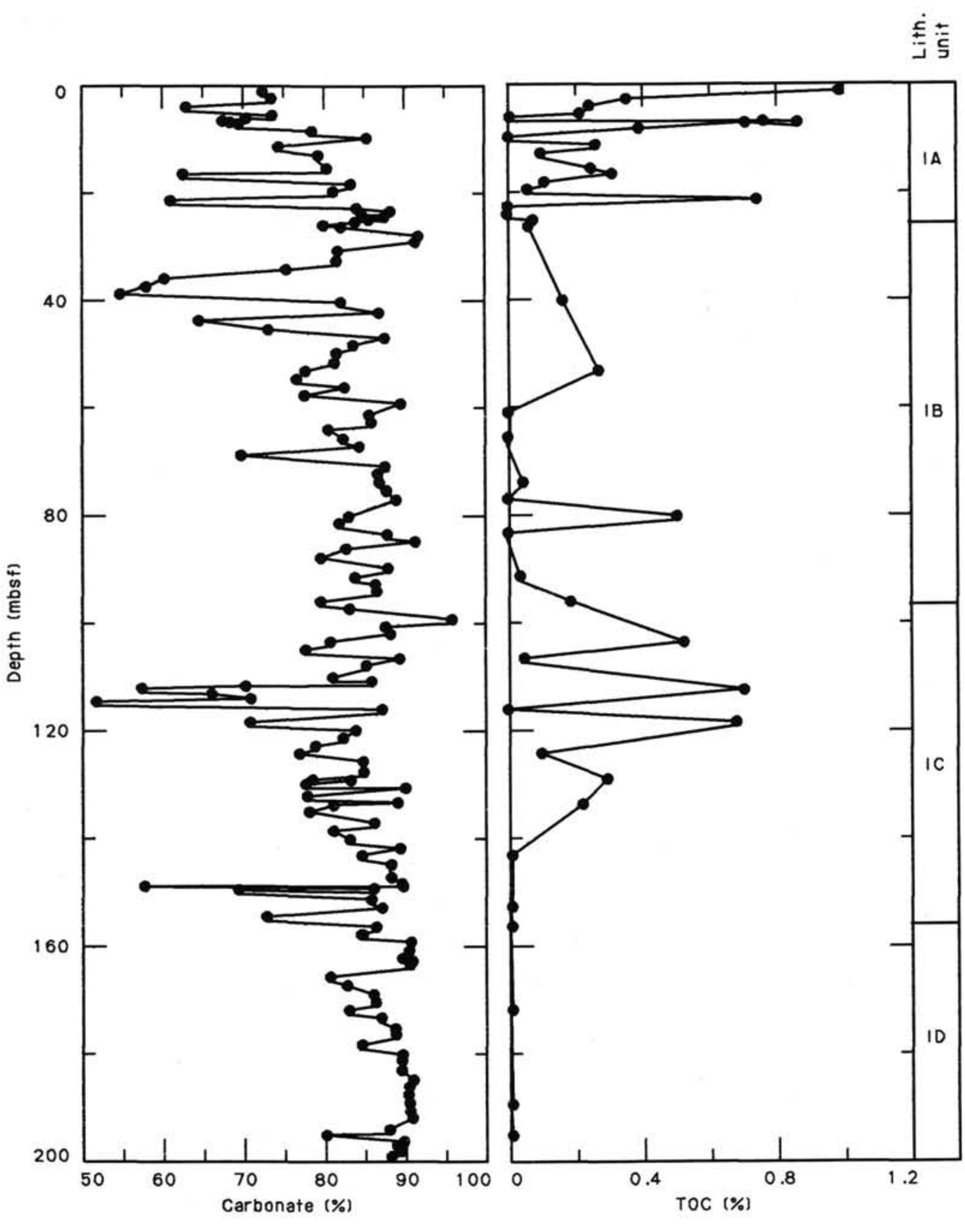


Figure 5. Carbonate and organic-carbon contents of sediments at Site 662, Hole 662A. Also shown is the division of the unit into subunits.

nannofossil ooze interbedded with pelagic carbonates. The carbonate content of the sediments in this subunit ranges from 60% to 90%. The foraminifer-nannofossil and nannofossil oozes are commonly white, light gray, or gray, depending on the clay and biogenic-silica contents. The siliceous nannofossil ooze is gray to light gray. All sediment types are moderately bioturbated. Two thin (< 10 cm), sandy foraminifer turbidites occur near the top of Cores 108-662A-2H and -662A-3H and in the middle of Cores 108-662B-2H and -662B-3H.

The depth of the base of this subunit in Hole 662B can be estimated only minimally as the next two core intervals were washed and the subunit boundary was not cored.

### Subunit IB

Cores 108-662A-4H-3, 100 cm, through 662A-11H-5, 150 cm; depth, 26.2–96.2 mbsf; age, Pleistocene.

Cores 108-662B-3H through 662B-5H-5, 150 cm; depth, 36.2–100.7 mbsf; age, Pleistocene.

Subunit IB is composed of interbedded foraminifer-nannofossil and nannofossil oozes with minor (10% to 25%) amounts of clay, diatoms, radiolarians and sponge spicules. Sediments are white, light gray, and gray. The carbonate content of this subunit generally ranges from 80% to 90%, with the exception of a clayey silt interval around 40 mbsf (Hole 662A) having carbonate values as low as 55%. This subunit is defined on the basis of deformation features, particularly three slumps (mass flows?). These slumps are characterized by folded, dipping, and vertically stretched bedding planes. Microfaulting and slide planes are common within the slumped intervals. Erosional contacts and graded bedding (turbidites?) are common in Core 108-662A-5H-7H and Cores 108-662B-3H through -662B-5H. Intervals between the slumps appear to be normal pelagic units. The precise upper boundary of this subunit in Hole 662B is unknown as it occurs in a washed interval.

### Subunit IC

Cores 108-662A-11H-6 through -662A-17H, CC, 12 cm; depth, 96.2–154.64 mbsf; age, late Pliocene to Pleistocene.

Cores 108-662B-5H through -662B-9H-1, 100 cm; depth, 100.7–151.2 mbsf; age, late Pliocene to Pleistocene.

Subunit IC is composed primarily of nannofossil ooze, with minor amounts of clay, diatoms, radiolarians, sponge spicules, and foraminifers. In addition, Cores 108-662A-13H and -662A-14H contain siliceous nannofossil ooze interbedded with the nannofossil ooze. The carbonate content of this subunit generally ranges from 75% to 90%, with two intervals of lower (50% to 70%) carbonate content (115–120 and 150–155 mbsf; Hole 662A). The nannofossil ooze is generally white to light gray, and the siliceous nannofossil ooze is olive gray. Both sediment types are moderately bioturbated and contain numerous green and black laminae. Erosional contacts and graded bedding (turbidites) occur in Cores 108-662A-12H, -662A-13H, -662-17H, and -662B-5H.

The precise location of the lower boundary of this Hole 662B subunit is unknown. The boundary was determined from variations in carbonate content in Hole 662A. Carbonate data were not generated for Hole 662B. Therefore, the Hole 662B boundary is based on correlation of light to dark color variations with those of Hole 662A.

### Subunit ID

Cores 108-662A-18H through -662A-22H, CC, 21 cm; depth, 154.64–203.00 mbsf; age, Pliocene.

Cores 108-662B-9H-1, 100 cm, through -662B-12H, CC, 17 cm; depth, 151.2–188.2 mbsf; age, Pliocene.

Subunit ID is composed primarily of nannofossil and foraminifer-nannofossil oozes, with minor (0% to 10%) amounts of clay, radiolarians, and diatoms. The carbonate content of this subunit is generally high (85% to 90%), with less apparent variability than in the other subunits. The foraminifer-nannofossil ooze is generally white, while the foraminifer-bearing nannofossil ooze is light gray to light olive gray. Both sediment types are weakly to moderately bioturbated, and black and green microlaminae are common.

### Depositional History

The depositional history of the stratigraphic section recovered at Site 662 shows normal calcareous and siliceous-calcareous pelagic sedimentation typical of highly productive equatorial locations. These pelagic deposits are interrupted by slumps and turbidites of similar lithology originating from surrounding topographic highs. Three slumps flowed over the pelagic beds, tilting these beds slightly, but not deforming them extensively. After each slumping episode, normal pelagic sedimentation resumed.

## BIOSTRATIGRAPHY

Two holes were cored at Site 662, located in a water depth of 3813.8 m, to investigate the history of divergence in the equatorial Atlantic. Hole 662A was cored continuously to a depth of 200 mbsf, while Hole 662B was cored discontinuously. Only selected intervals of sediments (0–19.0, 36.2–45.7, 64.7–74.2, 93.2–102.7, and 121.7–188.2 mbsf) were recovered from this hole. The oldest sediments cored are early Pliocene in age. Zonal assignments for the cores are shown in Figures 6 and 7.

Calcareous nannofossils and planktonic foraminifers are abundant at this site. The nannofossils are generally moderately well preserved, with occasional poor preservation caused by dissolution. The planktonic foraminifers are characterized by good-to-moderate preservation. Numerous reworked specimens identified throughout the record are attributed to the presence of extensive slumps and turbidites, especially within the Pleistocene section. Diatoms are generally common to abundant, with moderate-to-poor preservation, and benthic foraminifers range from rare to common, with good preservation.

The planktonic fauna and flora are characterized variously by both cool and warm taxa and may be recording glacial/interglacial intervals, especially in the upper one-half of both holes. Shore-based investigations at closer sampling intervals should clarify the floral and faunal records of climate changes at this site.

### Calcareous Nannofossils

Calcareous nannofossils are abundant in all sediment samples investigated from Site 662. Most assemblages are moderately well preserved, but in many samples poorer preservation occurs caused by dissolution. Reworked specimens (e.g., discoasters in the late Pleistocene) were observed in most samples investigated. Generally, this background "noise level" of reworking was moderate above Section 108-662A-10H-6 and below Section 108-662A-12H-2, except in scattered samples in the upper one-half of the cored sequence, which is characterized by extensive turbidite deposition. Pliocene and Pleistocene nannofossil assemblages commonly are intermixed severely between these two sections. Within the slump deposits in Cores 108-662A-11H and -662A-12H, sediments of older age sometimes overlie younger sediments.

All major slumps occur from Section 108-662A-12H-2 upward, shortly above the extinction level of *Calcidiscus macintyrei* (at the Core 108-662A-12H/108-662A-13H boundary, 1.45 Ma). The slumped material (e.g., in Samples 108-662A-10H, CC and -662A-11H, CC) seems derived mostly from the latest part of Zone NN18, within the *Discoaster triradiatus* acme interval (1.89 to 2.07 Ma).

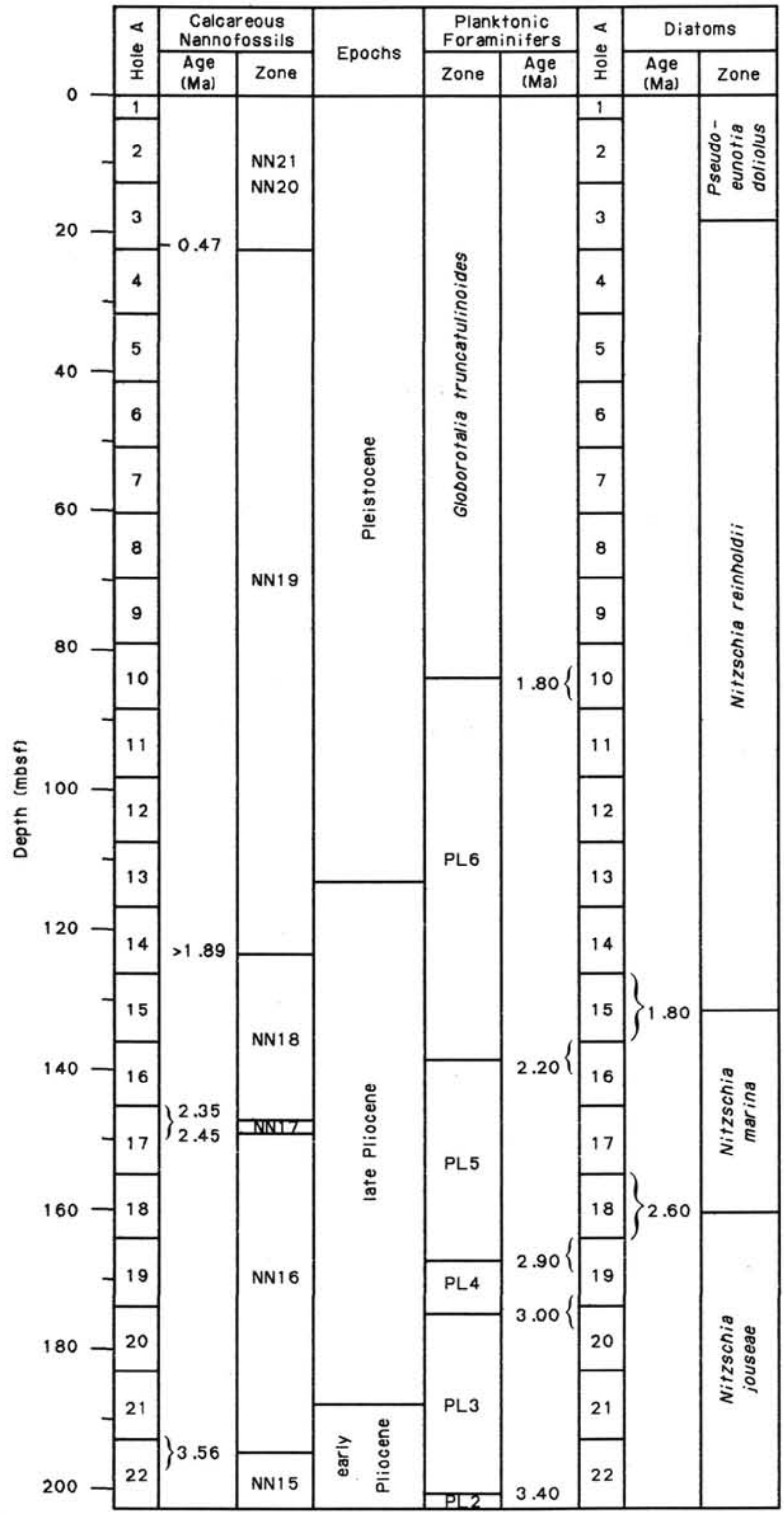


Figure 6. Zonal assignments for cores recovered from Hole 662A.

The extinction of *Reticulofenestra pseudoumbilica* occurs in the deepest core retrieved (Core 108-662A-22H), implying that the latest part of the early Pliocene was reached. The Pliocene and Pleistocene nannofossil assemblages at Site 662 are similar in composition to those observed in previous Leg 108 sites, perhaps with the exception that *Umbilicosphaera mirabilis* makes up a greater share of the total assemblage at Site 662. Gephyrocapsids and reticulofenestrids dominate the Pliocene and Pleistocene assemblages, respectively. Ceratoliths, pontosphaerids, and scyphosphaerids are rare in both the Pliocene and Pleistocene samples, whereas common elements consist of *Helicosphaera carteri, Helicosphaera sellii* (the latter is found up to

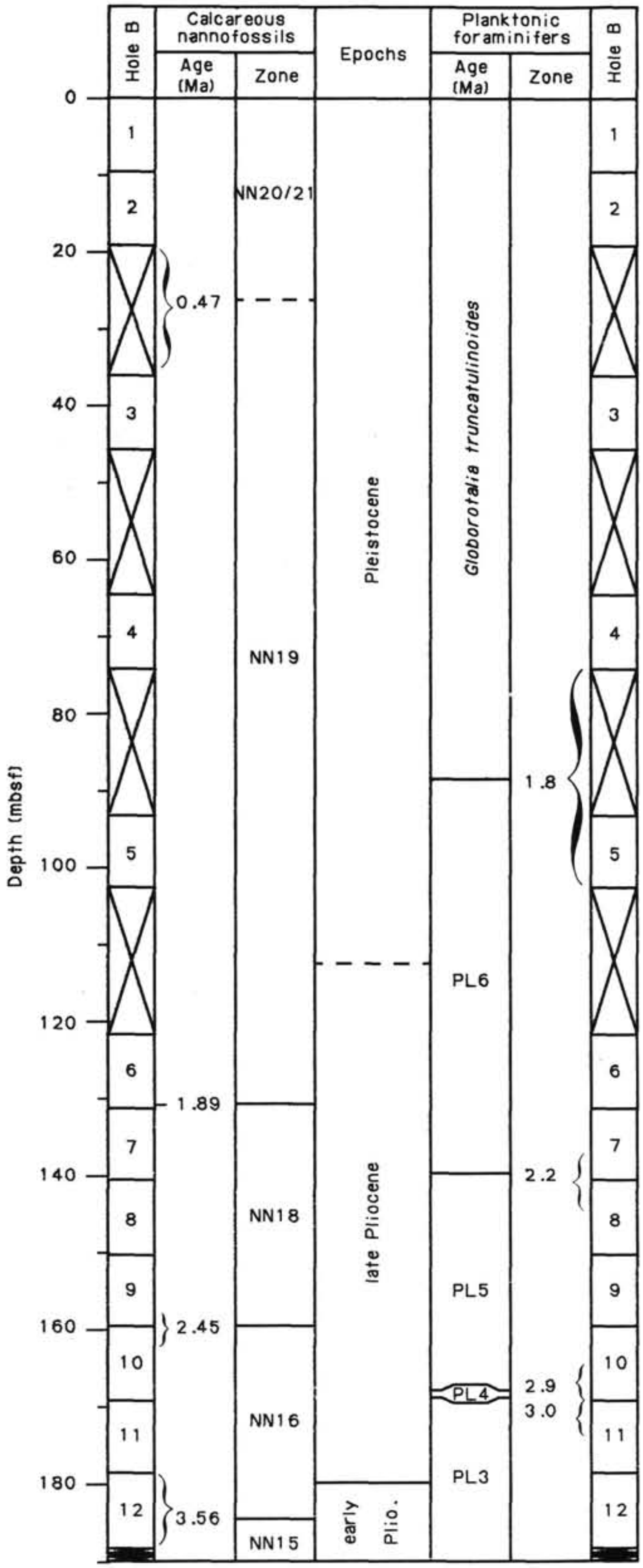


Figure 7. Zonal assignments for cores recovered from Hole 662B. The interval representing calcareous-nannofossil Zone NN17 was not identified in this hole.

immediately below the slumped interval in Section 108-662A-12H-2), *Calcidiscus leptoporus, C. macintyrei, Pseudoemiliania lacunosa*, rhabdosphaerids, and syracosphaerids.

Two assemblage features are particularly noteworthy. First, in light of the equatorial location of Site 662, we were surprised to find that discoasters are minor components of the total assemblage. More detailed sampling within cores showed distinct abundance fluctuations of the discoasters; however, they never contributed more than 5% to 10% of the total assemblage. We hope that by quantifying their fluctuations in abundance we can gain insight as to the cause of their low relative abundances at this low-latitude site. Second, *Coccolithus pelagicus* never was present in any of the middle or upper Pleistocene assemblages, except within slumps of older age, but this species was a consistent if rare component of upper Pliocene and lowermost Pleistocene assemblages.

Late Pliocene nannofossil biostratigraphy is based entirely on discoaster events. Combined with reworking, the low abundance of discoasters at Site 662 suggests that more precise determinations of these late Pliocene markers can be made only through detailed quantitative analysis and then judged in relation to the background level of reworking.

### *Pleistocene*

*Pseudoemiliania lacunosa* is fairly common below Sample 108-662A-4H-1, 100 cm, rare in 108-662A-3H, CC, and absent from 108-662A-3H-6, 150 cm, and upward. In Hole 662B, *P. lacunosa* disappears between Cores 108-662B-3H and -662B-2H.

*Helicosphaera sellii* was present in sediments immediately below the slump, which begins in Section 108-662A-12H-2. *Calcidiscus macintyrei* was observed in Sample 108-662A-13H-1, 75 cm, and downward, but was not observed above Sample 108-662A-12H-6, 110 cm (except within slumped intervals). Hole 662B was spot cored; these two events occur within the uncored interval between Cores 108-662B-5H and -662B-6H.

### *Pliocene*

*Discoaster brouweri* and *D. triradiatus* disappear between Samples 108-662A-14H-4, 150 cm, and 108-662A-14H-5, 75 cm. Rare specimens of *D. brouweri* were observed in Samples 108-662A-14H-4, 150 cm, and 108-662A-14H-4, 75 cm, but these were considered to be reworked. In Hole 662B, these events probably occur in Core 108-662B-6H, but the ages are difficult to determine because of intense reworking of the core-catcher sample. Sample 108-662B-7H, CC was deposited before the acme interval of *D. triradiatus*. This acme interval begins with the lower one-half of Section 108-662B-15H-5 in Hole 662B.

Neither *D. pentaradiatus* nor *D. surculus* was observed in Sample 108-662A-17H-1, 75 cm. Occurrences at shallower levels most likely result from reworking. *Discoaster pentaradiatus* has its last occurrence (LO) in Sample 108-662A-17H-2, 142 cm, and *D. surculus* in Sample 108-662A-17H-3, 118 cm. Both species are rare toward the end of their indicated ranges, and present assignments of their extinctions to specific samples should be considered tentative. *Discoaster tamalis* disappears in the lower part of Core 108-662A-18H. The less-refined sampling intervals in Hole 662B, restricted to core-catcher samples, were too coarse to yield conclusive results regarding the extinctions of *D. pentaradiatus* and *D. surculus*. Judging from the depths below the seafloor, one would expect to find these events in Sample 108-662B-8H, CC. However, only a trace of *D. surculus* was observed in this sample; thus, it was considered as being reworked. Abundant *D. brouweri* and rare *D. triradiatus* were observed in Sample 108-662B-9H, CC, although *D. pentaradiatus* and *D. surculus* were absent. Both these species were present in Sample 108-662B-10H, CC, together with *D. tamalis*. We consider that in Hole 662B too-wide sampling intervals, sediment mixing, and generally low relative abundances of discoasters prevented us from identifying the true extinction levels of *D. pentaradiatus* and *D. surculus*. In Hole 662B, *D. tamalis* disappeared in the upper part of Core 108-662B-18H. Closer sampling intervals within this section did not improve the precision owing to very low relative abundances of discoasters.

*Sphenolithus abies* and *Sphenolithus neoabies* persist into the lower one-half of Core 108-662A-21H, whereas *Reticulofenestra pseudoumbilica* showed a distinct extinction between Samples 108-662A-22H-3, 50 cm, and -662A-22H-1, 70 cm. Hole 662B was not cored deeply enough to reach these events.

### Planktonic Foraminifers

A record of planktonic foraminifers extending to the early Pliocene was recovered at Site 662. Although two holes were drilled, only Hole 662A was cored continuously and, hence, gives a clearer picture of distribution of the planktonic zones in the sediments. With few exceptions, planktonic foraminifers were abundant at this site, with preservation ranging from good to moderate. The fauna is tropical, typically containing common *Neogloboquadrina dutertrei, Globigerinoides ruber, Globigerinoides trilobus*, or *Globorotalia menardii*, with rarer, yet consistently present, *Pulleniatina obliquiloculata, Orbulina universa, Globigerinoides sacculifer, Globigerina decoraperta*, and *Globorotalia scitula*. The presence of common *Neogloboquadrina pachyderma* (right-coiling) and *Globorotalia inflata* in the top 60 m of Hole 662A may reflect intensification of glaciations since 1 Ma.

Berggren's (1973) PL zones were recognized easily at this site. The PL6/*Globorotalia truncatulinoides* zonal boundary, marked by the LO of *Globigerinoides obliquus*, fell between Samples 108-662A-10H-3, 9 cm, and -662A-10H-5, 49 cm, in Hole 662A and between Samples 108-662B-4H, CC and -662B-5H, CC in Hole 662B. A short overlapping (<0.1 Ma) in the ranges of *G. truncatulinoides* and *G. obliquus* was not observed and may indicate that *G. obliquus* is too rare at the top of its range to be used with confidence. The few specimens of *G. obliquus*, identified well within the *Globorotalia truncatulinoides* Zone, are believed to be reworked, a conclusion supported by the presence of numerous slumps and turbidites within the Pleistocene section.

The PL6/PL5 zonal boundary, dated at 2.2 Ma and based on the LO of *Globorotalia miocenica*, lies between Samples 108-662A-16H-1, 137 cm, and -662A-16H-3, 136 cm, and Samples 108-662B-7H-5, 135 cm, and -662B-7H, CC. The transition between *Globorotalia puncticulata* and *G. inflata* occurs within these samples. Zone PL5 is characterized by increasing numbers of *G. decoraperta* and *Neogloboquadrina humerosa*. The short Zone PL4 (2.9 to 3.0 Ma), which occurs between the last occurrences of *Spaeroidinellopsis seminulina* and *Dentogloboquadrina altispira*, was identified at both holes—in Samples 108-662A-19H-3, 74 cm, and -662B-10H-6, 131 cm. Zone PL3 starts above Samples 108-662A-19H, CC and -662B-10H, CC. Only Hole 662A reaches the early to late Pliocene boundary marked by the top of Zone PL2. The top of this zone, however, is based on the LO of *Globorotalia margaritae*, which has proved an unreliable marker at previous Leg 108 sites. Therefore, the PL3/PL2 boundary, as found between Samples 108-662A-22H-3, 135 cm and -662A-22-5, 135 cm, may be in sediments older than 3.4 Ma if the LO of *G. margaritae* follows the same pattern as at previous sites. This possibility appears to be borne out by nannofossil data. Finally, the LO of *Pulleniatina praecursor*, dated at 3.3 Ma (Berggren et al., 1985) was identified between Samples 108-662A-20H, CC and -662A-21H, CC.

### Benthic Foraminifers

Benthic foraminifers occurred in all core-catcher samples examined from Site 662A. Samples 108-662A-1H, CC through -662A-16H, CC contain rare-to-common and well-preserved specimens. The characteristic species of the assemblage are consistent throughout this interval, but their abundances vary from sample to sample. In Sample 108-662A-2H, CC, *Chilostomella oolina, Melonis pompilioides*, and *Melonis barleeanus* are relatively abundant. Core-catcher Samples 108-662A-3H and -662A-6H are characterized by high diversity and the dominance of uvigerinids. *Oridorsalis tener* and *Sphaeroidina bulloides* are the dominant species in Sample 108-662A-5H, CC. *Globobulimina auriculata* occurs frequently in Sample 108-662A-7H, CC and in Samples 108-662A-13H, CC through -662A-17H, CC. This species is most abundant (about 70%) in Sample 108-662A-13H, CC. *Globobulimina auriculata* typically is associated with North Atlantic Deep Water (Schnitker, 1979) and suggests relatively warm deep water. In core-catcher Samples 108-662A-10H through -662A-20H, the agglutinated foraminifers, such as *Eggerella bradyi* and *Karreriella bradyi*, are relatively common. Core-catcher Samples 108-662A-17H through -662A-22H contain rare and poorly to moderately well-preserved specimens. The LO of *Bulimina alazanensis* occurs in Sample 108-662A-20H, CC (3.2 Ma). This age is similar to that reported by Lutze (1977).

### Diatoms

Diatoms are present in all samples examined from Hole 662A. The assemblage is dominated by warm- to cool-water taxa indicative of moderate-to-high productivity. Common to abundant diatoms occur in all samples except Samples 108-662A-13H, CC and -662A-21H, CC, where few diatoms are present. Preservation varies from moderate to poor, with no systematic trend evident. The species composition varies and may reflect glacial/interglacial changes. Samples dominated by *Pseudoeunotia doliolus, Thalassionema nitzschioides* vars., and fragments of *Ethmodiscus rex* suggest glacial intervals, whereas samples with greater numbers of *Coscinodiscus nodulifer, Thalassiosira eccentrica*, and *Roperia tesselata* probably were deposited under interglacial conditions. Windblown freshwater diatoms, predominantly *Melosira* spp., also occur in varying numbers. Sampling density is insufficient to delineate specific climatic trends or cycles among either marine or windblown diatoms. Because of time constraints, no samples from Hole 662B were examined.

The sporadic occurrences of *Rhizosolenia praebergonii* and *R. praebergonii* var. *robustus* required that Burckle's zonation (1977), defined for the eastern equatorial Pacific, be exchanged for that defined by Baldauf (1984) for the North Atlantic, thus replacing the *Rhizosolenia praebergonii* Zone with the *Nitzschia marina* Zone. Increased sampling resolution during subsequent studies will determine the stratigraphic continuity of *R. praebergonii*.

Samples 108-662A-1H, CC and -662A-2H, CC are assigned to the *Pseudoeunotia doliolus* Zone, based on the presence of *P. doliolus* stratigraphically above the LO of *N. reinholdii*. Samples 108-662A-3H, CC through -662A-14H, CC are assigned to the *Nitzschia reinholdii* Zone, based on the co-occurrence of these two species.

The LO of the silicoflagellate *Mesocena quadrangula* has an approximate age of 0.70 Ma in the middle latitudes of the Atlantic (Baldauf et al., 1987) and an age of 0.79 Ma in the eastern equatorial Pacific (Barron, 1980). The LO of *Nitzschia fossilis* has an approximate age of 0.58 to 0.64 Ma in the middle latitudes of the Atlantic (Baldauf et al., 1987) and approximates the LO of *Mesocena quadrangula* (0.79 Ma) in the eastern equatorial Pacific (Barron, 1980). The last occurrences of both *M. quadrangula* and *N. fossilis* occur between Samples 108-662A-5-1, 30 cm, and -662A-4H, CC. However, this interval contains numerous slumps and turbidites, which may result in the reworking of these taxa. The last consistent, common occurrence of *M. quadrangula* occurs in Sample 108-662A-7H-1, 150 cm, whereas that of *N. fossilis* occurs in the upper part of Section 108-662A-7H-6. Additional studies using quantitative methods will be required to determine the actual LO of these species.

Based on the first occurrence (FO) of *P. doliolus*, Sample 108-662A-14H, CC represents the base of the *Nitzschia reinholdii* Zone. Comparison with the planktonic-foraminifer and calcareous-nannofossil stratigraphies suggests an age of 2.0 to 2.1 Ma for this sample, rather than the accepted date of 1.8 Ma (Barron, 1980) for the LO of *P. doliolus*. The older date, which is similar to the estimated age of this event at Site 658 (this volume), suggests that *P. doliolus* occurred earlier (0.2 to 0.3 m.y.) in the equatorial Atlantic and later spread to the Pacific. This finding is similar to those of L. Burckle and E. Fortanier (pers. comm., 1984); however, correlation of the LO of *P. doliolus* to absolute time will be required to verify this hypothesis.

The *Nitzschia marina* Zone (Baldauf, 1984), which is defined as the interval from the LO of *Nitzschia jouseae* to the FO of *P. doliolus*, occurs in Samples 108-662A-14H, CC through 662A-18H, CC. The LO of *Thalassiosira convexa* s. ampl. in Sample 108-662A-17H, CC suggests an age of approximately 2.1 Ma; however, the LO of *N. jouseae* (2.6 Ma) in Sample 108-662A-18H, CC argues that the LO of *T. convexa* in Core 108-662A-17H is anomalously early (about 0.2 Ma). In the equatorial Pacific, the abundance of this species decreases near the end of its stratigraphic range (Baldauf, 1985). A similar decrease in abundance at Site 662 or ecological exclusion may explain the earlier occurrence of this event. The occurrence of *N. jouseae* in core-catcher Samples 108-662A-18H through -662A-22H allows us to place these samples into the *Nitzschia jouseae* Zone of Baldauf (1984).

The FO of substantial numbers of windblown, siliceous microfossils occurs in Sample 108-662A-17H, CC. Below this level, opal phytoliths are absent, and freshwater *Melosira* spp. occur only in Sample 108-662A-20H, CC. Below Sample 108-662A-7H-1, 142 cm, *Melosira* spp. invariably outnumber phytoliths. From this sample to the top of Core 108-662A-1H, phytoliths frequently outnumber *Melosira* spp.

## PALEOMAGNETISM

### Paleomagnetics

Archive halves of sections were measured from Cores 108-662A-1H through -662A-6H, 108-662A-8H, and 108-662A-13H through -662A-15H. No cores were measured from Hole 662B. Intensities were weak, and vector data were highly scattered. Duplicate measurements of the same section exclude noise from instruments as the cause of the scatter. Rather, poor agreement between archive and working halves suggests that continued magnetic grain mobility is responsible. We do not know whether the incoherence is a consequence of coring disturbance or an inherent property of the sediments. No discrete samples could be measured using our shipboard equipment owing to extremely weak magnetizations.

### Magnetic Susceptibility

We measured whole-core volume susceptibilities for Cores 108-662A-1H through -662A-21H and for Cores 108-662B-1H through -662B-8H. Susceptibilities were low (often less than 10 $\times$ $10^{-6}$ SI units), and in many cores the record obviously was dominated by contaminants. No between-hole correlations were possible.

## SEDIMENT-ACCUMULATION RATES

Sediment-accumulation rates were calculated for Hole 662A, based on 16 nannofossil, planktonic-foraminifer, and diatom biostratigraphic events (Table 2). The resulting curve (Fig. 8)

**Table 2. Biostratigraphic and magnetostratigraphic events, their stratigraphic placement, and estimated ages for Hole 662A.**

| | Datum | Depth (mbsf) | Age (Ma) |
|---|---|---|---|
| LO | *Pseudoemiliania lacunosa* | 21.7-22.2 | 0.47 |
| LO | *Nitzschia reinholdii* | 12.7-22.2 | 0.65 |
| LO | *Calcidiscus macintyrei* | 106.8-108.5 | 1.45 |
| FO | *Pseudoeunotia doliolus* | 126.7-136.2? | 1.80 |
| LO | *Discoaster brouweri* | 123.2-124.0 | 1.89 |
| FO | *D. triradiatus* acme | 133.5-134.2 | 2.07 |
| LO | *Globorotalia miocenica* | 137.5-140.5 | 2.20 |
| LO | *Thalassiosira convexa* | 145.7-155.2 | 2.20 |
| LO | *Discoaster pentaradiatus* | 146.5-148.6 | 2.35 |
| LO | *D. surculus* | 148.6-149.9 | 2.45 |
| LO | *N. jouseae* | 155.2-164.7 | 2.65 |
| LO | *Discoaster tamalis* | 155.3-159.8 | 2.65 |
| LO | *Dentogloboquadrina altispira* | 166.9-168.5 | 2.90 |
| LO | *Sphaeroidinellopsis seminulina* | 174.2-175.5 | 3.00 |
| LO | *Pulleniatina* | 183.7-193.2 | 3.30 |
| LO | *Reticulofenestra pseudoumbilica* | 193.9-196.7 | 3.56 |

Note: LO = last occurrence. FO = first occurrence.

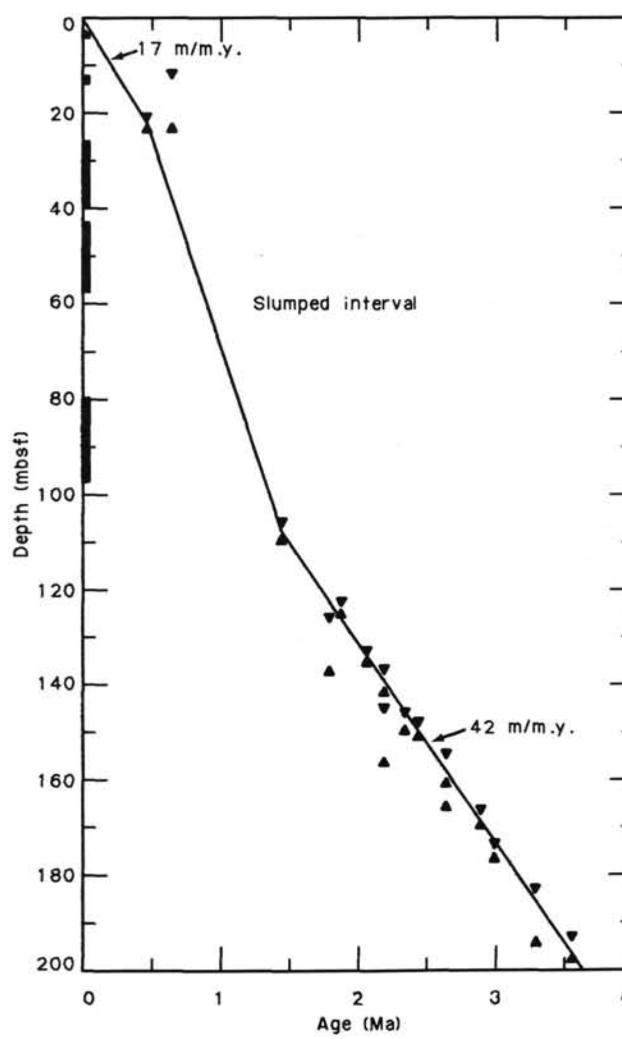


Figure 8. Sediment-accumulation rates for Hole 662A. Identifiable slumps and turbidites indicated by black bars on left. Uncertainties in the depth placement of the datums are delineated by points of the triangles.

suggests a continuous average accumulation rate of ~42 m/m.y. from the late to early Pliocene through the early Pleistocene, at which time the accumulation rate more than doubles to ~87 m/m.y. During the latest Pleistocene (<0.5 Ma), the accumulation rate falls to the pre-Pleistocene level. Of all biostratigraphic markers used, only three diatom events, the FO of *Pseudoeunotia doliolus* and the last occurrences of *Nitzschia reinholdii* and *Thalassiosira convexa*, fall off the curve. This most likely results from the sporadic occurrences of *P. doliolus* and *T. convexa* near the limits of their stratigraphic ranges, and the diachronous LO of *N. reinholdii* between the equatorial Pacific and Atlantic (Baldauf, 1986). The last occurrences of *Globorotalia margaritae* (3.4 Ma) and *Globigerinoides obliquus* (1.8 Ma) were not used because of their scarcity at the tops of their ranges.

The apparent doubling of accumulation rates in the Pleistocene is not caused by an increase in pelagic sedimentation, but results from the presence of numerous turbidites and slumps between 25 and 100 mbsf that contribute a minimum of 43.2 m of sediments to the Pleistocene interval (see "Composite-Depth Section," this chapter). The actual depths of datums below 100 m thus were converted to "no-turbidite/slump" depths (Table 3) by subtracting 43.2 m from each depth and are replotted in Figure 9.

Figure 9 more accurately represents the pelagic sedimentary history at Site 662, with an apparent accumulation rate of ~42.0 m/m.y. over the last 3.6 m.y. All the nannofossil and planktonic-foraminifer datums fall on or very close to the line in Figure 9. Thus, in spite of the extensive slumping that has occurred, we see no evidence of major hiatuses in the pelagic sedimentary record at this site.

## INORGANIC GEOCHEMISTRY

Interstitial-water samples were squeezed from six sediment samples routinely recovered approximately every 50 m from Hole 662A. Values for pH and alkalinity were measured in conjunction, using a Metrohm 605 pH-meter, followed by titration with 0.1N HCl. Salinities were measured using an optical refractometer, and chlorinities were determined by titration with silver nitrate to a potassium chromate end point.

Magnesium and sulfate analyses were performed by ion chromatography using a Dionex 2120i instrument. Results from all analyses are presented in Table 4.

**Table 3. Biostratigraphic and magnetostratigraphic events, their stratigraphic placement, and estimated ages in the absence of 43.2 m of identifiable slumps and turbidites for Hole 662A.**

| | Datum | Depth (mbsf) | Age (Ma) |
|---|---|---|---|
| LO | *Pseudoemiliania lacunosa* | 21.7-22.2 | 0.47 |
| LO | *Nitzschia reinholdii* | 12.7-22.2 | 0.65 |
| LO | *Calcidiscus macintyrei* | 63.6-65.3 | 1.45 |
| LO | *Discoaster brouweri* | 80.0-81.8 | 1.89 |
| FO | *D. triradiatus* acme | 90.3-91.0 | 2.07 |
| LO | *Globorotalia miocenica* | 94.3-97.3 | 2.20 |
| LO | *Discoaster pentaradiatus* | 103.3-105.4 | 2.35 |
| LO | *D. surculus* | 105.4-106.7 | 2.45 |
| LO | *N. jouseae* | 112.0-121.5 | 2.65 |
| LO | *Discoaster tamalis* | 112.1-116.6 | 2.65 |
| LO | *Dentogloboquadrina altispira* | 123.7-125.3 | 2.90 |
| LO | *Sphaeroidinellopsis seminulina* | 131.0-132.3 | 3.00 |
| LO | *Pulleniatina* | 140.5-150.0 | 3.30 |
| LO | *Reticulofenestra pseudoumbilica* | 150.7-153.5 | 3.56 |

Note: LO = last occurrence. FO = first occurrence.

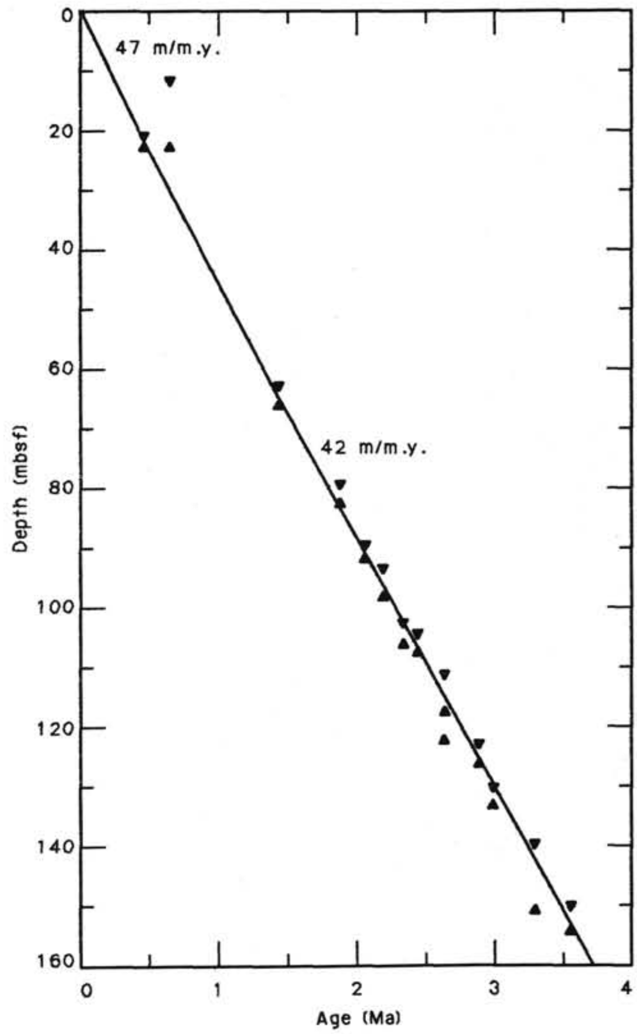


Figure 9. Sediment-accumulation rates for Hole 662A in the absence of 43.2 m of identifiable slumps and turbidites. Uncertainties in the depth placement of the datums are delineated by points of the triangles.

## ORGANIC GEOCHEMISTRY

At Site 662, Hole 662A, 126 physical-properties samples were used for determining carbonate content. Of these, 45 samples from throughout the sequence also were analyzed for total-organic-carbon (TOC) contents. No analyses were performed on samples from Hole 662B.

### Organic and Inorganic Carbon

Inorganic-carbon (IC) content was measured on the Coulometrics Carbon Dioxide Coulometer, while total-carbon (TC) values were determined using the Perkin Elmer 240C Elemental Analyzer. TOC values were calculated by difference. Analytical methods are discussed, and data presented in the Appendix (this volume).

The boundary between sedimentary Subunits IC and ID (see "Lithostratigraphy and Sedimentology" section, this chapter) may be observed in the carbonate curve (Fig. 10), found within Core 108-662A-17H (155 mbsf; about 2.65 Ma). Subunits IA through ID are characterized by variations in carbonate contents of from 52% to 97%, with most samples lying within the range of 75% to 90%. In contrast, Subunit ID displays rela-

**Table 4. Results of inorganic-geochemical analyses conducted for Site 662.**

| Core/ section | pH | Alkalinity (mmol/L) | Salinity (‰) | Chlorinity (mmol/L) | $SO_4^{2-}$ (mmol/L) | $Mg^{2+}$ (mmol/L) | $Ca^{2+}$ (mmol/L) |
|---|---|---|---|---|---|---|---|
| 1-5 | 7.60 | 4.33 | 33.9 | 554.4 | 20.48 | 52.59 | ** |
| 3-3 | 7.43 | 5.59 | 34.3 | 561.03 | 19.82 | 46.99 | ** |
| 4-3 | 7.26 | 5.84 | 34.0 | 560.05 | 20.69 | 49.15 | ** |
| 6-5 | 7.48 | 6.72 | 34.1 | 557.5 | 17.52 | 52.81 | ** |
| 16-5 | 7.31 | 7.27 | 33.9 | 557.5 | 17.37 | 56.04 | ** |
| 21-5 | 7.43 | 7.19 | 33.8 | 557.5 | 16.96 | 54.53 | ** |

**No data are available from this site for calcium because of problems with instruments.

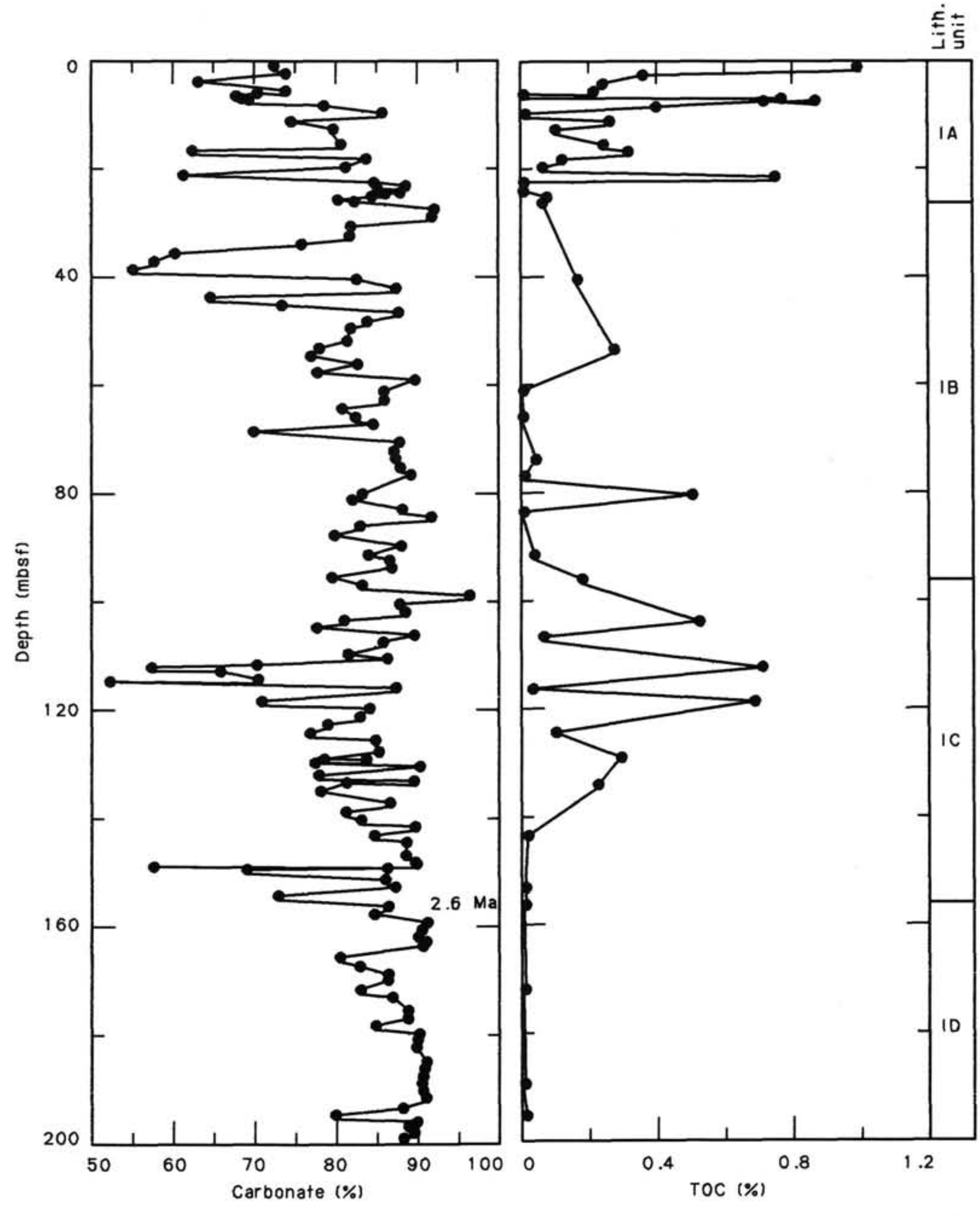


Figure 10. Carbonate and total-organic-carbon (TOC) records from Site 662, Hole 662A.

tively constant, high-carbonate contents that vary from 80% to 90%; cyclic variations appear weaker in Subunit ID.

TOC values fluctuate between 0.0% and 1.0% in the upper part of the sequence, corresponding to Subunits IA through IC (see "Lithostratigraphy and Sedimentology" section, this chapter). Subunit ID, however, appears to be characterized by very low or zero TOC contents (0.0% to 0.04%; Fig. 10), although more samples should be analyzed to confirm this pattern.

### Discussion

Sediments at Site 662 display highly variable, but generally rather low, TOC contents that range from 0.0% to 1.0%. Subunit ID contains little or no organic carbon. The highest values lie within Subunits IA and IC. These values generally correlate with levels containing high proportions of biogenic-siliceous debris (see "Lithostratigraphy and Sedimentology" section, this chapter) and relatively low-carbonate content (Fig. 10). Thus, all evidence suggests that surface productivity was low before approximately 2.65 Ma and that after this time, productivity fluctuated.

## PHYSICAL PROPERTIES

Techniques used for shipboard physical-properties measurements at Site 662 are outlined in the "Introduction and Explanatory Notes" chapter (this volume). Index-properties and vane-shear-strength measurements were conducted on cores from Holes 662A and 662B. Continuous *P*-wave-velocity records also were obtained from these holes. Tables 5 and 6 show index-properties and vane-shear-strength data for Holes 662A and 662B, respectively. Table 7 gives a synthesis of *P*-wave-logger velocity data for Hole 662A. Most data for Hole 662A are presented graphically in Figures 11 through 17 (the calcium carbonate profile is shown in Figure 15 for comparison with the other properties). No data presented in this summary were screened for bad data points. All whole-core sections were logged continuously using the GRAPE.

Site 662 had a high calcium carbonate content throughout the cored interval (200 mbsf), as illustrated in Figure 15. Most of the sediments had a carbonate content of 80% to 90%, with some low values of about 60%. Wet- and dry-bulk densities (Fig. 11) correlate positively with the carbonate content (Fig. 15).

Vane shear strength also correlates positively with the carbonate content (Fig. 16). This illustrates that the vane-shear-strength test probably becomes progressively less valid as the carbonate contents increase, which in turn suggests that permeability increases as carbonate content increases. Hence, it is likely that mean grain size also increases with increasing carbonate content.

A synthesis profile of *P*-wave-logger velocity data (Fig. 17) shows only a slight velocity gradient over the 200 m cored. The average velocity is about 1.53 km/s, with velocity spikes of up to 1.65 km/s that occur in the coarser turbidite or winnowed lithologies.

An experiment was performed on Core 662B-12H to investigate the repeatability of the *P*-wave logs, the physical heterogeneity of the cores, and their shock sensitivity. Results of this experiment are illustrated in Figure 18. Profile 1 is a normal log obtained with the double line on the liner facing upward. Profile 2 is a repeat log of the same core, except that the double line faces horizontally (i.e., at 90° to profile 1). These two profiles illustrate that much of the higher frequency fluctuations are not common to both profiles. However, these fluctuations are not caused by instrument noise, as demonstrated by profiles 3 and 4. We concluded, therefore, that these higher frequency fluctuations result from a "physical noise" within the sediments. The small-scale changes in velocity, which manifest themselves as this physical noise, must be caused by local density fluctuations. Profiles 1 and 2 are different because the *P*-wave logger effectively "looks" at only a thin section through the core; this section can vary, depending on orientation of the core. It probably would be useful in highly calcareous sediments to obtain an average whole-core velocity. Spinning the core along its axis should produce this effect. A profile similar to *A* (Fig. 18) should result; *A* is an "eye-ball" estimate of the common mode present in profiles 1 and 2.

To investigate the velocity sensitivity to rough handling of high-carbonate cores, Section 108-662A-4H was subjected to a significant shock after profile 4 had been run. A significant acceleration was produced (possibly as much as 5 G) when the section collided horizontally with the deck. This impact is not dissimilar to that suffered by the core when opened after splitting (depending on the marine technician on duty and other factors). A computer-based, risk-analysis model had shown that the chance of accidentally splitting the liner and remolding its sediments on deck immediately after impact was significant. Nevertheless, we felt that this risk was acceptable. The velocity profile recorded after impact is shown as trace 5 (Fig. 18). Our semi-controlled test then was repeated (the estimated acceleration for this second impact was 7.5 G), and the velocity profile recorded (profile 6, Fig. 18). These geotechnical impact tests illustrate a slight sensitivity of high-carbonate cores to rough handling (the sharp peak in the velocity profile broadens after impact, indicating some dilation and grain mobilization), but the overall nature of the signature remains the same. It might be instructive for the global physical-properties community if this experiment were repeated on a clay-rich section (assuming that the risk-analysis model can be refined sufficiently to make chances of disaster much less).

## SEISMIC STRATIGRAPHY

The water-gun seismic-profiler records obtained during our approach to Site 662 have four seismic units within the 0.267 s of two-way traveltime roughly equivalent to the interval cored at that site. These four units (Fig. 19) are described as follows:

Seismic unit 1: 0–0.05 s, an upper unit with a false acoustic signal caused by the water guns. This unit should equate to approximately the upper 38 m of sediment.

Seismic unit 2: 0.05–0.08 s, an irregular, finely laminated unit with a wavelike pattern that occasionally rises into the overlying unit and may be masked by an artificial acoustic overprint. This unit should equate to an interval of about 38 to 61 m in the sediment section.

Seismic unit 3: 0.08–0.13 s, a more transparent unit with faint acoustic returns between 0.08 and 0.10 s, but with near-transparency below this interval. This unit should equate to an interval of about 61 to 97 m in the sediment section.

Seismic unit 4: 0.13–0.32 s, a unit of evenly spaced, moderately reflective layering that shows some relief laterally. The top of this unit should equate to a depth of about 97 m in the sediment section, with its bottom lying below the cored interval.

We used a mean sound velocity of 760 m/s for the entire sediment section at Site 662 (see "Physical Properties" section, this chapter) to evaluate correlations of both seismic and lithologic units (Fig. 19). Seismic unit 1 is an artifact. Seismic units 2 and 3 are equivalent in depth to the mid-Pleistocene interval of slumps and turbidites (lithologic Subunit IB), perhaps indicating partial destruction of the acoustic layering by slump deformation. The top of Seismic unit 4 corresponds to the late Pliocene to mid-Pleistocene interval of normal pelagic deposition (lithologic Subunit IC), with the acoustic layering apparently returning because of the absence of deformation.

**Table 5. Index-properties and vane-shear-strength data for Hole 662A.**

| Core/ section | Interval (cm) | Depth (mbsf) | Grain density ($g/cm^3$) | Wet-water content (%) | Dry-water content (%) | Wet-bulk density ($g/cm^3$) | Dry-bulk density ($g/cm^3$) | Porosity (%) | Vane shear strength (kPa) |
|---|---|---|---|---|---|---|---|---|---|
| 108-662A-1H-1 | 121 | 1.21 | 2.47 | 68.78 | 220.26 | 1.25 | 0.42 | 84.47 | 2.60 |
| 108-662A-1H-2 | 111 | 2.61 | 2.43 | 60.87 | 155.55 | 1.32 | 0.56 | 78.98 | 4.80 |
| 108-662A-2H-1 | 121 | 4.10 | 2.41 | 62.74 | 168.40 | 1.30 | 0.52 | 80.19 | 5.60 |
| 108-662A-2H-2 | 121 | 5.60 | 2.58 | 58.60 | 141.52 | 1.36 | 0.59 | 78.39 | 7.00 |
| 108-662A-2H-3 | 121 | 7.10 | 2.59 | 65.43 | 189.26 | 1.29 | 0.48 | 83.02 | 6.60 |
| 108-662A-2H-4 | 121 | 8.60 | 2.53 | 55.77 | 126.10 | 1.39 | 0.64 | 76.01 | 9.00 |
| 108-662A-2H-5 | 121 | 10.10 | 2.62 | 49.64 | 98.56 | 1.47 | 0.79 | 71.89 | 11.40 |
| 108-662A-2H-6 | 121 | 11.60 | 2.06 | 64.54 | 182.00 | 1.24 | 0.48 | 78.98 | 10.80 |
| 108-662A-3H-1 | 26 | 12.96 | 2.48 | 54.54 | 120.00 | 1.39 | 0.67 | 74.68 | 15.00 |
| 108-662A-3H-2 | 149 | 15.69 | 2.36 | 52.24 | 109.38 | 1.40 | 0.69 | 71.90 | 15.00 |
| 108-662A-3H-3 | 120 | 16.90 | 2.39 | 63.04 | 170.56 | 1.29 | 0.52 | 80.26 | 13.00 |
| 108-662A-3H-4 | 121 | 18.41 | 2.58 | 52.50 | 110.51 | 1.43 | 0.72 | 73.89 | 20.00 |
| 108-662A-3H-5 | 111 | 19.81 | 2.58 | 54.09 | 117.81 | 1.41 | 0.70 | 75.06 | 16.00 |
| 108-662A-3H-6 | 121 | 21.41 | 2.64 | 63.94 | 177.35 | 1.31 | 0.51 | 82.36 | 18.00 |
| 108-662A-4H-1 | 121 | 23.41 | 2.57 | 46.06 | 85.39 | 1.51 | 0.86 | 68.49 | 26.00 |
| 108-662A-4H-2 | 39 | 23.95 | 2.75 | 47.44 | 90.24 | 1.52 | 0.84 | 71.04 | 21.00 |
| 108-662A-4H-2 | 99 | 24.55 | 2.50 | 47.22 | 89.46 | 1.48 | 0.81 | 68.90 | 20.00 |
| 108-662A-4H-2 | 121 | 24.77 | 2.55 | 47.58 | 90.77 | 1.49 | 0.81 | 69.60 | 24.00 |
| 108-662A-4H-3 | 99 | 26.05 | 2.53 | 53.62 | 115.59 | 1.41 | 0.69 | 74.34 | 13.00 |
| 108-662A-4H-4 | 121 | 27.77 | 2.51 | 53.33 | 114.29 | 1.41 | 1.31 | 74.00 | 0.00 |
| 108-662A-4H-5 | 121 | 29.27 | 2.69 | 51.93 | 108.03 | 1.45 | 0.73 | 74.20 | 0.00 |
| 108-662A-4H-6 | 121 | 30.77 | 2.31 | 48.01 | 92.33 | 1.44 | 0.44 | 67.94 | 31.00 |
| 108-662A-5H-1 | 122 | 32.92 | 2.55 | 51.33 | 105.49 | 1.44 | 0.74 | 72.76 | 30.00 |
| 108-662A-5H-2 | 121 | 34.38 | 2.29 | 53.54 | 115.23 | 1.37 | 0.68 | 72.40 | 38.00 |
| 108-662A-5H-3 | 121 | 35.88 | 2.47 | 55.92 | 126.88 | 1.38 | 0.64 | 75.67 | 40.00 |
| 108-662A-5H-4 | 121 | 37.38 | 2.43 | 57.60 | 135.82 | 1.35 | 0.61 | 76.64 | 29.00 |
| 108-662A-5H-5 | 121 | 38.88 | 2.67 | 59.26 | 145.49 | 1.36 | 0.59 | 79.41 | 28.00 |
| 108-662A-5H-6 | 121 | 40.38 | 2.52 | 48.34 | 93.58 | 1.47 | 0.80 | 70.01 | 31.00 |
| 108-662A-6H-1 | 121 | 42.41 | 2.67 | 47.09 | 88.99 | 1.51 | 0.83 | 70.13 | 28.00 |
| 108-662A-6H-2 | 121 | 43.91 | 2.49 | 55.63 | 125.36 | 1.38 | 0.64 | 75.61 | 30.00 |
| 108-662A-6H-3 | 121 | 45.41 | 2.68 | 51.50 | 106.17 | 1.46 | 0.75 | 73.83 | 31.00 |
| 108-662A-6H-4 | 121 | 46.91 | 2.55 | 42.82 | 74.89 | 1.55 | 0.92 | 65.39 | 40.00 |
| 108-662A-6H-5 | 121 | 48.41 | 2.65 | 45.97 | 85.07 | 1.53 | 0.86 | 69.01 | 37.00 |
| 108-662A-6H-6 | 121 | 49.91 | 2.48 | 48.42 | 93.86 | 1.46 | 0.80 | 69.74 | 38.00 |
| 108-662A-7H-1 | 121 | 51.91 | 2.50 | 50.57 | 102.31 | 1.44 | 0.75 | 71.72 | 32.00 |
| 108-662A-7H-2 | 121 | 53.41 | 2.58 | 49.32 | 97.30 | 1.47 | 0.77 | 71.35 | 40.00 |
| 108-662A-7H-3 | 121 | 54.91 | 2.62 | 50.33 | 101.32 | 1.46 | 0.76 | 72.47 | 37.00 |
| 108-662A-7H-4 | 121 | 56.41 | 2.75 | 46.08 | 85.46 | 1.54 | 0.86 | 69.93 | 40.00 |
| 108-662A-7H-5 | 121 | 57.91 | 2.53 | 46.43 | 86.66 | 1.50 | 0.83 | 68.47 | 39.00 |
| 108-662A-7H-6 | 121 | 59.41 | 2.62 | 42.18 | 72.94 | 1.58 | 0.94 | 65.38 | 39.00 |
| 108-662A-8H-1 | 121 | 61.41 | 2.46 | 43.86 | 78.13 | 1.52 | 0.91 | 65.57 | 50.00 |
| 108-662A-8H-2 | 121 | 62.71 | 2.67 | 46.21 | 85.91 | 1.53 | 0.86 | 69.42 | 40.00 |
| 108-662A-8H-3 | 121 | 64.21 | 2.52 | 45.62 | 83.88 | 1.51 | 0.86 | 67.63 | 54.00 |
| 108-662A-8H-4 | 121 | 65.71 | 2.59 | 44.22 | 79.28 | 1.54 | 0.91 | 66.98 | 56.00 |
| 108-662A-8H-5 | 121 | 67.21 | 2.58 | 45.90 | 84.84 | 1.52 | 0.86 | 68.46 | 49.00 |
| 108-662A-8H-6 | 121 | 68.71 | 2.52 | 49.75 | 99.01 | 1.46 | 0.77 | 71.20 | 51.00 |
| 108-662A-9H-1 | 121 | 70.91 | 2.54 | 47.33 | 89.86 | 1.49 | 0.83 | 69.29 | 23.00 |
| 108-662A-9H-2 | 121 | 72.40 | 2.43 | 48.38 | 93.74 | 1.46 | 0.80 | 69.29 | 19.00 |
| 108-662A-9H-3 | 121 | 73.90 | 2.55 | 46.98 | 88.61 | 1.50 | 0.84 | 69.13 | 24.00 |
| 108-662A-9H-4 | 121 | 75.40 | 2.42 | 47.21 | 89.43 | 1.47 | 0.84 | 68.18 | 24.00 |
| 108-662A-9H-5 | 121 | 76.90 | 2.59 | 47.07 | 88.94 | 1.50 | 0.84 | 69.55 | 25.00 |
| 108-662A-10H-1 | 121 | 80.41 | 2.56 | 47.78 | 91.50 | 1.49 | 0.81 | 69.84 | 31.00 |
| 108-662A-10H-2 | 65 | 81.35 | 2.46 | 47.13 | 89.15 | 1.48 | 0.82 | 68.51 | 51.00 |
| 108-662A-10H-2 | 121 | 81.91 | 2.54 | 45.57 | 83.71 | 1.51 | 0.87 | 67.79 | 52.00 |
| 108-662A-10H-3 | 121 | 83.41 | 2.56 | 44.50 | 80.18 | 1.53 | 0.89 | 66.96 | 49.00 |
| 108-662A-10H-4 | 121 | 84.91 | 2.53 | 43.50 | 76.98 | 1.54 | 0.93 | 65.87 | 45.00 |
| 108-662A-10H-5 | 121 | 86.41 | 2.55 | 42.58 | 74.15 | 1.56 | 0.93 | 65.20 | 66.00 |
| 108-662A-10H-6 | 143 | 87.98 | 2.52 | 44.50 | 80.20 | 1.52 | 0.88 | 66.69 | 46.00 |
| 108-662A-11H-1 | 121 | 89.91 | 2.53 | 41.88 | 72.07 | 1.56 | 0.95 | 64.36 | 53.00 |
| 108-662A-11H-2 | 121 | 91.41 | 2.53 | 43.44 | 76.90 | 1.54 | 0.91 | 65.74 | 51.00 |
| 108-662A-11H-3 | 121 | 92.91 | 2.50 | 41.05 | 69.62 | 1.57 | 0.98 | 63.23 | 54.00 |
| 108-662A-11H-4 | 121 | 94.41 | 2.60 | 42.30 | 73.30 | 1.57 | 0.95 | 65.30 | 52.00 |
| 108-662A-11H-5 | 121 | 95.91 | 2.44 | 45.89 | 84.81 | 1.49 | 0.87 | 67.20 | 58.00 |
| 108-662A-11H-6 | 121 | 97.41 | 2.49 | 38.27 | 62.00 | 1.61 | 1.04 | 60.44 | 94.00 |
| 108-662A-12H-1 | 121 | 99.41 | 2.55 | 39.02 | 64.00 | 1.61 | 1.03 | 61.73 | 32.00 |
| 108-662A-12H-2 | 121 | 100.91 | 2.58 | 48.71 | 94.98 | 1.48 | 0.79 | 70.83 | 15.00 |
| 108-662A-12H-3 | 121 | 102.41 | 2.60 | 46.28 | 86.16 | 1.51 | 0.87 | 68.93 | 25.00 |
| 108-662A-12H-4 | 121 | 103.91 | 2.50 | 47.47 | 90.38 | 1.48 | 0.82 | 69.12 | 30.00 |
| 108-662A-12H-5 | 121 | 105.41 | 2.44 | 49.86 | 99.44 | 1.44 | 0.78 | 70.66 | 29.00 |
| 108-662A-12H-6 | 121 | 106.91 | 2.64 | 42.66 | 74.41 | 1.57 | 0.95 | 65.98 | 26.00 |
| 108-662A-13H-1 | 121 | 108.91 | 2.44 | 47.27 | 89.65 | 1.47 | 0.82 | 68.44 | 24.00 |
| 108-662A-13H-2 | 121 | 110.41 | 2.43 | 48.96 | 95.93 | 1.45 | 1.07 | 69.78 | 24.00 |
| 108-662A-13H-3 | 121 | 111.91 | 2.43 | 49.80 | 99.21 | 1.44 | 0.76 | 70.48 | 50.00 |
| 108-662A-13H-4 | 121 | 113.41 | 2.48 | 49.67 | 98.69 | 1.45 | 0.64 | 70.80 | 68.00 |
| 108-662A-13H-5 | 121 | 114.91 | 2.52 | 52.00 | 108.34 | 1.43 | 0.64 | 73.06 | 68.00 |
| 108-662A-13H-6 | 121 | 116.41 | 2.54 | 45.27 | 82.70 | 1.52 | 0.88 | 67.52 | 32.00 |

**Table 5 (continued).**

| Core/ section | Interval (cm) | Depth (mbsf) | Grain density (g/cm³) | Wet-water content (%) | Dry-water content (%) | Wet-bulk density (g/cm³) | Dry-bulk density (g/cm³) | Porosity (%) | Vane shear strength (kPa) |
|---|---|---|---|---|---|---|---|---|---|
| 108-662A-14H-1 | 121 | 118.41 | 2.56 | 52.08 | 108.67 | 1.43 | 0.73 | 73.43 | 47.00 |
| 108-662A-14H-2 | 121 | 119.91 | 2.59 | 43.91 | 78.29 | 1.54 | 0.91 | 66.71 | 33.00 |
| 108-662A-14H-3 | 121 | 121.41 | 2.59 | 44.76 | 81.02 | 1.53 | 0.90 | 67.50 | 49.00 |
| 108-662A-14H-4 | 121 | 122.91 | 2.54 | 44.71 | 80.88 | 1.52 | 0.88 | 67.01 | 38.00 |
| 108-662A-14H-5 | 121 | 124.41 | 2.44 | 44.76 | 81.03 | 1.50 | 0.89 | 66.16 | 40.00 |
| 108-662A-14H-6 | 121 | 125.91 | 2.59 | 41.88 | 72.05 | 1.57 | 0.96 | 64.84 | 45.00 |
| 108-662A-15H-1 | 121 | 127.89 | 2.60 | 43.92 | 78.30 | 1.55 | 0.90 | 66.82 | 31.00 |
| 108-662A-15H-2 | 121 | 129.39 | 2.43 | 42.58 | 74.16 | 1.53 | 0.94 | 64.07 | 30.00 |
| 108-662A-15H-3 | 121 | 130.89 | 2.60 | 41.04 | 69.60 | 1.59 | 0.98 | 64.14 | 31.00 |
| 108-662A-15H-4 | 121 | 132.39 | 2.69 | 43.88 | 78.19 | 1.57 | 0.96 | 67.57 | 44.00 |
| 108-662A-15H-5 | 121 | 133.89 | 2.69 | 42.74 | 74.65 | 1.58 | 0.95 | 66.52 | 41.00 |
| 108-662A-15H-6 | 121 | 135.39 | 2.12 | 48.86 | 95.53 | 1.39 | 0.76 | 66.74 | 58.00 |
| 108-662A-16H-1 | 121 | 137.41 | 2.57 | 41.29 | 70.34 | 1.58 | 0.98 | 64.13 | 45.00 |
| 108-662A-16H-2 | 121 | 138.85 | 2.53 | 43.64 | 77.42 | 1.54 | 0.94 | 65.94 | 48.00 |
| 108-662A-16H-3 | 121 | 140.35 | 2.53 | 39.23 | 64.55 | 1.60 | 1.02 | 61.71 | 35.00 |
| 108-662A-16H-4 | 121 | 141.85 | 2.49 | 40.13 | 67.02 | 1.58 | 1.00 | 62.22 | 41.00 |
| 108-662A-16H-5 | 121 | 143.35 | 2.41 | 42.52 | 73.98 | 1.53 | 0.92 | 63.86 | 51.00 |
| 108-662A-17H-1 | 121 | 146.91 | 2.56 | 40.76 | 68.81 | 1.58 | 1.01 | 63.52 | 41.00 |
| 108-662A-17H-2 | 121 | 148.41 | 2.54 | 41.48 | 70.87 | 1.57 | 0.98 | 64.02 | 33.00 |
| 108-662A-17H-3 | 82 | 149.52 | 2.42 | 44.89 | 81.44 | 1.50 | 0.88 | 66.13 | 78.00 |
| 108-662A-17H-4 | 121 | 151.41 | 2.53 | 39.76 | 65.99 | 1.59 | 1.01 | 62.27 | 56.00 |
| 108-662A-17H-5 | 121 | 152.91 | 2.45 | 41.95 | 72.26 | 1.54 | 0.95 | 63.66 | 51.00 |
| 108-662A-17H-6 | 121 | 154.41 | 2.46 | 42.65 | 74.36 | 1.53 | 0.94 | 64.38 | 60.00 |
| 108-662A-18H-1 | 121 | 156.41 | 2.43 | 44.65 | 80.67 | 1.50 | 0.90 | 66.00 | 27.00 |
| 108-662A-18H-2 | 121 | 157.91 | 2.52 | 41.62 | 71.30 | 1.56 | 0.95 | 63.97 | 32.00 |
| 108-662A-18H-3 | 121 | 159.36 | 2.46 | 42.46 | 73.80 | 1.54 | 0.93 | 64.20 | 20.00 |
| 108-662A-18H-4 | 121 | 160.86 | 2.63 | 39.03 | 64.02 | 1.63 | 1.05 | 62.44 | 30.00 |
| 108-662A-18H-5 | 121 | 162.36 | 2.50 | 41.15 | 69.92 | 1.57 | 0.95 | 63.36 | 25.00 |
| 108-662A-18H-6 | 121 | 163.86 | 2.47 | 41.81 | 71.85 | 1.55 | 0.96 | 63.68 | 25.00 |
| 108-662A-19H-1 | 121 | 165.76 | 2.71 | 42.02 | 72.48 | 1.60 | 0.97 | 66.04 | 39.00 |
| 108-662A-19H-2 | 121 | 167.26 | 2.58 | 42.81 | 74.85 | 1.56 | 0.93 | 65.60 | 55.00 |
| 108-662A-19H-3 | 121 | 168.76 | 2.73 | 40.22 | 67.29 | 1.63 | 1.01 | 64.44 | 57.00 |
| 108-662A-19H-5 | 114 | 170.15 | 2.73 | 40.73 | 68.72 | 1.62 | 1.01 | 64.96 | 72.00 |
| 108-662A-19H-6 | 125 | 171.76 | 2.50 | 42.64 | 74.35 | 1.54 | 0.92 | 64.77 | 48.00 |
| 108-662A-20H-1 | 121 | 175.41 | 2.58 | 44.97 | 81.73 | 1.53 | 0.98 | 67.60 | 43.00 |
| 108-662A-20H-2 | 121 | 176.88 | 2.55 | 42.71 | 74.55 | 1.55 | 0.94 | 65.24 | 44.00 |
| 108-662A-20H-3 | 121 | 178.38 | 2.57 | 42.25 | 73.16 | 1.57 | 0.95 | 65.06 | 53.00 |
| 108-662A-20H-4 | 121 | 179.88 | 2.58 | 41.36 | 70.54 | 1.58 | 0.97 | 64.31 | 53.00 |
| 108-662A-20H-5 | 111 | 181.28 | 2.62 | 40.37 | 67.70 | 1.60 | 1.03 | 63.63 | 53.00 |
| 108-662A-20H-6 | 121 | 182.88 | 2.57 | 41.36 | 70.53 | 1.58 | 0.96 | 64.17 | 44.00 |
| 108-662A-21H-1 | 121 | 184.91 | 2.48 | 41.26 | 70.24 | 1.56 | 0.97 | 63.24 | 32.00 |
| 108-662A-21H-2 | 121 | 186.41 | 2.59 | 42.35 | 73.45 | 1.57 | 0.96 | 65.25 | 33.00 |
| 108-662A-21H-3 | 121 | 187.91 | 2.64 | 40.27 | 67.41 | 1.61 | 1.01 | 63.78 | 38.00 |
| 108-662A-21H-4 | 121 | 189.41 | 2.65 | 41.51 | 70.98 | 1.59 | 0.99 | 65.02 | 39.00 |
| 108-662A-21H-5 | 121 | 190.91 | 2.59 | 40.49 | 68.04 | 1.60 | 0.99 | 63.51 | 49.00 |
| 108-662A-21H-6 | 111 | 192.31 | 2.50 | 43.45 | 76.85 | 1.53 | 0.91 | 65.55 | 34.00 |
| 108-662A-22H-1 | 121 | 194.41 | 2.62 | 43.02 | 75.49 | 1.56 | 0.93 | 66.14 | 20.00 |
| 108-662A-22H-2 | 121 | 195.91 | 2.55 | 39.97 | 66.58 | 1.60 | 1.00 | 62.71 | 72.00 |

## COMPOSITE-DEPTH SECTION

Several difficulties were encountered when making between-hole correlations at Site 662. The magnetic-susceptibility measurements revealed no measurable signal. The *P*-wave logs were reliable only for small parts of the section. In addition, numerous slumps and other disturbances in the depth range of approximately 26 to 100 mbsf made correlations impossible. Nevertheless, we were able to use the strong $CaCO_3$-induced color layering visible in our core photographs to correlate between the holes and to create a composite-depth section within two depth intervals.

Table 8 shows the correlation levels we used as a pathway to produce a continuous composite-depth section between the two holes. This composite-depth section was chosen so as to use Hole 662B only for short sequences to fill core-break gaps in Hole 662A. Figure 20 shows the general configuration of slumps and pelagic sediments, including a line representing the extrapolated age-depth curve, defined at the top and bottom of the sediment section (see "Sediment-Accumulation Rates" section, this chapter).

The first interval spanned the top several cores in the pelagic interval at each hole (Fig. 20), which we correlated as shown in Table 8. This produced a composite-depth section 21.5 m long that represents the last 500,000 yr of the Pleistocene.

Because of slumps and turbidites encountered in Hole 662A, we recovered only a few cores in Hole 662B within the range of 26 to 100 mbsf, coring only at levels of relatively little disturbance. This generally precludes assembling a composite-depth section in this interval. Core 108-662B-4H (64.7–74.2 mbsf) was positioned to bridge the gap between Cores 108-662A-8H and -662A-9H in the undeformed interval from 63 to 80 mbsf (Fig. 20). However, we were not able to correlate these cores based solely on photographs.

We did see a correlation of Core 108-662A-12H with Core -662B-5H as both contained the base of the slumped section. The next interval for which overlapped coring in the two holes allowed us to create a continuous composite-depth section began with Cores 108-662A-14H and -662B-6H (Table 8). We used the ODP depth of 117.35 mbsf for the top of Core 108-662A-14H as a reference point to begin the next composite-depth section.

**Table 6. Index-properties and vane-shear-strength data for Hole 662B.**

| Core/ section | Interval (cm) | Depth (mbsf) | Wet-water content (%) | Dry-water content (%) | Porosity (%) | Wet-bulk density (g/cm³) | Dry-bulk density (g/cm³) | Vane shear strength (kPa) |
|---|---|---|---|---|---|---|---|---|
| 108-662B-1H-1 | 121 | 1.21 | 60.78 | 154.97 | 79.18 | 1.36 | 0.55 | 6.00 |
| 108-662B-1H-2 | 121 | 2.71 | 62.30 | 165.28 | 80.16 | 1.35 | 0.53 | 6.00 |
| 108-662B-1H-3 | 121 | 4.21 | 53.15 | 113.46 | 73.84 | 1.45 | 0.69 | 12.00 |
| 108-662B-1H-4 | 121 | 5.71 | 64.77 | 183.82 | 81.71 | 1.32 | 0.48 | 7.50 |
| 108-662B-1H-5 | 121 | 7.21 | 62.73 | 168.33 | 80.44 | 1.34 | 0.52 | 12.00 |
| 108-662B-1H-6 | 121 | 8.71 | 61.50 | 159.72 | 79.64 | 1.36 | 0.54 | 11.00 |
| 108-662B-2H-1 | 121 | 10.71 | 63.13 | 171.24 | 80.69 | 1.34 | 0.51 | 10.00 |
| 108-662B-2H-2 | 121 | 12.16 | 54.61 | 120.33 | 74.92 | 1.43 | 0.66 | 14.00 |
| 108-662B-2H-3 | 121 | 13.66 | 60.60 | 153.80 | 79.06 | 1.37 | 0.55 | 10.00 |
| 108-662B-2H-4 | 121 | 15.16 | 52.86 | 112.16 | 73.62 | 1.45 | 0.70 | 16.00 |
| 108-662B-2H-5 | 116 | 16.61 | 57.45 | 135.03 | 76.93 | 1.40 | 0.61 | 14.00 |
| 108-662B-2H-6 | 121 | 18.16 | 52.71 | 111.47 | 73.51 | 1.46 | 0.70 | 14.00 |
| 108-662B-3H-1 | 121 | 37.41 | 48.39 | 93.76 | 70.13 | 1.51 | 0.79 | 32.00 |
| 108-662B-3H-2 | 121 | 38.77 | 46.45 | 86.74 | 68.53 | 1.54 | 0.83 | 37.00 |
| 108-662B-3H-3 | 121 | 40.27 | 47.04 | 88.82 | 69.02 | 1.53 | 0.82 | 39.00 |
| 108-662B-3H-4 | 111 | 41.67 | 50.45 | 101.83 | 71.78 | 1.48 | 0.75 | 36.00 |
| 108-662B-3H-5 | 121 | 43.27 | 51.02 | 104.15 | 72.22 | 1.48 | 0.74 | 37.00 |
| 108-662B-3H-6 | 121 | 44.77 | 44.33 | 79.63 | 66.71 | 1.57 | 0.88 | 38.00 |
| 108-662B-5H-3 | 121 | 97.36 | 46.63 | 87.38 | 68.68 | 1.53 | 0.83 | 72.00 |
| 108-662B-5H-4 | 121 | 98.86 | 38.64 | 62.97 | 61.44 | 1.65 | 1.02 | 85.00 |
| 108-662B-5H-6 | 121 | 101.86 | 45.49 | 83.46 | 67.72 | 1.55 | 0.86 | 36.00 |
| 108-662B-6H-2 | 121 | 124.41 | 45.10 | 82.14 | 67.38 | 1.56 | 0.86 | 35.00 |
| 108-662B-6H-3 | 121 | 125.91 | 41.15 | 69.91 | 63.84 | 1.61 | 0.96 | 48.00 |
| 108-662B-7H-1 | 121 | 132.41 | 39.84 | 66.22 | 62.60 | 1.63 | 0.99 | 36.00 |
| 108-662B-7H-2 | 121 | 133.87 | 45.14 | 82.29 | 67.42 | 1.55 | 0.86 | 50.00 |
| 108-662B-7H-3 | 121 | 135.37 | 44.04 | 78.69 | 66.45 | 1.57 | 0.89 | 96.00 |
| 108-662B-7H-4 | 121 | 136.87 | 43.70 | 77.62 | 66.15 | 1.57 | 0.90 | 62.00 |
| 108-662B-7H-5 | 121 | 138.37 | 39.10 | 64.21 | 61.89 | 1.64 | 1.01 | 42.00 |
| 108-662B-7H-6 | 121 | 139.87 | 40.41 | 67.82 | 63.15 | 1.62 | 0.98 | 72.00 |
| 108-662B-8H-1 | 121 | 141.91 | 39.09 | 64.18 | 61.88 | 1.64 | 1.01 | 32.00 |
| 108-662B-8H-2 | 121 | 143.41 | 40.37 | 67.71 | 63.11 | 1.62 | 0.98 | 22.00 |
| 108-662B-8H-3 | 121 | 144.91 | 44.06 | 78.77 | 66.48 | 1.57 | 0.89 | 36.00 |
| 108-662B-8H-4 | 121 | 146.39 | 42.71 | 74.56 | 65.27 | 1.59 | 0.92 | 36.00 |
| 108-662B-8H-5 | 121 | 147.89 | 43.91 | 78.27 | 66.34 | 1.57 | 0.89 | 63.00 |
| 108-662B-8H-6 | 121 | 149.39 | 44.12 | 78.94 | 66.52 | 1.57 | 0.89 | 28.00 |
| 108-662B-9H-1 | 121 | 151.41 | 41.20 | 70.07 | 63.89 | 1.61 | 0.96 | 32.00 |
| 108-662B-9H-2 | 121 | 152.86 | 41.82 | 71.89 | 64.46 | 1.60 | 0.94 | 43.00 |
| 108-662B-9H-3 | 121 | 154.36 | 41.67 | 71.43 | 64.32 | 1.60 | 0.95 | 29.00 |
| 108-662B-9H-4 | 121 | 155.86 | 42.90 | 75.13 | 65.44 | 1.59 | 0.92 | 34.00 |
| 108-662B-9H-5 | 121 | 157.36 | 42.61 | 74.25 | 65.18 | 1.59 | 0.92 | 36.00 |
| 108-662B-9H-6 | 121 | 158.83 | 42.13 | 72.81 | 64.75 | 1.60 | 0.93 | 29.00 |
| 108-662B-10H-1 | 121 | 160.91 | 38.54 | 62.70 | 61.35 | 1.65 | 1.02 | 44.00 |
| 108-662B-10H-2 | 121 | 162.41 | 41.77 | 71.74 | 64.42 | 1.60 | 0.94 | 43.00 |
| 108-662B-10H-3 | 121 | 163.91 | 40.80 | 68.93 | 63.52 | 1.62 | 0.97 | 43.00 |
| 108-662B-10H-4 | 121 | 165.41 | 41.23 | 70.14 | 63.91 | 1.61 | 0.96 | 46.00 |
| 108-662B-10H-5 | 121 | 166.91 | 39.56 | 65.45 | 62.34 | 1.64 | 1.00 | 49.00 |
| 108-662B-10H-6 | 121 | 168.41 | 39.73 | 65.91 | 62.50 | 1.63 | 0.99 | 57.00 |
| 108-662B-11H-1 | 121 | 170.41 | 40.62 | 68.39 | 63.34 | 1.62 | 0.97 | 42.00 |
| 108-662B-11H-2 | 121 | 171.91 | 41.70 | 71.53 | 64.35 | 1.60 | 0.94 | 45.00 |
| 108-662B-11H-3 | 121 | 173.41 | 41.85 | 71.98 | 64.49 | 1.60 | 0.94 | 43.00 |
| 108-662B-11H-4 | 121 | 174.91 | 42.15 | 72.87 | 64.76 | 1.60 | 0.93 | 44.00 |
| 108-662B-11H-5 | 121 | 176.41 | 42.75 | 74.67 | 65.30 | 1.59 | 0.92 | 53.00 |
| 108-662B-11H-6 | 121 | 177.91 | 42.59 | 74.18 | 65.16 | 1.59 | 0.92 | 48.00 |
| 108-662B-12H-1 | 121 | 180.01 | 40.52 | 68.13 | 63.25 | 1.62 | 0.97 | 37.00 |
| 108-662B-12H-2 | 121 | 181.51 | 41.07 | 69.69 | 63.76 | 1.61 | 0.96 | 38.00 |
| 108-662B-12H-3 | 121 | 183.01 | 41.60 | 71.22 | 64.25 | 1.61 | 0.95 | 53.00 |
| 108-662B-12H-4 | 121 | 184.51 | 40.25 | 67.36 | 62.99 | 1.63 | 0.98 | 40.00 |
| 108-662B-12H-5 | 121 | 186.01 | 40.80 | 68.91 | 63.51 | 1.62 | 0.97 | 41.00 |
| 108-662B-12H-6 | 121 | 187.51 | 41.12 | 69.84 | 63.81 | 1.61 | 0.96 | 30.00 |

From this point, we were able to correlate unambiguously down to the base of Core 108-662B-12H, at a composite depth of 184.73 mbsf. This 67.38-m section represents an interval of time from approximately 1.3 to 3.3 Ma. Thus, the only time interval for which we could not assemble a composite-depth section was that between 0.5 and 1.3 Ma.

Correlations between the two holes generally indicate a loss of sediment across core breaks. The amount lost ranges from 0 to 150 cm, averaging about 50 cm. At the mean depositional rate for this part of the record, this represents gaps of about 12,000 yr that otherwise would be lost without using overlapped cores.

## REFERENCES


Baldauf, J. G., 1984. Cenozoic diatom biostratigraphy and paleoceanography of the Rockall Plateau region, North Atlantic, Deep Sea Drilling Project Leg 81. *In* Roberts, D. G., Schnitker, D., et al., *Init. Repts. DSDP*, 81: Washington (U.S. Govt. Printing Office), 439–478.

________, 1985. A high resolution late Miocene-Pliocene diatom biostratigraphy for the eastern equatorial Pacific. *In* Mayer, L., Theyer, E., et al., *Init. Repts. DSDP*, 85: Washington (U.S. Govt. Printing Office), 457–475.

________, 1986. Diatom biostratigraphy and paleoceanographic interpretations for the middle to high latitude North Atlantic Ocean. *In*

Summerhayes, C. P., and Shackleton, N. J. (Eds.), *North Atlantic Paleoceanography*: Geol. Soc. London Spec. Publ., 21:243-252.

Baldauf, J. G., Thomas, E., Clement, B., Takayama, T., Weaver, P.P.E., Backman, J., Jenkins, G., Mudie, P. J., and Westberg-Smith, M. J., 1987. Magnetostratigraphic and biostratigraphic synthesis, Deep Sea Drilling Project Leg 94. *In* Ruddiman, W., Kidd, R., Thomas, E., et al., *Init. Repts. DSDP*, 94 (Pt. 2): Washington (U.S. Govt. Printing Office), 1159-1205.

Barron, J. A., 1980. Upper Pliocene and Quaternary diatom biostratigraphy of Deep Sea Drilling Project Leg 54, tropical eastern Pacific. *In* Rosendahl, B. R., Hekinian, R., et al., *Init. Repts. DSDP*, 54: Washington (U.S. Govt. Printing Office), 455-485.

Berggren, W. A., 1973. The Pliocene timescale: calibration of planktonic foraminiferal and calcareous nannoplankton zones. *Nature*, 243:391-397.

Berggren, W. A., Kent, D. V., and Van Couvering, J. A., 1985. Neogene geochronology and chronostratigraphy. *In* Snelling, P. J. (Ed.), *The Chronology of the Geological Record*: Geol. Soc. London Mem., 10:211-259.

Burckle, L. H., 1977. Pliocene and Pleistocene diatom datum levels from the equatorial pacific. *Quat. Geol.*, 7:330-340.

CLIMAP Project Members, 1981. Seasonal reconstructions of the earth's surface at the last glacial maximum. *Geol. Soc. Am.* Map Chart Ser. MC-36.

Lutze, G. F., 1977. Neogene benthic foraminifera from Site 369, Leg 41, Deep Sea Drilling Project. *In* Lancelot, Y., Seibold, E., et al., *Init. Repts. DSDP*, 41: Washington (U.S. Govt. Printing Office), 659-660.

McIntyre, A., Ruddiman, W. F., Mix, A. C., and Karlin, K., in prep. Late Pleistocene variations in equatorial Atlantic sea-surface temperature.

Pokras, E., and Mix, A., 1985. Hemispheric asymmetry of late Pleistocene climate in tropical West Africa: aeolian diatom evidence. *Quat. Res.*, 24:137-148.

Schnitker, D., 1979. The deep waters of the western North Atlantic during the past 24,000 years, and the re-initiation of the Western Boundary Undercurrent. *Mar. Micropaleontol.*, 4:265-280.

**Table 7. *P*-wave-logger velocity data for Hole 662A.**

| Depth (mbsf) | *P*-wave velocity (km/s) | Depth (mbsf) | *P*-wave velocity (km/s) | Depth (mbsf) | *P*-wave velocity (km/s) |
|---|---|---|---|---|---|
| 0.50 | 1.534 | 48.20 | 1.529 | 108.20 | 1.532 |
| 1.00 | 1.504 | 49.50 | 1.570 | 111.70 | 1.528 |
| 1.70 | 1.520 | 49.90 | 1.510 | 114.70 | 1.520 |
| 2.10 | 1.510 | 51.70 | 1.520 | 117.70 | 1.530 |
| 4.00 | 1.554 | 53.70 | 1.530 | 118.90 | 1.544 |
| 4.40 | 1.520 | 55.70 | 1.510 | 119.20 | 1.525 |
| 5.20 | 1.519 | 56.20 | 1.650 | 121.20 | 1.521 |
| 5.60 | 1.539 | 56.70 | 1.520 | 123.20 | 1.535 |
| 5.80 | 1.515 | 57.40 | 1.640 | 125.20 | 1.530 |
| 7.70 | 1.530 | 58.50 | 1.520 | 127.70 | 1.536 |
| 8.20 | 1.514 | 58.70 | 1.588 | 130.70 | 1.555 |
| 8.40 | 1.526 | 58.90 | 1.508 | 131.70 | 1.524 |
| 10.20 | 1.512 | 59.80 | 1.551 | 135.20 | 1.525 |
| 11.70 | 1.505 | 61.70 | 1.555 | 137.70 | 1.555 |
| 12.20 | 1.529 | 62.30 | 1.584 | 139.70 | 1.555 |
| 13.30 | 1.556 | 62.40 | 1.527 | 140.20 | 1.535 |
| 14.60 | 1.505 | 63.60 | 1.514 | 143.40 | 1.523 |
| 15.50 | 1.540 | 64.00 | 1.555 | 146.70 | 1.530 |
| 15.70 | 1.509 | 65.70 | 1.510 | 148.70 | 1.560 |
| 17.10 | 1.523 | 66.70 | 1.660 | 149.70 | 1.530 |
| 19.70 | 1.502 | 67.50 | 1.522 | 151.20 | 1.516 |
| 20.20 | 1.535 | 71.20 | 1.532 | 152.70 | 1.524 |
| 21.20 | 1.506 | 73.70 | 1.530 | 156.20 | 1.540 |
| 23.20 | 1.525 | 76.70 | 1.552 | 158.70 | 1.532 |
| 25.70 | 1.540 | 79.70 | 1.528 | 161.20 | 1.542 |
| 26.20 | 1.522 | 81.70 | 1.537 | 162.40 | 1.528 |
| 27.20 | 1.541 | 82.20 | 1.570 | 165.50 | 1.563 |
| 28.70 | 1.550 | 83.20 | 1.516 | 166.10 | 1.530 |
| 29.70 | 1.580 | 83.90 | 1.556 | 167.00 | 1.560 |
| 30.70 | 1.515 | 85.20 | 1.569 | 169.40 | 1.520 |
| 34.20 | 1.507 | 87.20 | 1.545 | 170.80 | 1.551 |
| 35.90 | 1.508 | 87.90 | 1.602 | 172.70 | 1.526 |
| 36.30 | 1.552 | 88.60 | 1.516 | 174.60 | 1.561 |
| 36.70 | 1.500 | 89.50 | 1.565 | 176.20 | 1.522 |
| 36.90 | 1.620 | 91.20 | 1.539 | 179.60 | 1.522 |
| 37.10 | 1.530 | 92.10 | 1.579 | 182.00 | 1.540 |
| 37.20 | 1.615 | 92.50 | 1.530 | 185.70 | 1.535 |
| 37.40 | 1.507 | 94.30 | 1.528 | 188.40 | 1.543 |
| 37.90 | 1.560 | 95.20 | 1.596 | 188.70 | 1.522 |
| 38.70 | 1.510 | 96.20 | 1.534 | 189.90 | 1.539 |
| 41.20 | 1.545 | 97.20 | 1.605 | 191.70 | 1.516 |
| 42.00 | 1.510 | 97.70 | 1.538 | 193.10 | 1.539 |
| 42.50 | 1.558 | 99.70 | 1.577 | 195.20 | 1.535 |
| 43.20 | 1.507 | 103.70 | 1.505 | 198.20 | 1.520 |
| 44.70 | 1.535 | 104.70 | 1.536 | 200.90 | 1.543 |
| 47.20 | 1.518 | 106.40 | 1.514 | 202.70 | 1.531 |

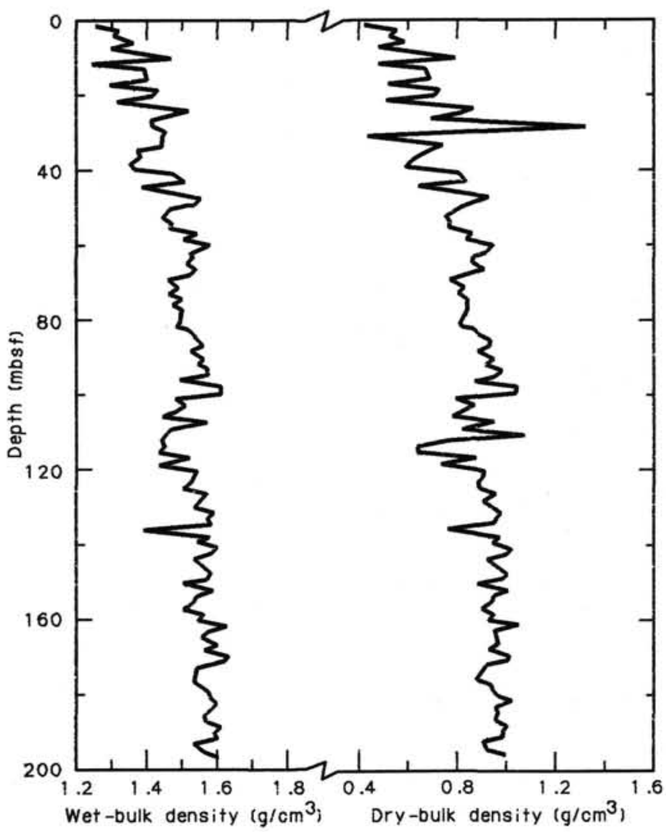


Figure 11. Wet- and dry-bulk-density profiles for Hole 662A.

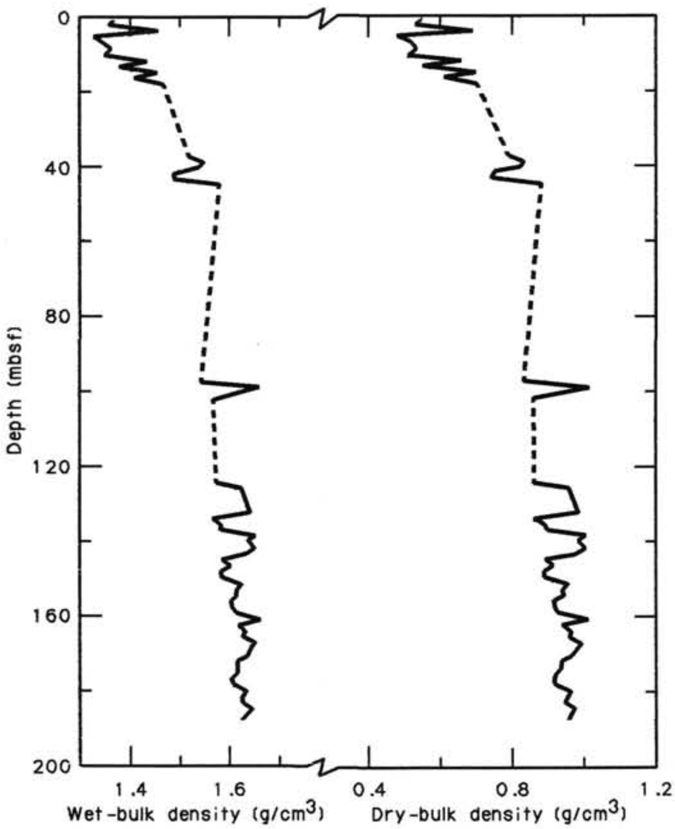


Figure 12. Wet- and dry-bulk-density profiles for Hole 662B.

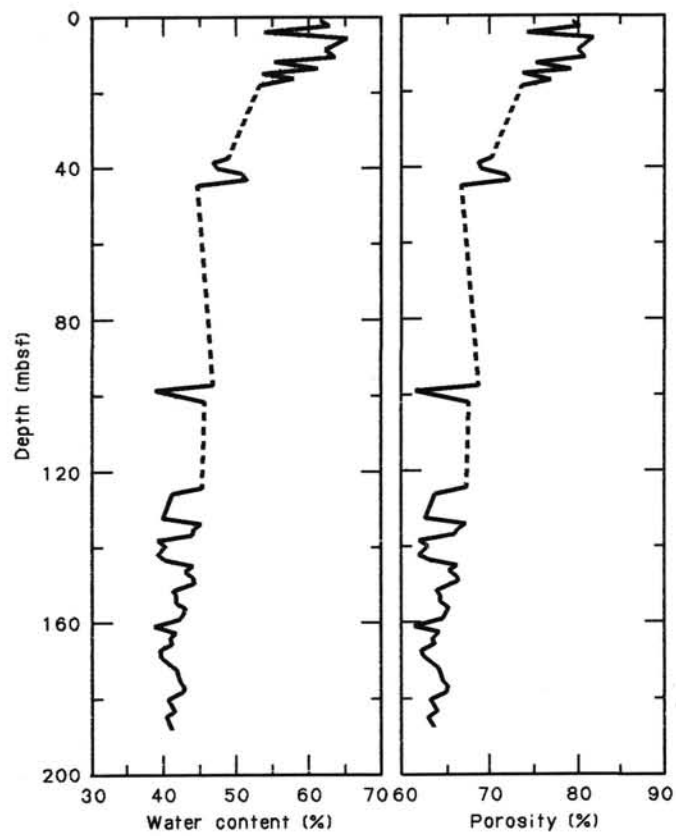


Figure 14. Water-content and porosity profiles for Hole 662B.

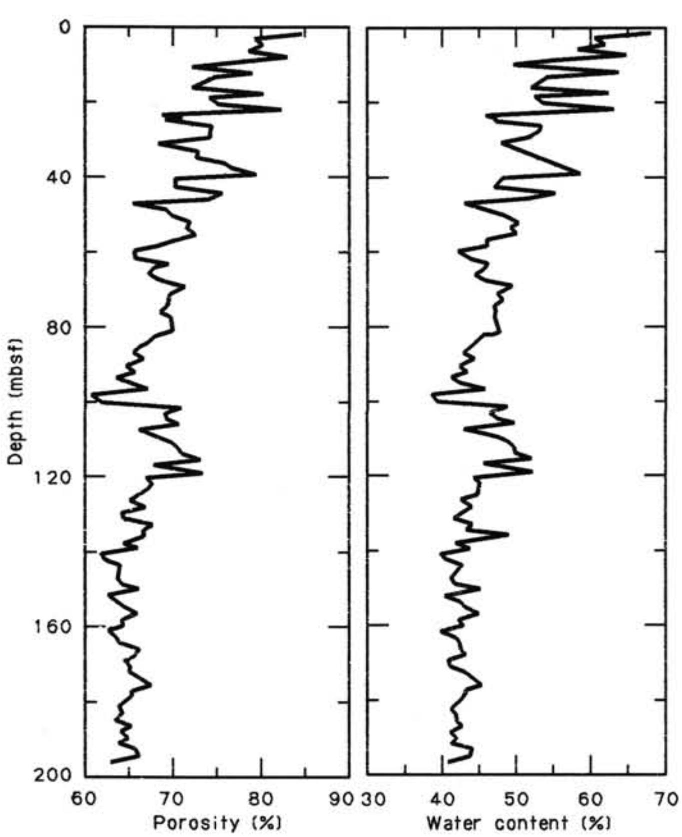


Figure 13. Water-content and porosity profiles for Hole 662B.

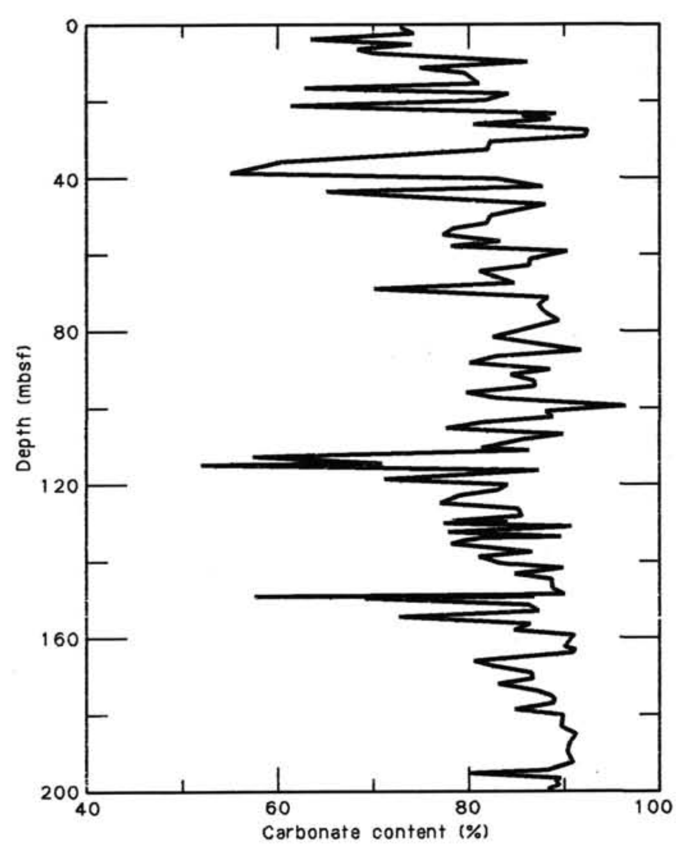


Figure 15. Carbonate-content profile for Hole 662A.

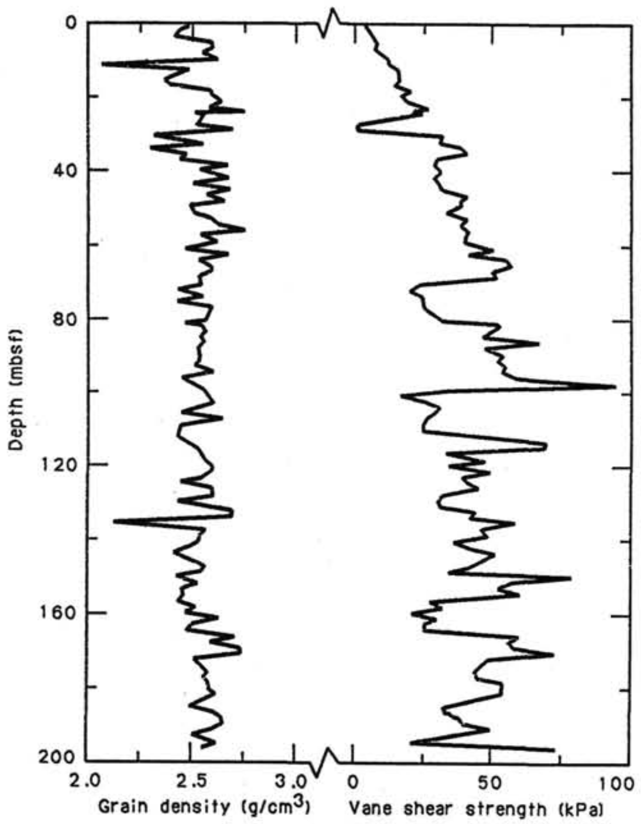


Figure 16. Vane-shear-strength and grain-density profiles for Hole 662A.

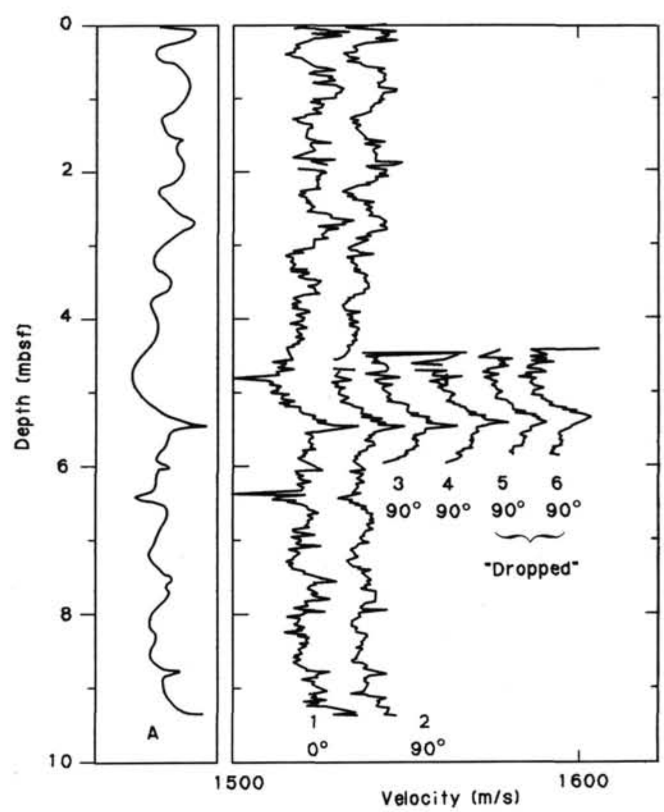


Figure 18. *P*-wave-velocity profile for Core 108-662B-12H (see text for details).

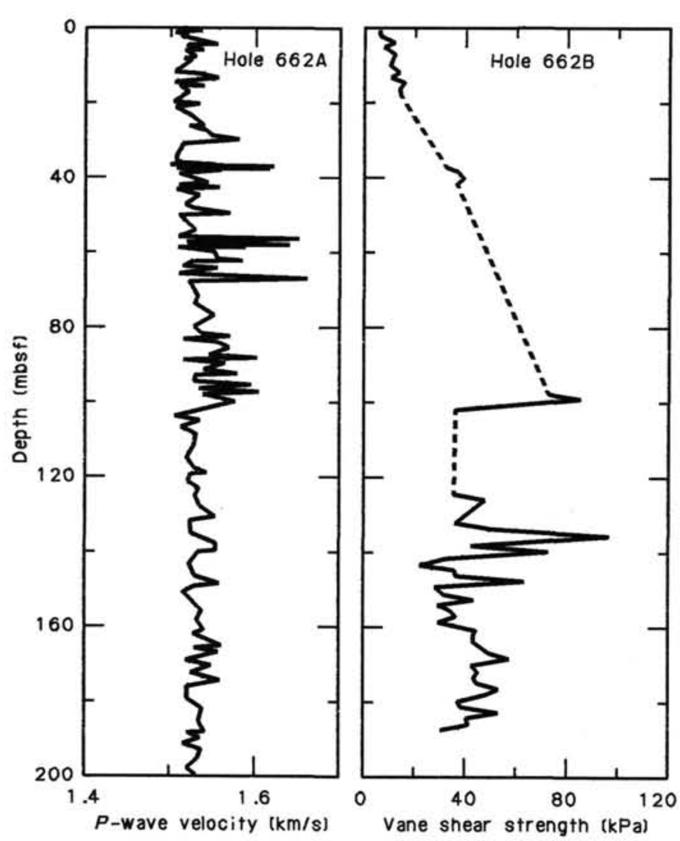


Figure 17. *P*-wave-logger velocity profile for Hole 662A and vane-shear-strength profile for Hole 662B.

**Table 8. Composite-depth sections between Holes 662A and 662B.**

| Hole 662A interval (cm) | Hole 662B interval (cm) | Composite depth (mbsf) |
|---|---|---|
| 1H-1, 0 | — | 0 |
| [a]1H-3, 0 | 1H-2, 75 | 3.0 |
| 2H-2, 25 | 1H-3, 118 | 4.93 |
| 2H-6, 137 | 2H-1, 92 | 12.05 |
| 3H-1, 127 | 2H-3, 100 | 15.13 |
| 3H-7, 15 | — | 21.51 |
| 14H-1, 15 | | [b]117.35 |
| 14H-7, 5 | 6H-3, 72 | 126.25 |
| 15H-3, 86 | 6H-6, 95 | 130.98 |
| 15H-7, 20 | 7H-3, 35 | 136.32 |
| 16H-1, 73 | 7H-4, 10 | 137.57 |
| [a]16H-5, 90 | 8H-1, 70 | 143.74 |
| 17H-1, 12 | 8H-3, 75 | 146.79 |
| 17H-6, 117 | 9H-2, 90 | 155.34 |
| 18H-1, 105 | [c]9H-4, 51 | 157.95 |
| 18H-7, 39 | 10H-4, 8 | 166.29 |
| 19H-2, 77 | 10H-5, 141 | 169.12 |
| 19H-6, 96 | 11H-3, 130 | 175.31 |
| 20H-2, 50 | 11H-6, 132 | 179.83 |
| 20H-5, 90 | 12H-4, 20 | 184.73 |

[a] These correlations are approximate and should be refined by $CaCO_3$ analyses.
[b] This depth is not in true composite-depth units because of a break in the correlations.
[c] A dark layer in Core 108-662B-9H-6 from 60 to 105 cm has no counterpart in Core 108-662A-18H.

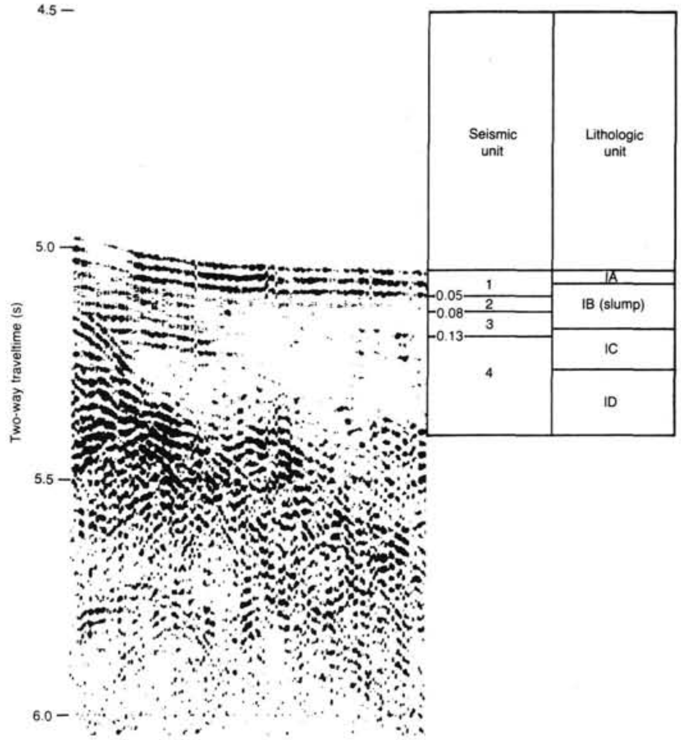


Figure 19. Comparison of Site 662 seismic units with lithologic units.

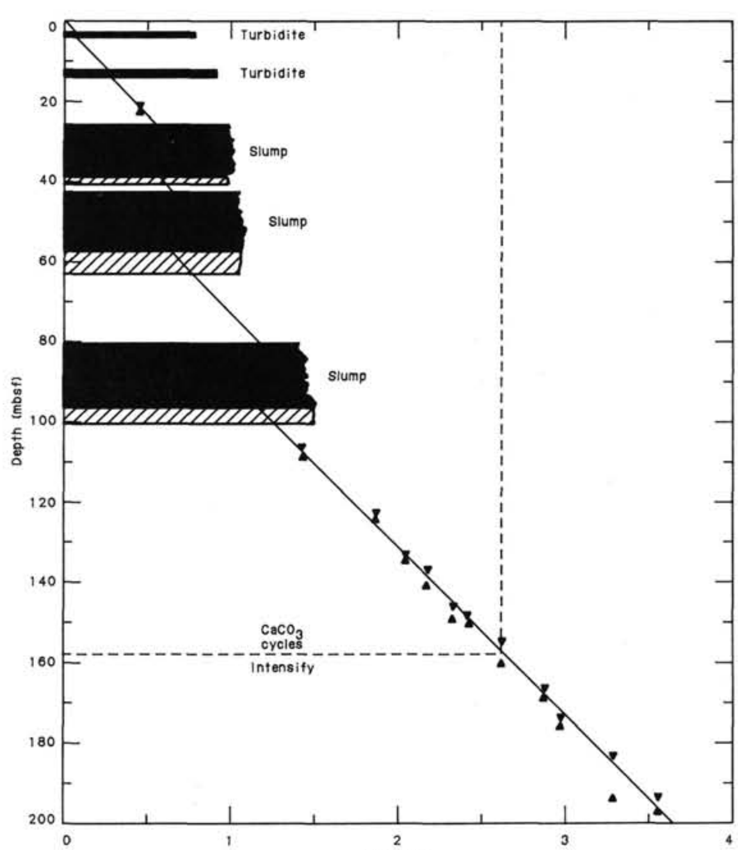


Figure 20. Age-depth curve for Site 662. Black layers are gravity-deposited sediments; white layers indicate pelagic deposition; diagonal pattern indicates slight deformation (tilting) of pelagic sediments. Age-depth biostratigraphic control points are shown by triangles.

## SITE 662 HOLE A CORE 1 H CORED INTERVAL 3814.0-3817.2 mbsl; 0-3.2 mbsf

| TIME-ROCK UNIT | FORAMINIFERS | NANNOFOSSILS | RADIOLARIANS | DIATOMS | BENTHIC FORAM. | PALEOMAGNETICS | PHYS. PROPERTIES | CHEMISTRY | SECTION | METERS |
|---|---|---|---|---|---|---|---|---|---|---|
| PLEISTOCENE TO HOLOCENE | *G. truncatulinoides* A/G | NN 20-21 A/M | | *P. doliolus* A/M | C/G | | | IC=72.6 TOC=0.99 | 1 | 0.5, 1.0 |
| | | | | | | | | IC=74.2 TOC=0.36 | 2 | |
| | | | | | | | | | CC | |

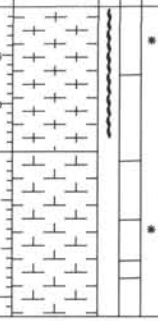

### LITHOLOGIC DESCRIPTION

FORAMINIFER-NANNOFOSSIL OOZE *and* CLAY-BEARING NANNOFOSSIL OOZE

Foraminifer-nannofossil ooze, white (5Y 8/1) to olive-gray (5Y 5/2); very disturbed by drilling and clay-bearing nannofossil ooze, gray (5Y 6/1, 5/1) to olive-gray (5Y 5/2); bioturbation not apparent.

SMEAR SLIDE SUMMARY (%):

| | 1, 38 M | 2, 80 D |
|---|---|---|
| TEXTURE: | | |
| Sand | 20 | 20 |
| Silt | 30 | 30 |
| Clay | 50 | 50 |
| COMPOSITION: | | |
| Clay | 10 | — |
| Foraminifers | 50 | 50 |
| Nannofossils | 50 | 40 |
| Diatoms | Tr | — |
| Radiolarians | Tr | — |
| Sponge spicules | Tr | — |

Chemistry: IC here refers to weight % $CaCO_3$.

## SITE 662 HOLE A CORE 2 H CORED INTERVAL 3817.2-3827.4 mbsl; 3.2-12.7 mbsf

| TIME-ROCK UNIT | FORAMINIFERS | NANNOFOSSILS | RADIOLARIANS | DIATOMS | BENTHIC FORAM. | PALEOMAGNETICS | PHYS. PROPERTIES | CHEMISTRY | SECTION | METERS |
|---|---|---|---|---|---|---|---|---|---|---|
| MIDDLE TO LATE PLEISTOCENE | *G. truncatulinoides* A/G | NN 20-21 A/M | | *P. doliolus* A/M | C/G | | | IC=63.3 TOC=0.25 | 1 | 0.5, 1.0 |
| | | | | | | | | IC=74.1 TOC=0.22 | 2 | |
| | | | | | | | | | 3 | |
| | | | | | | | | IC=78.8 TOC=0.04 | 4 | |
| | | | | | | | | IC=86.0 TOC=0.00 | 5 | |
| | | | | | | | | IC=74.6 TOC=0.27 | 6 | |
| | | | | | | | | | 7 | |
| | | | | | | | | | CC | |

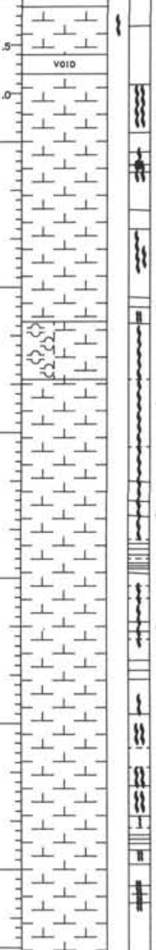


### LITHOLOGIC DESCRIPTION

SILICEOUS-BEARING, FORAMINIFER-BEARING NANNOFOSSIL OOZE to SILICEOUS-BEARING NANNOFOSSIL OOZE

Siliceous-bearing, foraminifer-bearing nannofossil ooze to siliceous-bearing nannofossil ooze, gray (5Y 6/1, 5/1), light gray (5Y 7/1, 7/2) or white (5Y 8/1); weak to moderate bioturbation with pyritic staining throughout core.

Minor lithology: Section 3, 37–94 cm: foraminifer-bearing, siliceous nannofossil ooze, gray (5Y 5/1); moderate bioturbation.

SMEAR SLIDE SUMMARY (%):

| | 1, 84 M | 3, 14 D | 3, 135 D | 4, 81 D | 5, 40 D |
|---|---|---|---|---|---|
| TEXTURE: | | | | | |
| Sand | 50 | 10 | 10 | 10 | 5 |
| Silt | 10 | 30 | 25 | 20 | 20 |
| Clay | 40 | 60 | 60 | 70 | 75 |
| COMPOSITION: | | | | | |
| Quartz | Tr | Tr | — | Tr | Tr |
| Clay | — | — | — | 10 | 10 |
| Accessory Minerals | — | — | 10 | — | — |
| Foraminifers | 60 | 15 | 10 | 10 | 5 |
| Nannofossils | 40 | 50 | 60 | 60 | 70 |
| Diatoms | — | 10 | 10 | 10 | 5 |
| Radiolarians | — | 10 | 5 | 5 | 5 |
| Sponge Spicules | — | 15 | 5 | 10 | 5 |

SITE 662 HOLE A CORE 3 H CORED INTERVAL 3827.4-3836.9 mbsl; 12.7-22.2 mbsf

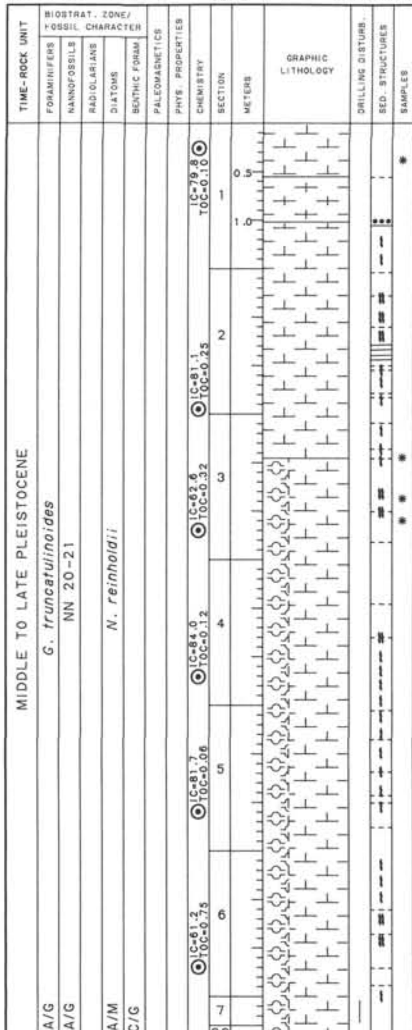


LITHOLOGIC DESCRIPTION

FORAMINIFER-BEARING, CLAY-BEARING, SILICEOUS NANNOFOSSIL OOZE; SILICEOUS-BEARING NANNOFOSSIL OOZE; and FORAMINIFER-BEARING, SILICEOUS NANNOFOSSIL OOZE

Foraminifer-bearing, clay-bearing, siliceous nannofossil ooze, gray (10Y 5/1, 6/1); slight bioturbation; siliceous nannofossil ooze, gray (10Y 6/1); and foraminifer-bearing, siliceous nannofossil ooze, light gray (10Y 7/1); little or no bioturbation.

Minor lithology: Section 1, 54–117 cm: foraminifer-nannofossil ooze, light-gray (5Y 7/1) with erosional lower contact and graded bedding.

SMEAR SLIDE SUMMARY (%):

| | 1, 38 D | 3, 37 D | 3, 85 D | 3, 110 D |
|---|---|---|---|---|
| TEXTURE: | | | | |
| Sand | — | 5 | 10 | 10 |
| Silt | 25 | 10 | 20 | 25 |
| Clay | 75 | 85 | 70 | 65 |
| COMPOSITION: | | | | |
| Clay | — | — | — | 10 |
| Accessory Minerals | — | — | — | Tr |
| Foraminifers | 5 | 5 | 15 | 15 |
| Nannofossils | 75 | 85 | 85 | 50 |
| Diatoms | 5 | — | 15 | 10 |
| Radiolarians | 10 | 10 | 10 | 10 |
| Sponge Spicules | 5 | Tr | 5 | 5 |

SITE 662 HOLE A CORE 4 H CORED INTERVAL 3836.9-3846.4 mbsl; 22.2-31.7 mbsf

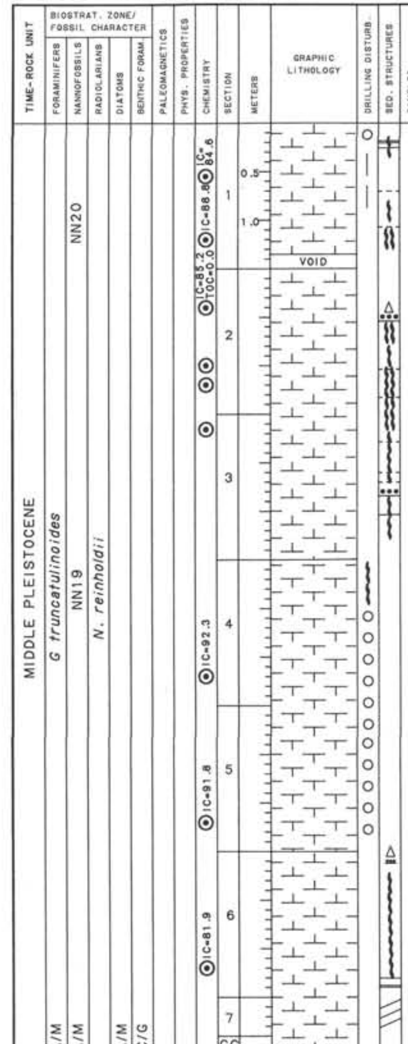


LITHOLOGIC DESCRIPTION

NANNOFOSSIL OOZE

Nannofossil ooze, light-gray (10Y 7/1), white (10Y 8/1), or gray (10Y 5/1, 6/1); moderate bioturbation; graded bedding in Sections 2 and 3; debris flow in Section 6.

Minor lithology: Section 4 through Section 6, 10 cm: foraminifer ooze, light-gray (10Y 7/1) with sharp erosional contact in Section 6, 10 cm; turbidite sequence.

SITE 662 HOLE A CORE 5 H CORED INTERVAL 3846.4-3855.9 mbsl; 31.7-41.2 mbsf

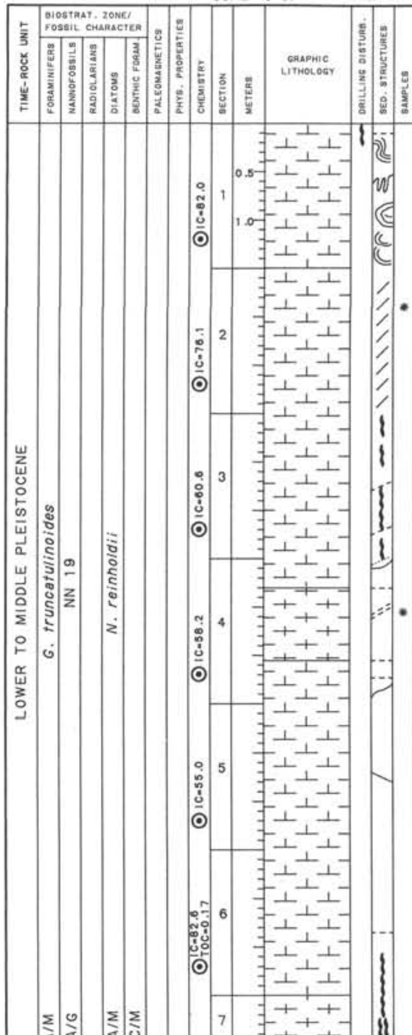


LITHOLOGIC DESCRIPTION

SILICEOUS-BEARING, FORAMINIFER-BEARING NANNOFOSSIL OOZE and SILICEOUS-BEARING FORAMINIFER-NANNOFOSSIL OOZE

Siliceous-bearing, foraminifer-bearing nannofossil ooze, light gray to gray (5Y 7/1, 6/1) and siliceous-bearing foraminifer-nannofossil ooze, light gray (10Y 7/1); contorted bedding with tilted beds; erosional contacts and graded bedding common.

SMEAR SLIDE SUMMARY (%):

| | 2, 46 D | 4, 65 D |
|---|---|---|
| TEXTURE: | | |
| Sand | 5 | 15 |
| Silt | 25 | 35 |
| Clay | 70 | 50 |
| COMPOSITION: | | |
| Clay | 5 | 5 |
| Foraminifers | 15 | 30 |
| Nannofossils | 65 | 50 |
| Diatoms | 5 | 5 |
| Radiolarians | 10 | 10 |

SITE 662 HOLE A CORE 6H CORED INTERVAL 3855.9-3865.4 mbsl; 41.2-50.7 mbsf

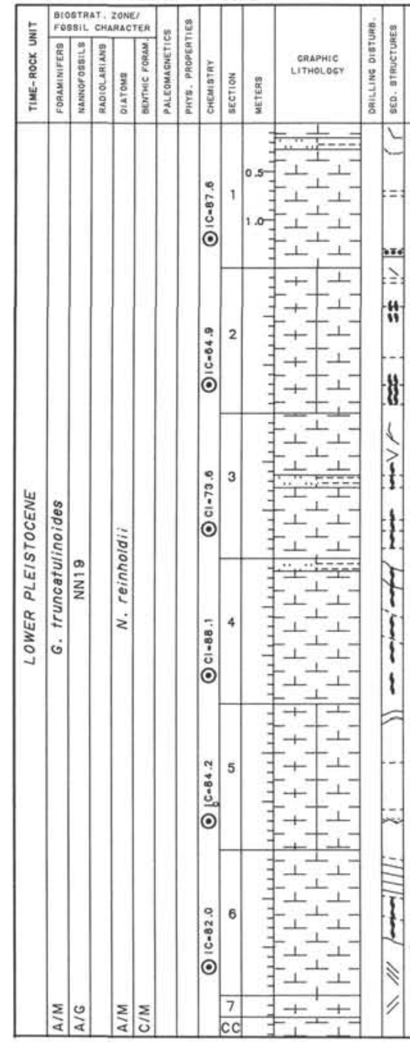


LITHOLOGIC DESCRIPTION

SILICEOUS-BEARING, FORAMINIFER-BEARING NANNOFOSSIL OOZE; SILTY CLAY; and FORAMINIFER-NANNOFOSSIL OOZE alternating with CLAY-BEARING, FORAMINIFER-BEARING NANNOFOSSIL OOZE

Siliceous-bearing, foraminifer-bearing nannofossil ooze, white (5Y 8/1) with little bioturbation; silty clay, greenish-gray (5G 5/1); and foraminifer-nannofossil ooze alternating with clay-bearing, foraminifer-bearing nannofossil ooze, dark gray (10Y 4/1), gray (10Y 6/1, 5/1), or greenish-gray (5GY 5/1).

Minor lithology: sharp, graded contacts (turbidites) in Section 1, 125–130 cm and Section 2, 110–115 cm. Slump structures present in Section 6, 70–100 cm.

SMEAR SLIDE SUMMARY (%):

| | 4, 70 D | 6, 110 D |
|---|---|---|
| TEXTURE: | | |
| Sand | 5 | 5 |
| Silt | 10 | 10 |
| Clay | 85 | 85 |
| COMPOSITION: | | |
| Quartz | 5 | 5 |
| Clay | 15 | — |
| Accessory Minerals | — | 5 |
| Foraminifers | 10 | 10 |
| Nannofossils | 65 | 80 |
| Radiolarians | 5 | — |

SITE 662 HOLE A CORE 7H CORED INTERVAL 3865.4-3874.9 mbsl; 50.7-60.2 mbsf

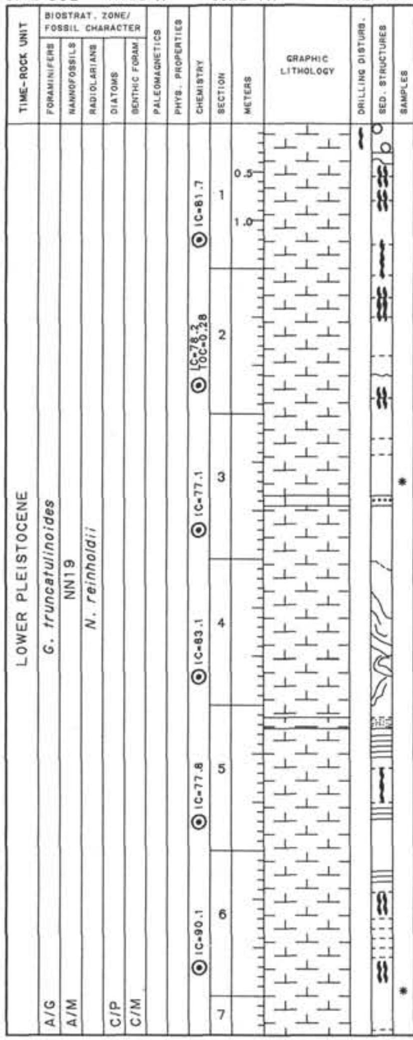


LITHOLOGIC DESCRIPTION

CLAY-BEARING NANNOFOSSIL OOZE; CLAY-BEARING, FORAMINIFER-BEARING NANNOFOSSIL OOZE; and MUD-BEARING, FORAMINIFER-BEARING NANNOFOSSIL OOZE

Clay-bearing nannofossil ooze, dark gray (5Y 4/1); clay-bearing, foraminifer-bearing nannofossil ooze, gray (5Y 6/1); and mud-bearing, foraminifer-bearing nannofossil ooze, light gray (5Y 7/1); strongly folded in Section 4.

Minor lithology: Section 3, 90 cm, and Section 5, 11–19 cm: foraminifer ooze, light-gray (5Y 7/1) with sharp lower contact and graded bedding.

SMEAR SLIDE SUMMARY (%):

| | 3, 70 M | 6, 146 D |
|---|---|---|
| TEXTURE: | | |
| Sand | 5 | 10 |
| Silt | 25 | 20 |
| Clay | 70 | 70 |
| COMPOSITION: | | |
| Clay | 10 | 5 |
| Accessory Minerals | 5 | 10 |
| Foraminifers | 15 | 15 |
| Nannofossils | 65 | 65 |
| Diatoms | 5 | 5 |

SITE 662 HOLE A CORE 8H CORED INTERVAL 3874.9-3884.4 mbsl; 50.7-60.2 mbsf

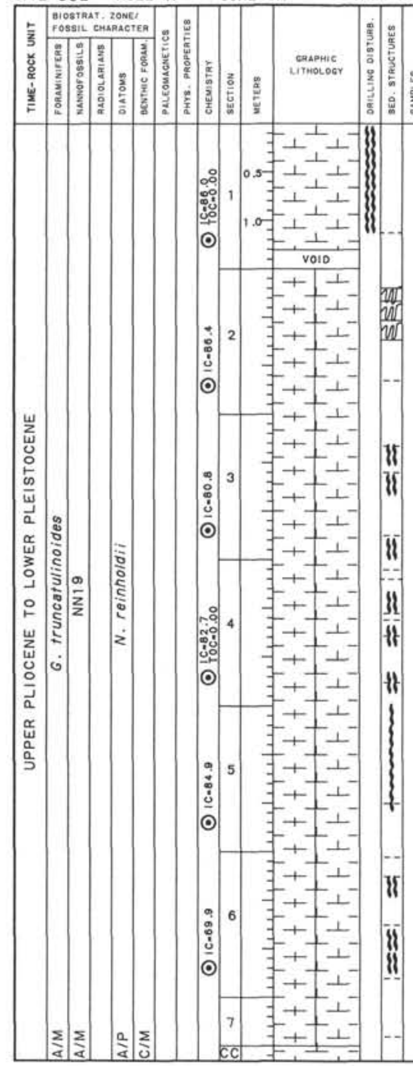


LITHOLOGIC DESCRIPTION

CLAY-BEARING, FORAMINIFER-BEARING NANNOFOSSIL OOZE, alternating with FORAMINIFER-NANNOFOSSIL OOZE

Clay-bearing foraminifer-bearing nannofossil ooze, alternating with foraminifer-nannofossil ooze, white (10Y 8/1), light gray (10Y 7/1) or gray (5Y 6/1); flow-in or slump structures in Section 1, 0–125 cm, and Section 2, 0–60 cm; weak to moderate bioturbation throughout core.

SITE 662 HOLE A CORE 9H CORED INTERVAL 3884.4-3893.5 mbsl; 69.7-79.2 mbsf

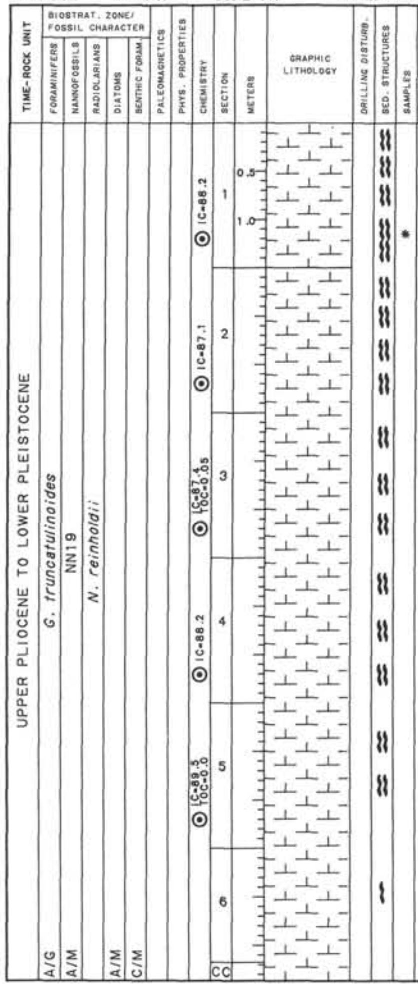


## LITHOLOGIC DESCRIPTION

NANNOFOSSIL OOZE

*Nannofossil ooze, white (2.5 8/0) with extensive olive-gray (10Y 5/2) mottling* in Sections 1 through 5. Minor void in Section 1, 148–150 cm.

SMEAR SLIDE SUMMARY (%):

| | 1, 120 D |
|---|---|
| TEXTURE: | |
| Sand | 5 |
| Silt | 10 |
| Clay | 85 |
| COMPOSITION: | |
| Quartz | 2 |
| Clay | 5 |
| Accessory Minerals | 3 |
| Foraminifers | 5 |
| Nannofossils | 80 |
| Diatoms | 5 |

SITE 662 HOLE A CORE 10H CORED INTERVAL 3893.5-3903.4 mbsl; 79.2-88.7 mbsf

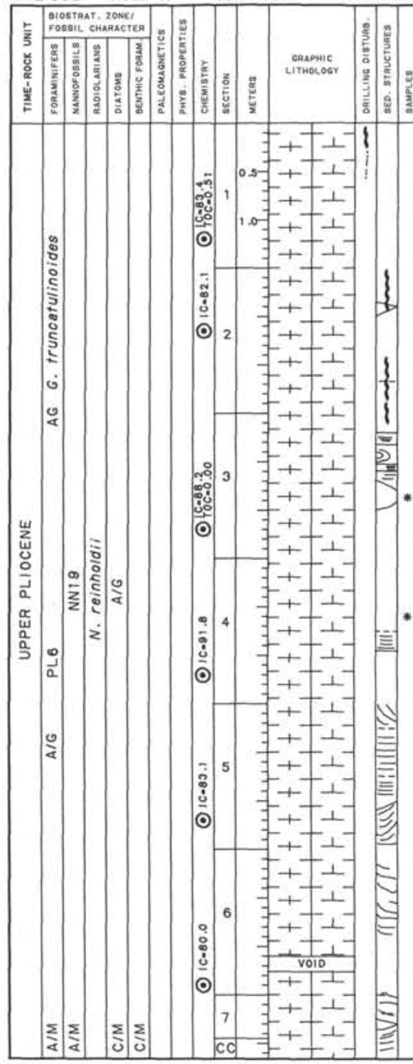


## LITHOLOGIC DESCRIPTION

SILICEOUS-BEARING, MUD-BEARING, FORAMINIFER-BEARING NANNOFOSSIL OOZE to FORAMINIFER-BEARING NANNOFOSSIL OOZE to CLAY-BEARING, FORAMINIFER-BEARING NANNOFOSSIL OOZE, alternating with CLAY-BEARING, SILICEOUS-BEARING FORAMINIFER NANNOFOSSIL OOZE

Siliceous-bearing, mud-bearing, foraminifer-bearing nannofossil ooze to foraminifer-bearing nannofossil ooze to clay-bearing, foraminifer-bearing nannofossil ooze, greenish-gray (5GY 6/1), light gray (5Y 7/1, or gray (5Y 6/1), alternating with clay-bearing, siliceous foraminifer-nannofossil ooze, white (10Y 8/1).

Minor lithology: Section 1 is contorted, possibly a slump. Section 3, 30–100 cm, contains folded slump deposits. Section 5 and Section 6, 0–109 cm, contain several tightly folded slump deposits that truncate each other.

SMEAR SLIDE SUMMARY (%):

| | 3, 90 *D* | 4, 65 *D* |
|---|---|---|
| TEXTURE: | | |
| Sand | 10 | 10 |
| Silt | 35 | 30 |
| Clay | 55 | 65 |
| COMPOSITION: | | |
| Clay | 20 | 15 |
| Accessory Minerals | 5 | 5 |
| Foraminifers | 20 | 25 |
| Nannofossils | 45 | 45 |
| Diatoms | 10 | 10 |

SITE 662 HOLE A CORE 11H CORED INTERVAL 3903.4-3912.9 mbsl; 88.7-98.2 mbsf

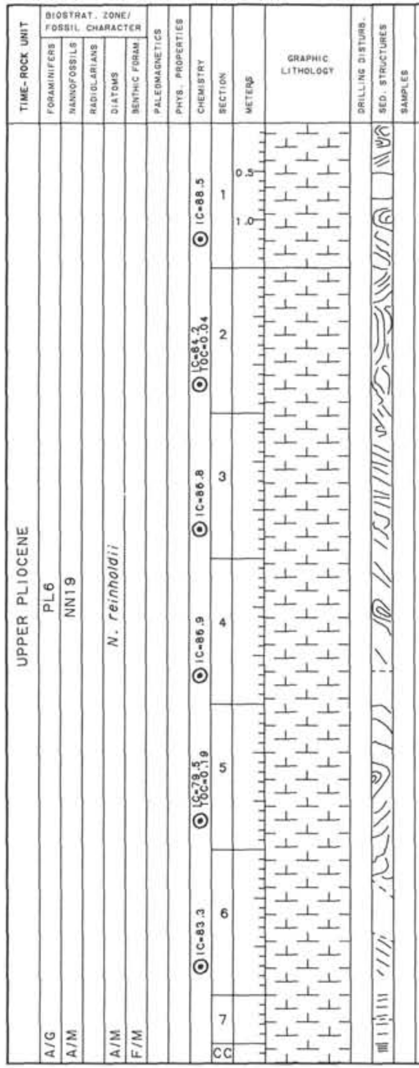


LITHOLOGIC DESCRIPTION

FORAMINIFER-BEARING, CLAY-BEARING NANNOFOSSIL OOZE to FORAMINIFER-BEARING NANNOFOSSIL OOZE to CLAY-BEARING NANNOFOSSIL OOZE

Foraminifer-bearing, clay-bearing nannofossil ooze to foraminifer-bearing nannofossil ooze to clay-bearing nannofossil ooze, white (5Y 8/1), light gray (5Y 7/1), or gray (5Y 6/1). Core consists mainly of tight folds, slumps and/or debris flows. Minor void in Section 1, 145–150 cm.

SITE 662 HOLE A CORE 12H CORED INTERVAL 3912.9-3922.4 mbsl; 982-107.7 mbsf

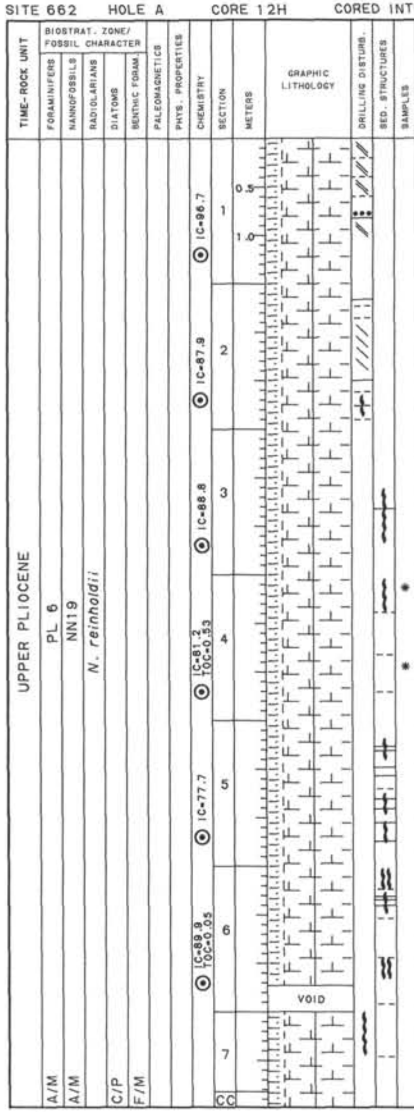


LITHOLOGIC DESCRIPTION

MUD-BEARING, SILICEOUS-BEARING, FORAMINIFER-BEARING NANNOFOSSIL OOZE, alternating with MUDDY NANNOFOSSIL OOZE

Mud-bearing, siliceous-bearing, foraminifer-bearing nannofossil ooze, light gray (10Y 7/2) and white (10Y 8/1), alternating with muddy nannofossil ooze, olive-gray (10Y 5/2) to light olive-gray (10Y 6/2); weak to moderate bioturbation with folding and turbidites in Sections 1 and 2.

SMEAR SLIDE SUMMARY (%):

| | 4, 20 D | 4, 100 D |
|---|---|---|
| TEXTURE: | | |
| Sand | 10 | 5 |
| Silt | 15 | 10 |
| Clay | 75 | 85 |
| COMPOSITION: | | |
| Quartz | 5 | 5 |
| Clay | 10 | 15 |
| Accessory Minerals | 5 | 10 |
| Foraminifers | 15 | 5 |
| Nannofossils | 55 | 40 |
| Diatoms | 10 | 15 |
| Radiolarians | — | 10 |

## SITE 662 HOLE A CORE 13H CORED INTERVAL 3922.4-3931.9 mbsl; 107.7-117.2 mbsf

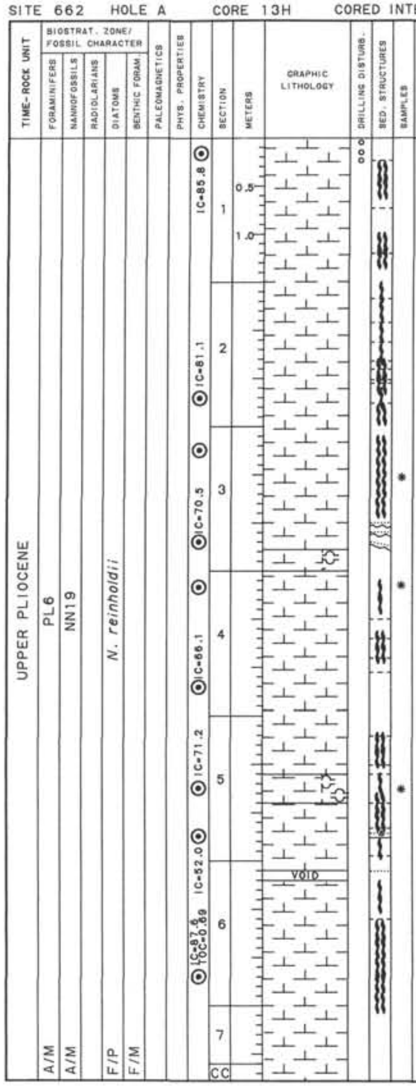


LITHOLOGIC DESCRIPTION

FORAMINIFER-BEARING, SILICEOUS-BEARING NANNOFOSSIL OOZE

Foraminifer-bearing, siliceous-bearing nannofossil ooze, white (10Y 8/1), light gray (10Y 7/1), or gray (10Y 5/1); weakly to moderately bioturbated; black laminations common throughout; graded beds and sharp contacts in Sections 3 and 5.

Minor lithology: Sections 3, 128–150 cm, and Section 5, 60–89 cm: siliceous nannofossil ooze, gray (10Y 5/1) to light-olive-gray (5Y 6/2).

SMEAR SLIDE SUMMARY (%):

| | 3, 60 D | 4, 26 D | 5, 82 D |
|---|---|---|---|
| **TEXTURE:** | | | |
| Sand | 20 | 10 | 5 |
| Silt | 30 | 20 | 35 |
| Clay | 50 | 70 | 60 |
| **COMPOSITION:** | | | |
| Quartz | — | Tr | — |
| Clay | — | — | 5 |
| Accessory Minerals | — | — | 5 |
| Foraminifers | 25 | 10–15 | 10 |
| Nannofossils | 50 | 65 | 50 |
| Diatoms | 10 | 5–10 | 15 |
| Radiolarians | 10 | 10 | 10 |
| Sponge spicules | <5 | 5 | 5 |
| Fish Remains | — | — | Tr |

## SITE 662 HOLE A CORE 14H CORED INTERVAL 3931.9-3941.4 mbsl; 117.2-126.7 mbsf

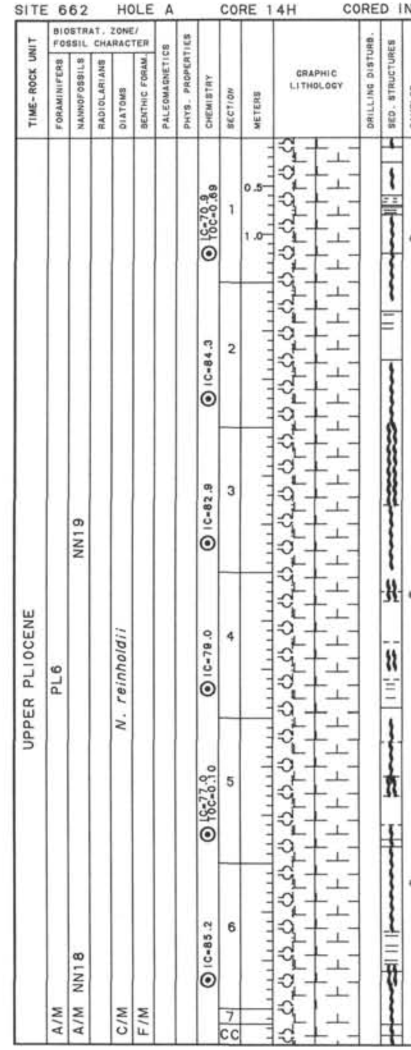


LITHOLOGIC DESCRIPTION

FORAMINIFER-BEARING NANNOFOSSIL OOZE to FORAMINIFER-BEARING, CLAY-BEARING, SILICEOUS-BEARING NANNOFOSSIL OOZE, alternating with SILICEOUS-NANNOFOSSIL OOZE

Foraminifer-bearing nannofossil ooze to foraminifer-bearing, clay-bearing, siliceous-bearing nannofossil ooze, white (5Y 8/1), to light olive-gray (5Y 6/2), alternating with siliceous-nannofossil ooze, olive-gray (5Y 5/2); moderate bioturbation with microlaminations throughout core.

SMEAR SLIDE SUMMARY (%):

| | 1, 100 D | 4, 24 D | 6, 125 D |
|---|---|---|---|
| **TEXTURE:** | | | |
| Sand | 10 | 10 | 10 |
| Silt | 25 | 30 | 10 |
| Clay | 75 | 60 | 80 |
| **COMPOSITION:** | | | |
| Clay | 10 | 15 | 10 |
| Foraminifers | 10 | 10 | 10 |
| Nannofossils | 60 | 45 | 75 |
| Diatoms | 20 | 10 | 5 |
| Radiolarians | | 10 | |
| Sponge spicules | — | 10 | — |

SITE 662 HOLE A CORE 15H CORED INTERVAL 3941.4-3950.9 mbsl; 126.7-136.2 mbsf

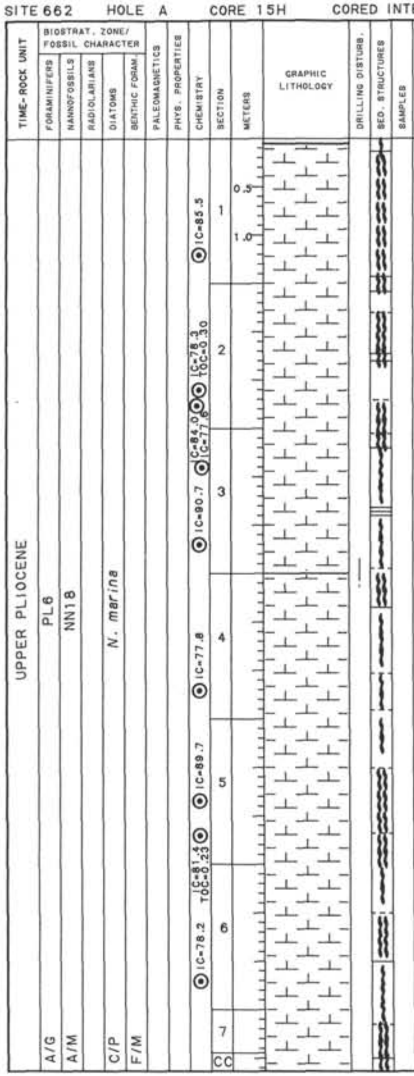


LITHOLOGIC DESCRIPTION

FORAMINIFER-BEARING NANNOFOSSIL OOZE alternating with FORAMINIFER-BEARING, CLAY-BEARING, SILICEOUS-BEARING NANNOFOSSIL OOZE

Foraminifer-bearing nannofossil ooze, white to light gray (5Y 8/1, 5Y 7/1), alternating with foraminifer-bearing, clay-bearing, siliceous-bearing nannofossil ooze, light olive-gray (5Y 6/2); weak to moderate bioturbation throughout; black microlaminations and burrows are common. Minor voids in Section 1, 0–2 cm, and Section 3, 143–150 cm.

SITE 662 HOLE A CORE 16H CORED INTERVAL 3950.9-3960.4mbsl; 136.2-145.7 mbsf

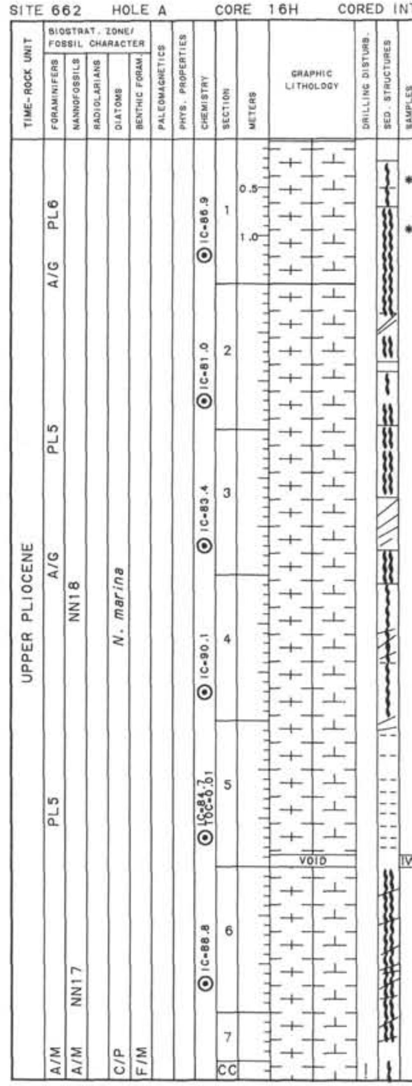


LITHOLOGIC DESCRIPTION

CLAY-BEARING, SILICEOUS-BEARING NANNOFOSSIL OOZE alternating with SILICEOUS-BEARING FORAMINIFER NANNOFOSSIL OOZE

Clay-bearing, siliceous-bearing nannofossil ooze, light olive-gray (5Y 6/2) to gray (5Y 6/1), alternating with siliceous-bearing foraminifer-nannofossil ooze, white (5Y 8/2); moderate to heavy bioturbation; slightly dipping black and green microlaminations common. Minor voids in Section 1, 0–3 and 145–150 cm.

SMEAR SLIDE SUMMARY (%):

| | 1, 40 D | 1, 90 D |
|---|---|---|
| TEXTURE: | | |
| Sand | 5 | 15 |
| Silt | 25 | 15 |
| Clay | 70 | 70 |
| COMPOSITION: | | |
| Clay | 15 | Tr |
| Accessory Minerals | 5 | — |
| Foraminifers | 5 | 25 |
| Nannofossils | 55 | 70 |
| Diatoms | 5 | 5 |
| Radiolarians | 10 | Tr |
| Sponge spicules | 5 | 5 |

SITE 662 HOLE A CORE 17H CORED INTERVAL 3960.4-3969.9 mbsl; 145.7-155.2 mbsf

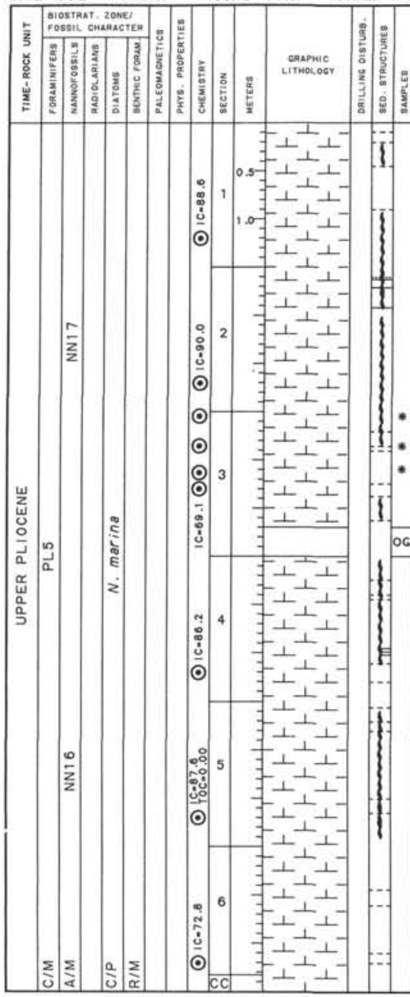


LITHOLOGIC DESCRIPTION

FORAMINIFER-BEARING NANNOFOSSIL OOZE, alternating with MUD-BEARING, SILICEOUS- BEARING NANNOFOSSIL OOZE and NANNOFOSSIL OOZE

Foraminifer-bearing nannofossil ooze, white (10Y 8/1), alternating with mud-bearing, siliceous-bearing nannofossil ooze, light olive-gray or olive-gray (10Y 6/2, 5/2) and nannofossil ooze, light gray (10Y 7/2); weak to moderate bioturbation; black and green microlaminations common.

SMEAR SLIDE SUMMARY (%):

| | 3, 6<br>D | 3, 36<br>D | 3, 60<br>D |
|---|---|---|---|
| TEXTURE: | | | |
| Sand | 13 | 5 | — |
| Silt | 32 | 20 | 25 |
| Clay | 55 | 75 | 75 |
| COMPOSITION: | | | |
| Quartz | Tr | 5 | 5 |
| Clay | — | 10 | — |
| Accessory Minerals | — | — | 5 |
| Foraminifers | 25 | 10 | 10 |
| Nannofossils | 65 | 70 | 70 |
| Diatoms | | | |
| Radiolarians | 10 | 5 | 10 |
| Sponge spicules | | | |

SITE 662 HOLE A CORE 18H CORED INTERVAL 3969.9-3979.4 mbsl; 155.2-164.7 mbsf

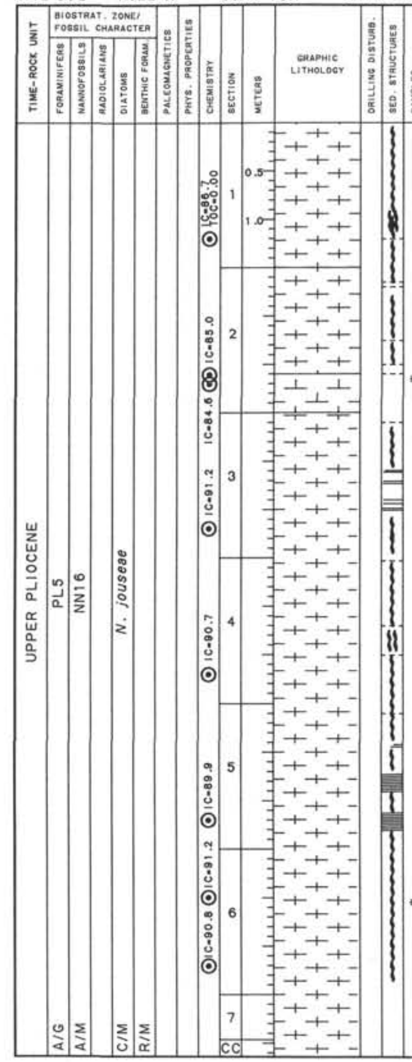


LITHOLOGIC DESCRIPTION

FORAMINIFER-NANNOFOSSIL OOZE and FORAMINIFER-BEARING, SILICEOUS-BEARING NANNOFOSSIL OOZE

Foraminifer-nannofossil ooze, white (10Y 8/1, 2.5Y 8/1), and foraminifer-bearing, siliceous-bearing nannofossil ooze, light olive-gray (10Y 6/2); black or green microlaminations and burrows common throughout; bioturbation weak to moderate throughout. Minor void in Section 1, 146–150 cm, and Section 2, 144–150 cm.

SMEAR SLIDE SUMMARY (%):

| | 2, 11<br>D | 26, 51<br>D |
|---|---|---|
| TEXTURE: | | |
| Sand | 5 | 20 |
| Silt | 20 | 15 |
| Clay | 75 | 65 |
| COMPOSITION: | | |
| Clay | 10 | — |
| Foraminifers | 5–10 | 30 |
| Nannofossils | 65 | 65 |
| Diatoms | 5 | 5 |
| Radiolarians | Tr | Tr |
| Sponge spicules | 5 | Tr |

SITE 662 HOLE A CORE 19H CORED INTERVAL 3979.4-3988.4 mbsl; 164.7-174.2 mbsf

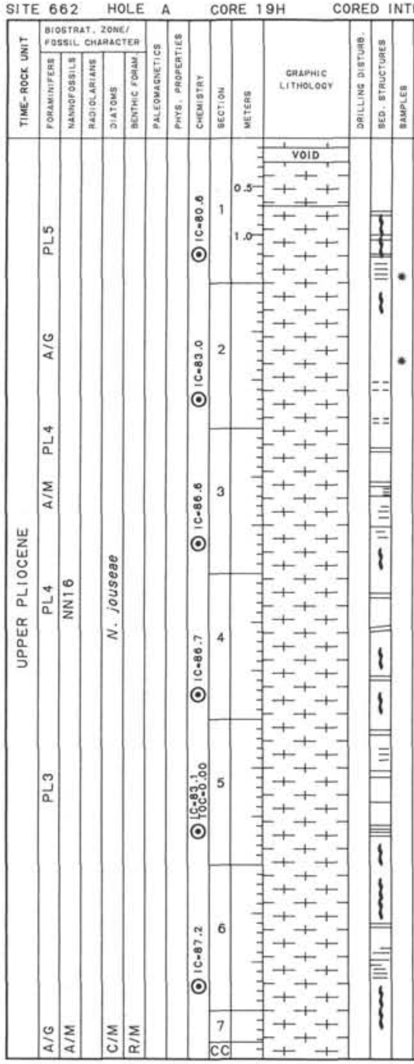


## LITHOLOGIC DESCRIPTION

FORAMINIFER-NANNOFOSSIL OOZE

Foraminifer-nannofossil ooze, white (2.5Y 8/0) with 2-5-cm thin layers, greenish-gray (5GY 6/2), throughout core; weak bioturbation. Minor void in Section 1, 66–70 cm.

SMEAR SLIDE SUMMARY (%):

| | 1, 145 M | 2, 70 D |
|---|---|---|
| TEXTURE: | | |
| Sand | 5 | 15 |
| Silt | 20 | 20 |
| Clay | 75 | 65 |
| COMPOSITION: | | |
| Quartz | — | Tr |
| Clay | 5 | — |
| Foraminifers | 15 | 25 |
| Nannofossils | 70 | 70 |
| Diatoms | 10 | 5 |

SITE 662 HOLE A CORE 20H CORED INTERVAL 3988.4-3998.4mbsl; 174.2-183.7 mbsf

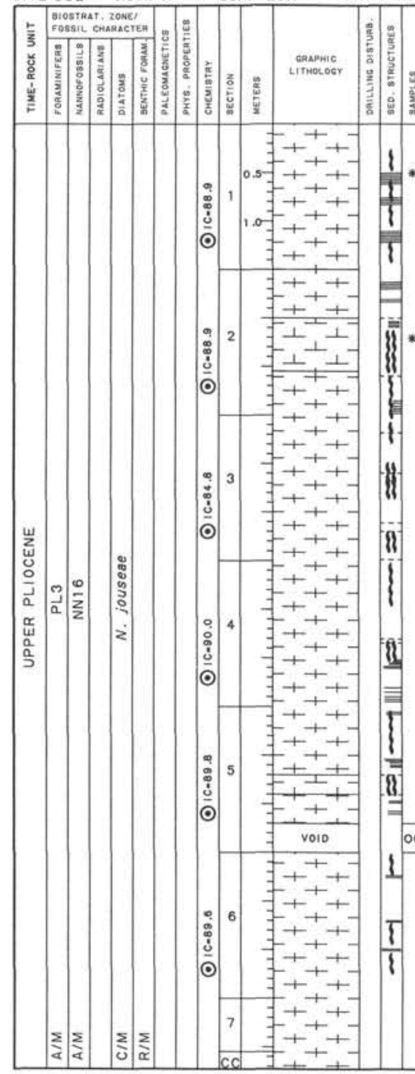


## LITHOLOGIC DESCRIPTION

FORAMINIFER-NANNOFOSSIL OOZE and FORAMINIFER-BEARING NANNOFOSSIL OOZE

Foraminifer-nannofossil ooze, white (10Y 7/1, 2.5Y 8/1), and foraminifer-bearing nannofossil ooze, light-olive-gray or light-gray (10Y 6/2, 6/1); black or green microlaminations and burrows common throughout; bioturbation weak to moderate throughout. Minor void in Section 1, 148–150 cm.

SMEAR SLIDE SUMMARY (%):

| | 1, 57 D | 2, 71 D |
|---|---|---|
| TEXTURE: | | |
| Sand | 15 | 5 |
| Silt | 25 | 25 |
| Clay | 60 | 70 |
| COMPOSITION: | | |
| Quartz | Tr | Tr |
| Clay | — | 5 |
| Foraminifers | 25 | 15 |
| Nannofossils | 70 | 75 |
| Diatoms | | |
| Radiolarians | 5 | 5 |
| Sponge spicules | | |

SITE 662 HOLE A CORE 21H CORED INTERVAL 3998.4-4008.9 mbsl; 183.7-193.2 mbsf

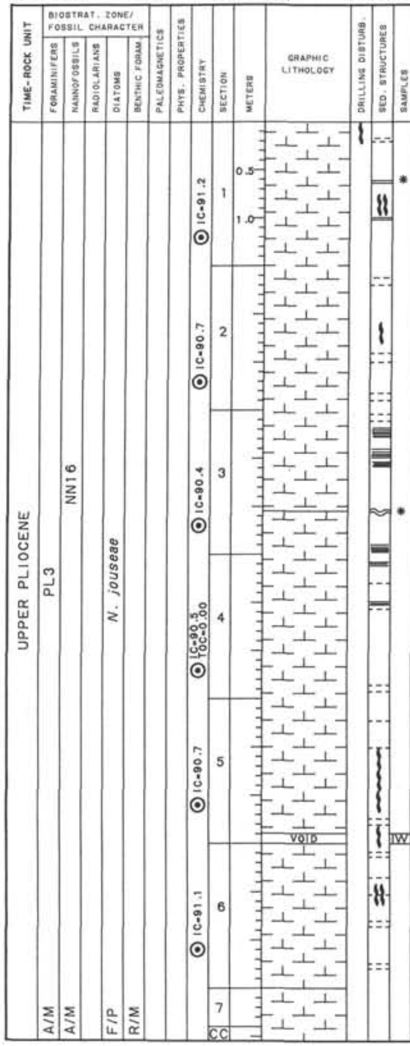


LITHOLOGIC DESCRIPTION

CLAY-BEARING, FORAMINIFER-BEARING NANNOFOSSIL OOZE

Clay-bearing, foraminifer-bearing nannofossil ooze, white (2.5Y 8/1) with blue-black and green microlaminations and burrows; bioturbation weak throughout. Minor void in Section 6, 146–150 cm.

Minor lithology: Section 3, 104 cm: clayey nannofossil ooze, light-gray (5Y 6/1).

SMEAR SLIDE SUMMARY (%):

| | 1, 60<br>D | 3, 105<br>M |
|---|---|---|
| TEXTURE: | | |
| Sand | 5 | — |
| Silt | 15 | 20 |
| Clay | 80 | 80 |
| COMPOSITION: | | |
| Clay | 20 | 25 |
| Accessory Minerals | Tr | — |
| Foraminifers | 10 | Tr |
| Nannofossils | 70 | 70 |
| Diatoms | Tr | 3 |
| Radiolarians | Tr | 2 |

SITE 662 HOLE A CORE 22H CORED INTERVAL 4008.9-4018.4 mbsl; 193.2-200.0 mbsf

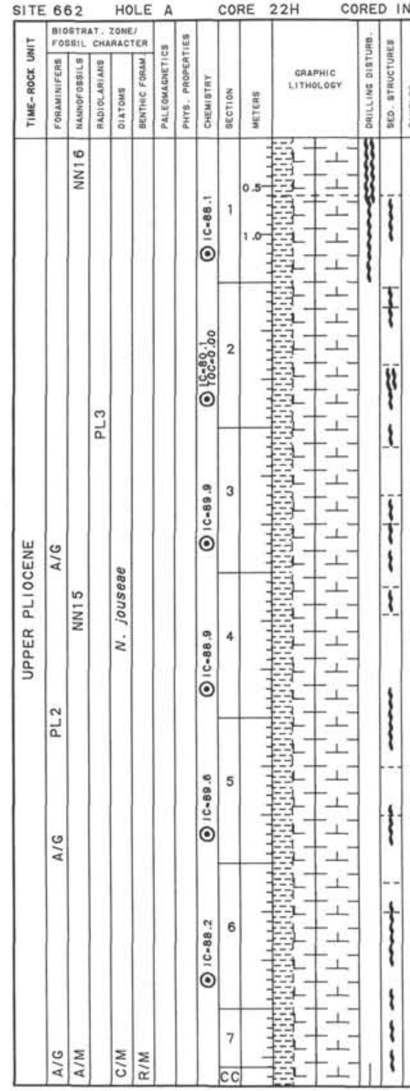


LITHOLOGIC DESCRIPTION

CLAY-BEARING, FORAMINIFER-BEARING NANNOFOSSIL OOZE, alternating with CLAY-BEARING NANNOFOSSIL OOZE

Clay-bearing, foraminifer-bearing nannofossil ooze, white (7.5YR 8/0), alternating with clay-bearing nannofossil ooze, white (5Y 8/1) or light gray (7/1); weak bioturbation; drilling breccia through upper 60 cm of Section 1.

SITE 662 HOLE B CORE 1 H CORED INTERVAL 3813.8-3823.3 mbsl; 0-9.5 mbsf

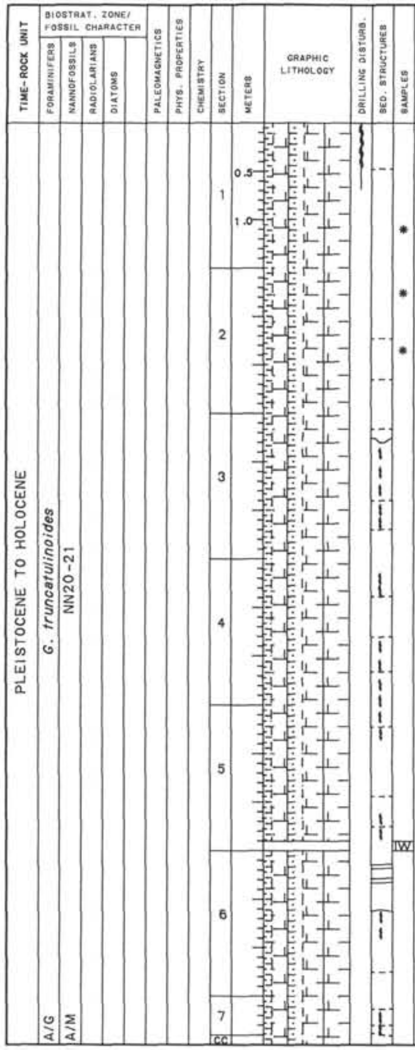


LITHOLOGIC DESCRIPTION

SILICEOUS-BEARING, FORAMINIFER-BEARING NANNOFOSSIL OOZE; FORAMINIFER-BEARING NANNOFOSSIL OOZE; and CLAY-BEARING FORAMINIFER-BEARING NANNOFOSSIL OOZE, alternating with CLAYEY NANNOFOSSIL OOZE and DIATOM-BEARING MUDDY NANNOFOSSIL OOZE

Siliceous-bearing, foraminifer-bearing nannofossil ooze, gray (5Y 6/1); foraminifer-bearing nannofossil ooze, white to light gray (5Y 8/1, 7/1); and clay-bearing foraminifer-bearing nannofossil ooze, white to gray (5Y 8/1, 6/1), alternating with clay-bearing nannofossil ooze, dark gray (5Y 4/1), and diatom-bearing, muddy nannofossil ooze, gray (5Y 6/1); weakly bioturbated throughout. Minor void in Section 5, 145–150 cm.

Minor lithology: Section 1 contains scattered shell fragments.

SMEAR SLIDE SUMMARY (%):

| | 1, 110 D | 2, 30 D | 2, 90 D |
|---|---|---|---|
| TEXTURE: | | | |
| Sand | 5 | 5 | 10 |
| Silt | 20 | 20 | 20 |
| Clay | 75 | 75 | 70 |
| COMPOSITION: | | | |
| Quartz | 5 | — | — |
| Clay | 30 | 5 | 5 |
| Accessory Minerals | 10 | 20 | 5 |
| Foraminifers | 5 | 5 | 10 |
| Nannofossils | 50 | 60 | 70 |
| Diatoms | Tr | 10 | 5 |
| Radiolarians | — | Tr | 5 |
| Sponge spicules | — | Tr | — |

SITE 662 HOLE B CORE 2 H CORED INTERVAL 3823.3-3832.8 mbsl; 9.5-14.0 mbsf

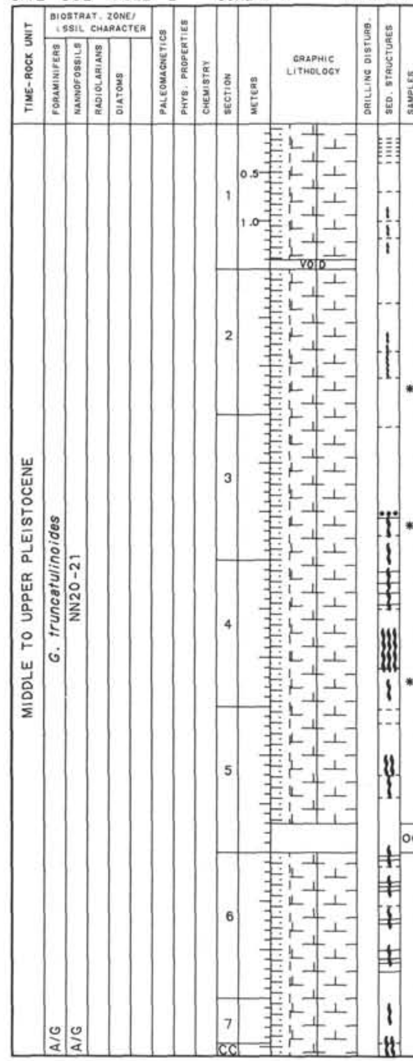


LITHOLOGIC DESCRIPTION

SILT-BEARING, FORAMINIFER-BEARING NANNOFOSSIL OOZE to FORAMINIFER-BEARING NANNOFOSSIL OOZE, alternating with MUDDY NANNOFOSSIL OOZE to FORAMINIFER-BEARING NANNOFOSSIL OOZE

Silt-bearing, foraminifer-bearing nannofossil ooze to foraminifer-bearing nannofossil ooze, white (5Y 8/1) to light gray (5Y 7/1), alternating with muddy nannofossil ooze to foraminifer-bearing nannofossil ooze, gray (5Y 6/1) to dark gray (5Y 4/1); weak to moderate bioturbation with microlaminations throughout core. Minor void in Section 1, 145–150 cm.

Minor lithology: Section 3, 15–85 cm, contains massive foraminifer turbidite.

SMEAR SLIDE SUMMARY (%):

| | 2, 120 D | 3, 120 D | 4, 130 D |
|---|---|---|---|
| TEXTURE: | | | |
| Sand | — | — | 5 |
| Silt | 20 | 25 | 25 |
| Clay | 80 | 75 | 70 |
| COMPOSITION: | | | |
| Quartz | 5 | 10 | 10 |
| Clay | 25 | 10 | — |
| Accessory Minerals | 10 | 10 | 5 |
| Foraminifers | 10 | — | 15 |
| Nannofossils | 50 | 70 | 70 |
| Diatoms | Tr | Tr | Tr |
| Radiolarians | Tr | Tr | — |

SITE 662 HOLE B CORE 3 H CORED INTERVAL 3832.8-3842.3 mbsl; 36.2-45.7 mbsf

TIME-ROCK UNIT: LOWER TO MIDDLE PLEISTOCENE

BIOSTRAT. ZONE/FOSSIL CHARACTER — FORAMINIFERS: *G. truncatulinoides* A/G; NANNOFOSSILS: NN19 A/M; RADIOLARIANS; DIATOMS

PALEOMAGNETICS | PHYS. PROPERTIES | CHEMISTRY | SECTION | METERS | GRAPHIC LITHOLOGY | DRILLING DISTURB. | SED. STRUCTURES | SAMPLES

SECTION: 1, 2, 3, 4, 5, 6, 7, CC

METERS: 0.5, 1.0

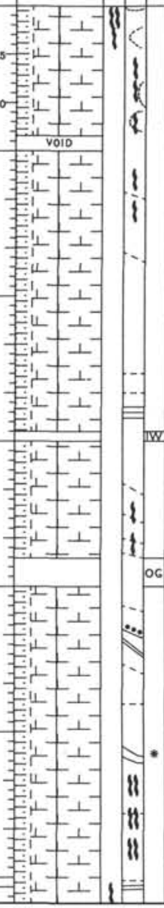


LITHOLOGIC DESCRIPTION

CLAY-BEARING, FORAMINIFER-BEARING NANNOFOSSIL OOZE to FORAMINIFER-BEARING NANNOFOSSIL OOZE, alternating with MUDDY NANNOFOSSIL OOZE

Clay-bearing, foraminifer-bearing nannofossil ooze to foraminifer-bearing nannofossil ooze, white (5Y 8/1, 7.5YR 8/0), light gray (N 7), or gray (5Y 6/1), alternating with muddy nannofossil ooze, dark gray (5Y 4/1) or light olive-gray (5Y 6/2); weak bioturbation with dark microlaminations in Sections 3 and 7; contacts dip slightly.

SMEAR SLIDE SUMMARY (%):

| | 6, 20 |
|---|---|
| | D |
| TEXTURE: | |
| Sand | 5 |
| Silt | 25 |
| Clay | 70 |
| COMPOSITION: | |
| Quartz | 5 |
| Clay | 20 |
| Foraminifers | 15 |
| Nannofossils | 50 |
| Diatoms | 5 |
| Radiolarians | Tr |

SITE 662 HOLE B CORE 4 H CORED INTERVAL 3842.3-3851.8 mbsl; 64.7-74.2 mbsf

TIME-ROCK UNIT: LOWER PLEISTOCENE

BIOSTRAT. ZONE/FOSSIL CHARACTER — FORAMINIFERS: *G. truncatulinoides* A/G; NANNOFOSSILS: NN19 A/M; RADIOLARIANS; DIATOMS

PALEOMAGNETICS | PHYS. PROPERTIES | CHEMISTRY | SECTION | METERS | GRAPHIC LITHOLOGY | DRILLING DISTURB. | SED. STRUCTURES | SAMPLES

SECTION: 1, 2, 3, 4, 5, 6, 7, CC

METERS: 0.5, 1.0

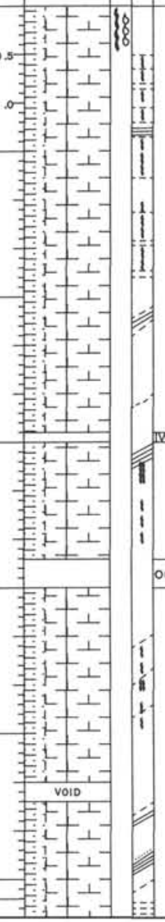


LITHOLOGIC DESCRIPTION

FORAMINIFER-BEARING NANNOFOSSIL OOZE, alternating with CLAY-BEARING, FORAMINIFER-BEARING NANNOFOSSIL OOZE and MUDDY NANNOFOSSIL OOZE

Foraminifer-bearing nannofossil ooze, white (5Y 8/1, 2.5Y 8/1), alternating with clay-bearing, foraminifer-bearing nannofossil ooze, gray (5Y 6/1), and muddy nannofossil ooze, gray to light gray (5Y 7/2, 6/1); weakly bioturbated throughout; greenish-gray and black microlaminations present in Sections 4 through 7; Sections 4 through 7 also dipping at approximately 30°.

SITE 662 HOLE B CORE 5 H CORED INTERVAL 3851.8-3861.3 mbsl; 93.2-102.7 mbsf

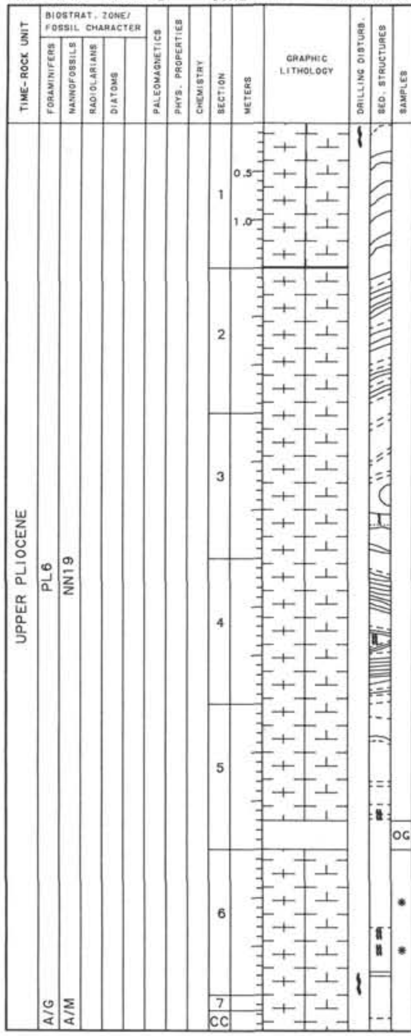


LITHOLOGIC DESCRIPTION

CLAY-BEARING, FORAMINIFER-BEARING NANNOFOSSIL OOZE, alternating with FORAMINIFER-NANNOFOSSIL OOZE

Clay-bearing, foraminifer-bearing nannofossil ooze, white to gray (7.5YR 8/0 and 5Y 6/1), alternating with foraminifer-nannofossil ooze, white (5Y 8/1). Beds are strongly folded and laminated with weak bioturbation. Minor void in Section 1, 145–150 cm.

SMEAR SLIDE SUMMARY (%):

| | 6, 50 D | 6, 100 D |
|---|---|---|
| **TEXTURE:** | | |
| Sand | 10 | 10 |
| Silt | 20 | 35 |
| Clay | 70 | 55 |
| **COMPOSITION:** | | |
| Clay | 10 | 10 |
| Accessory Minerals | 5 | 5 |
| Foraminifers | 10 | 25 |
| Nannofossils | 60 | 55 |
| Diatoms | 10 | 5 |
| Radiolarians | 5 | — |

SITE 662 HOLE B CORE 6 H CORED INTERVAL 3861.3-3870.8 mbsl; 121.7-131.2 mbsf

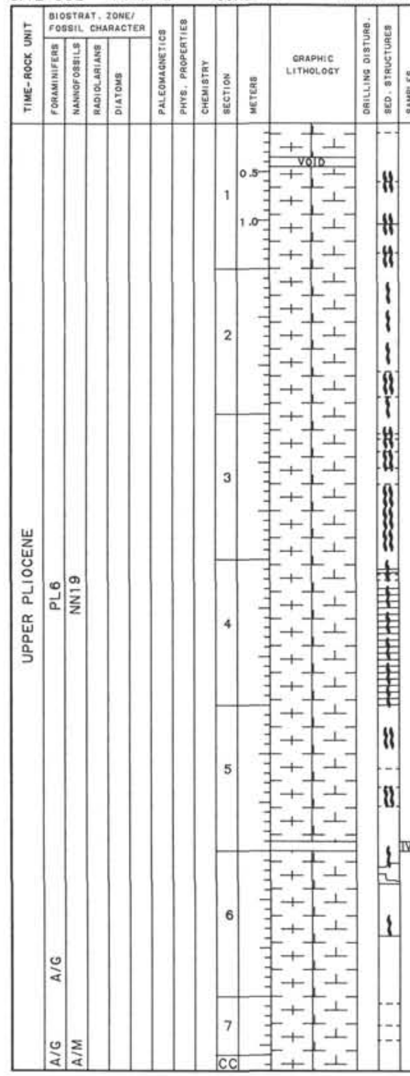


LITHOLOGIC DESCRIPTION

SILICEOUS-BEARING, CLAY-BEARING, FORMINIFER-BEARING NANNOFOSSIL OOZE, alternating with FORAMINIFER-NANNOFOSSIL OOZE

Siliceous-bearing, clay-bearing, foraminifer-bearing nannofossil ooze, gray (5Y 6/1) to olive-gray (10Y 5/2), alternating with foraminifer-nannofossil ooze, white (5Y 8/1, 7.5YR 8/0) or light gray (5Y 7/1); moderate bioturbation with dark microlaminations in Section 4. Minor void in Section 1, 36–43 cm.

SITE 662 HOLE B CORE 7 H CORED INTERVAL 3870.8-3880.3 mbsl; 131.2-140.7 mbsf

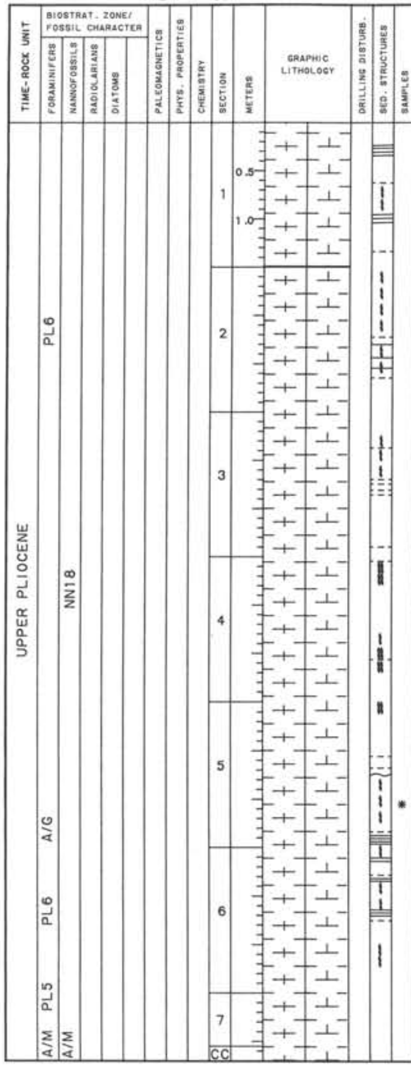


LITHOLOGIC DESCRIPTION

SILICEOUS-BEARING, CLAY-BEARING, FORAMINIFER-BEARING NANNOFOSSIL OOZE, alternating with CLAY-BEARING FORAMINIFER NANNOFOSSIL OOZE

Siliceous-bearing, clay-bearing, foraminifer-bearing nannofossil ooze, gray to light gray (5Y 6/1, 7/1), alternating with clay-bearing foraminifer-nannofossil ooze, white (7.5YR 8/0); black microlaminations and bioturbation structures common in the foraminifer-nannofossil ooze; bioturbation generally weak throughout. Minor void in Section 1, 146–150 cm.

SMEAR SLIDE SUMMARY (%):

| | 5, 110<br>D |
|---|---|
| TEXTURE: | |
| Sand | 10 |
| Silt | 30 |
| Clay | 60 |
| COMPOSITION: | |
| Clay | 10 |
| Foraminifers | 25 |
| Nannofossils | 60 |
| Diatoms | 5 |
| Radiolarians | |

SITE 662 HOLE B CORE 8 H CORED INTERVAL 3880.3-3889.8 mbsl; 140.7-150.2 mbsf

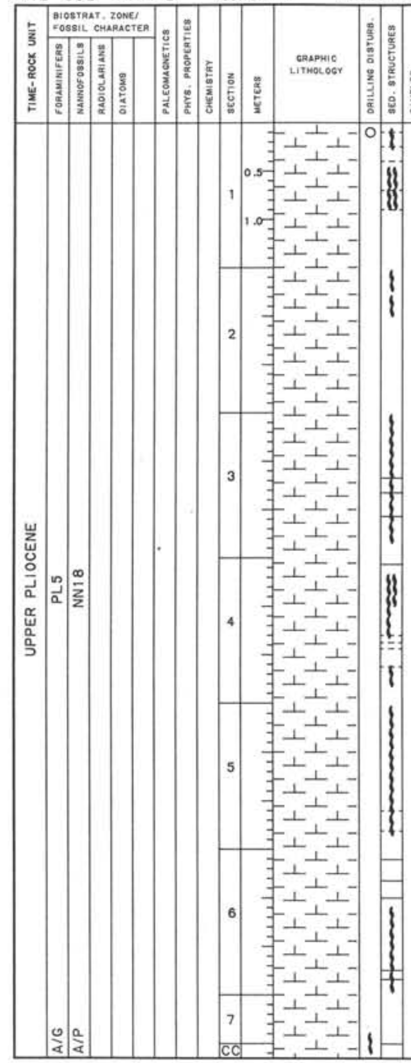


LITHOLOGIC DESCRIPTION

FORAMINIFER-BEARING NANNOFOSSIL OOZE to MUD-BEARING, SILICEOUS-BEARING, NANNOFOSSIL OOZE to FORAMINIFER-BEARING NANNOFOSSIL OOZE

Foraminifer-bearing nannofossil ooze, white (2.5Y 8/0), to mud-bearing, siliceous-bearing, nannofossil ooze, light olive-gray (10Y 6/2) to olive-gray (10Y 5/2), to foraminifer-bearing nannofossil ooze, light gray (10Y 7/1, 7/2); weak bioturbation with faint microlaminations in Sections 1 through 3.

SITE 662 HOLE B CORE 9 H CORED INTERVAL 3889.8-3899.3 mbsl; 150.2-159.7 mbsf

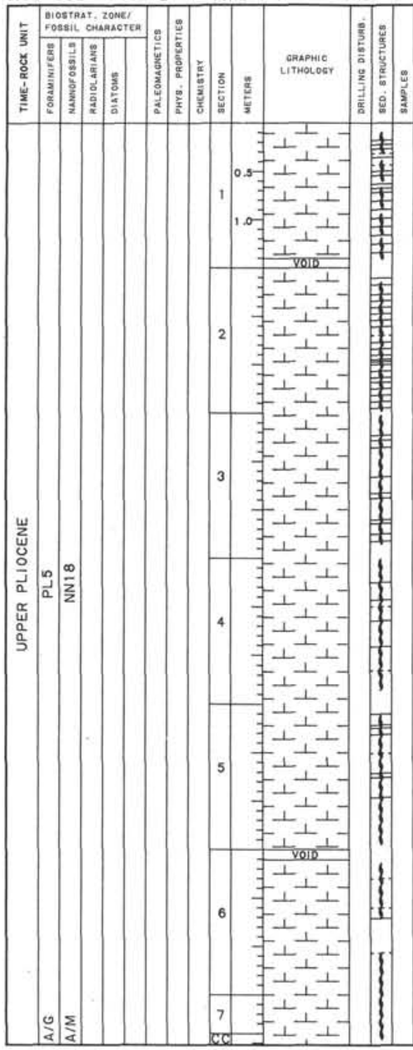


LITHOLOGIC DESCRIPTION

FORAMINIFER-BEARING NANNOFOSSIL OOZE to MUD-BEARING, SILICEOUS-BEARING NANNOFOSSIL OOZE to FORAMINIFER-BEARING NANNOFOSSIL OOZE

Foraminifer-bearing nannofossil ooze, white (2.5Y 8/0), to mud-bearing, siliceous-bearing, nannofossil ooze, light olive-gray (10Y 6/2) to olive-gray (10Y 5/2), to foraminifer-bearing nannofossil ooze, light gray (10Y 7/1, 7/2); moderate bioturbation with greenish-gray and black microlaminations concentrated in upper portion of core. Minor voids in Section 1, 144–150 cm, and Section 6, 0–3 cm.

SITE 662 HOLE B CORE 10 H CORED INTERVAL 3899.3-3908.8 mbsl; 159.7-169.2 mbsf

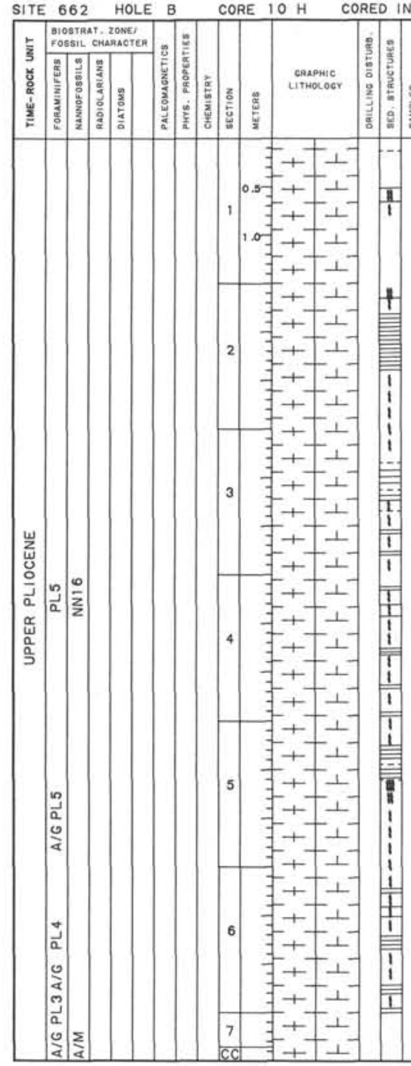


LITHOLOGIC DESCRIPTION

FORAMINIFER-BEARING NANNOFOSSIL OOZE, alternating with FORAMINIFER-NANNOFOSSIL OOZE

Foraminifer-bearing nannofossil ooze, white to light gray (7.5YR 8/0, 7/0, alternating with foraminifer-nannofossil ooze, white to light gray (7.5YR 8/0, 7/0); weak to moderate bioturbation throughout; laminations are common; mottles and black and green microlaminations.

SITE 662 HOLE B CORE 11 H CORED INTERVAL 3708.8-3918.3 mbsl; 169.2-178.7 mbsf

| TIME-ROCK UNIT | BIOSTRAT. ZONE/ FOSSIL CHARACTER: FORAMINIFERS | NANNOFOSSILS | RADIOLARIANS | DIATOMS | PALEOMAGNETICS | PHYS. PROPERTIES | CHEMISTRY | SECTION | METERS | GRAPHIC LITHOLOGY | DRILLING DISTURB. | SED. STRUCTURES | SAMPLES | LITHOLOGIC DESCRIPTION |
|---|---|---|---|---|---|---|---|---|---|---|---|---|---|---|
| UPPER PLIOCENE | PL3<br>A/G | NN16<br>A/P | | | | | | 1<br>2<br>3<br>4<br>5<br>6<br>7<br>CC | 0.5<br>1.0 | 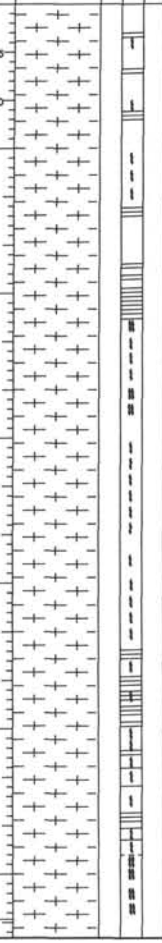 | | | | FORAMINIFER-NANNOFOSSIL OOZE<br><br>Foraminifer-nannofossil ooze, white to light greenish-gray (2.5Y 8/0, 5GY 7/1); microlaminations and mottles, black and green; bioturbation moderate in Sections 3 and 4; laminations common in Sections 5 and 6. |

SITE 662 HOLE B CORE 12 H CORED INTERVAL 3918.3-3827.8 mbsl; 178.7-188.2 mbsf

| TIME-ROCK UNIT | BIOSTRAT. ZONE/ FOSSIL CHARACTER: FORAMINIFERS | NANNOFOSSILS | RADIOLARIANS | DIATOMS | PALEOMAGNETICS | PHYS. PROPERTIES | CHEMISTRY | SECTION | METERS | GRAPHIC LITHOLOGY | DRILLING DISTURB. | SED. STRUCTURES | SAMPLES | LITHOLOGIC DESCRIPTION |
|---|---|---|---|---|---|---|---|---|---|---|---|---|---|---|
| UPPER PLIOCENE | PL3<br>A/G | NN15<br>A/P | | | | | | 1<br>2<br>3<br>4<br>5<br>6<br>7<br>CC | | 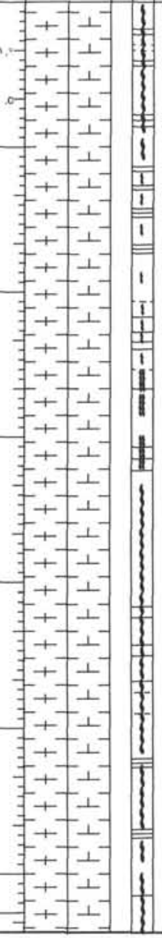 | | | | FORAMINIFER-BEARING NANNOFOSSIL OOZE, alternating with FORAMINIFER-NANNOFOSSIL OOZE<br><br>Foraminifer-bearing nannofossil ooze, white to light-greenish-gray (7.5Y 8/0, 5GY 7/1), alternating with foraminifer-nannofossil ooze, white (7.5YR 8/0); weakly bioturbated throughout; black, green or purple laminations common in Sections 1 through 3. |

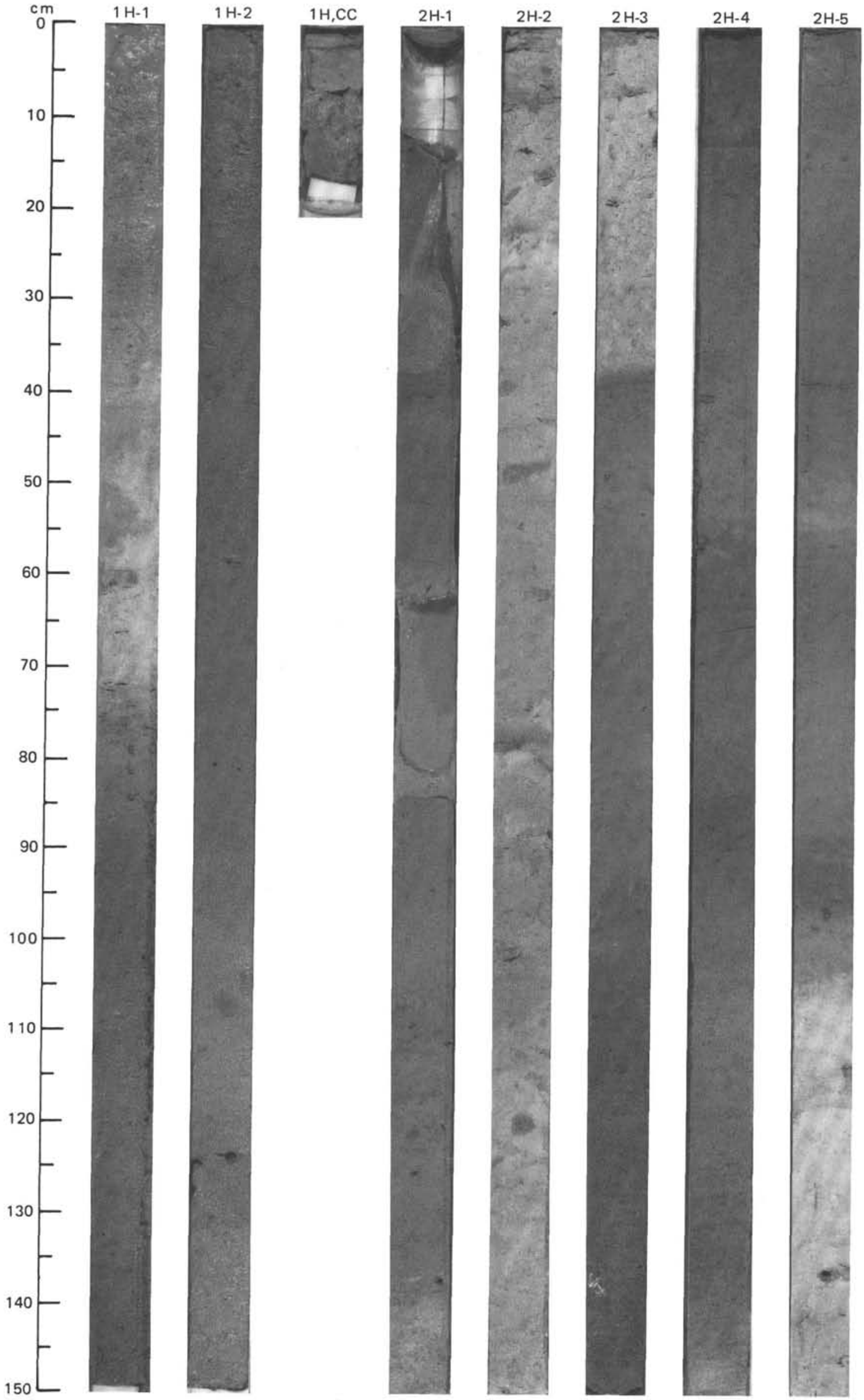
cm
0
10
20
30
40
50
60
70
80
90
100
110
120
130
140
150
1H-1
1H-2
1H,CC
2H-1
2H-2
2H-3
2H-4
2H-5

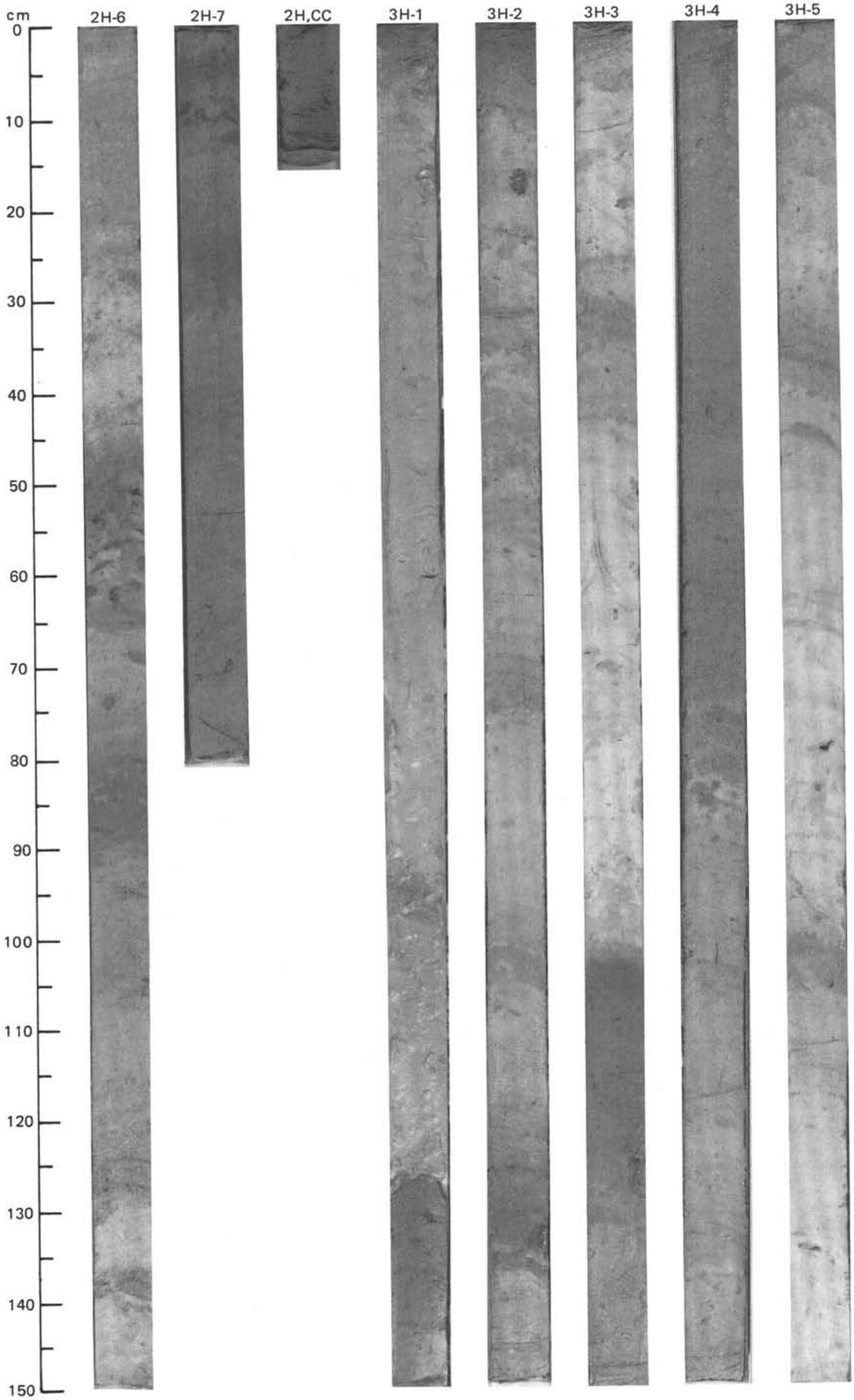
cm
0
10
20
30
40
50
60
70
80
90
100
110
120
130
140
150
2H-6
2H-7
2H,CC
3H-1
3H-2
3H-3
3H-4
3H-5

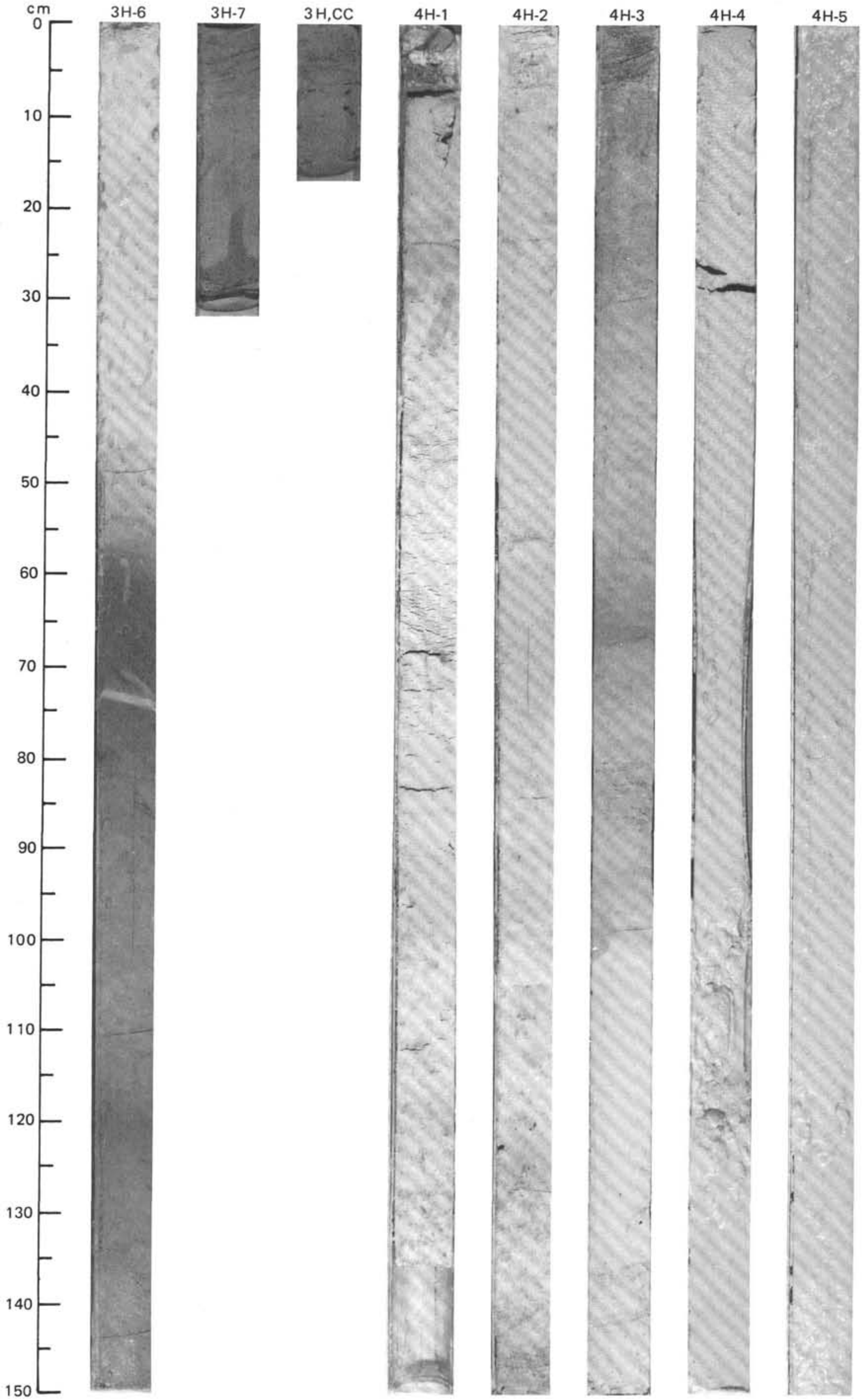
cm
0
10
20
30
40
50
60
70
80
90
100
110
120
130
140
150
3H-6
3H-7
3H,CC
4H-1
4H-2
4H-3
4H-4
4H-5

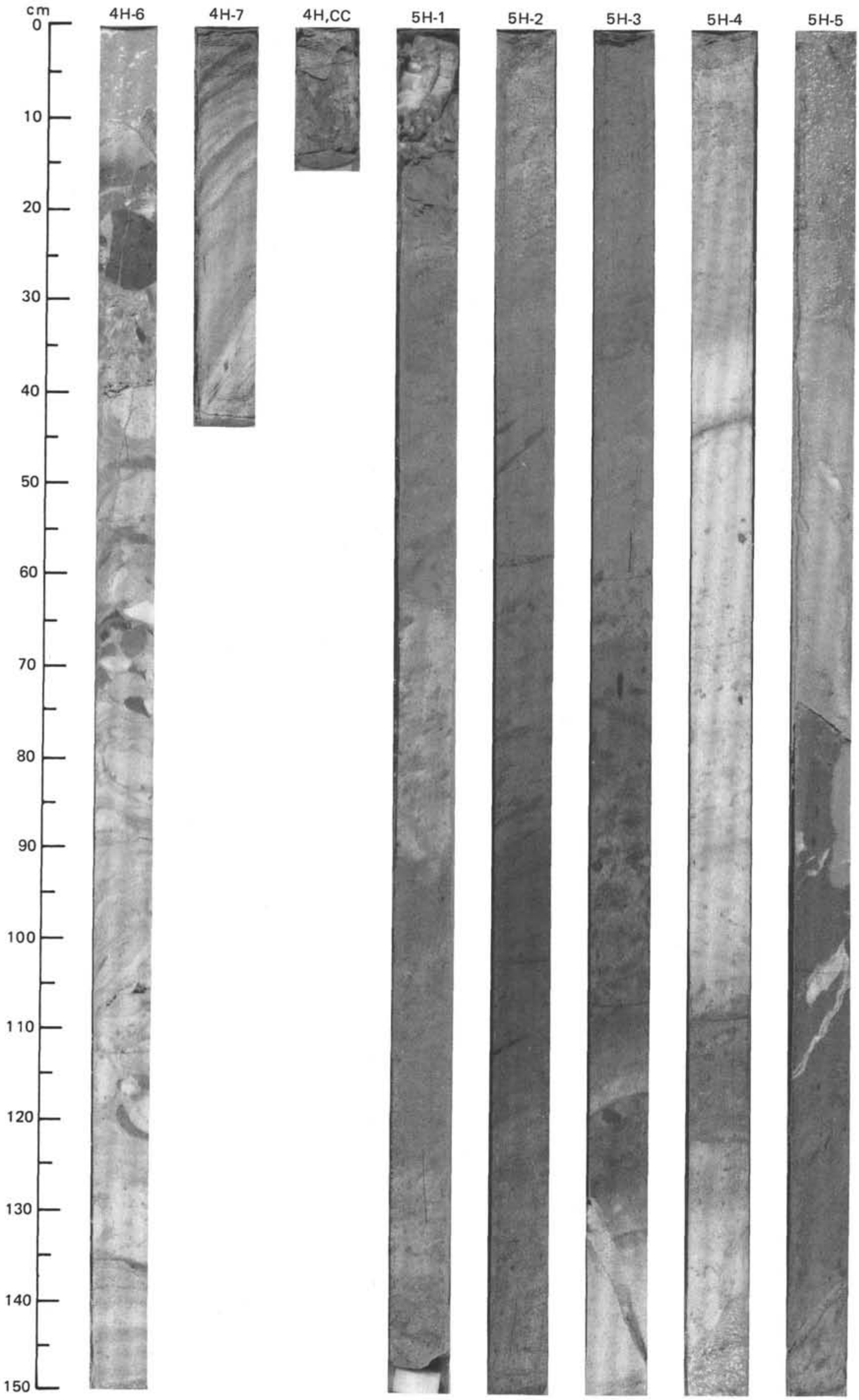
cm
0
10
20
30
40
50
60
70
80
90
100
110
120
130
140
150
4H-6
4H-7
4H,CC
5H-1
5H-2
5H-3
5H-4
5H-5

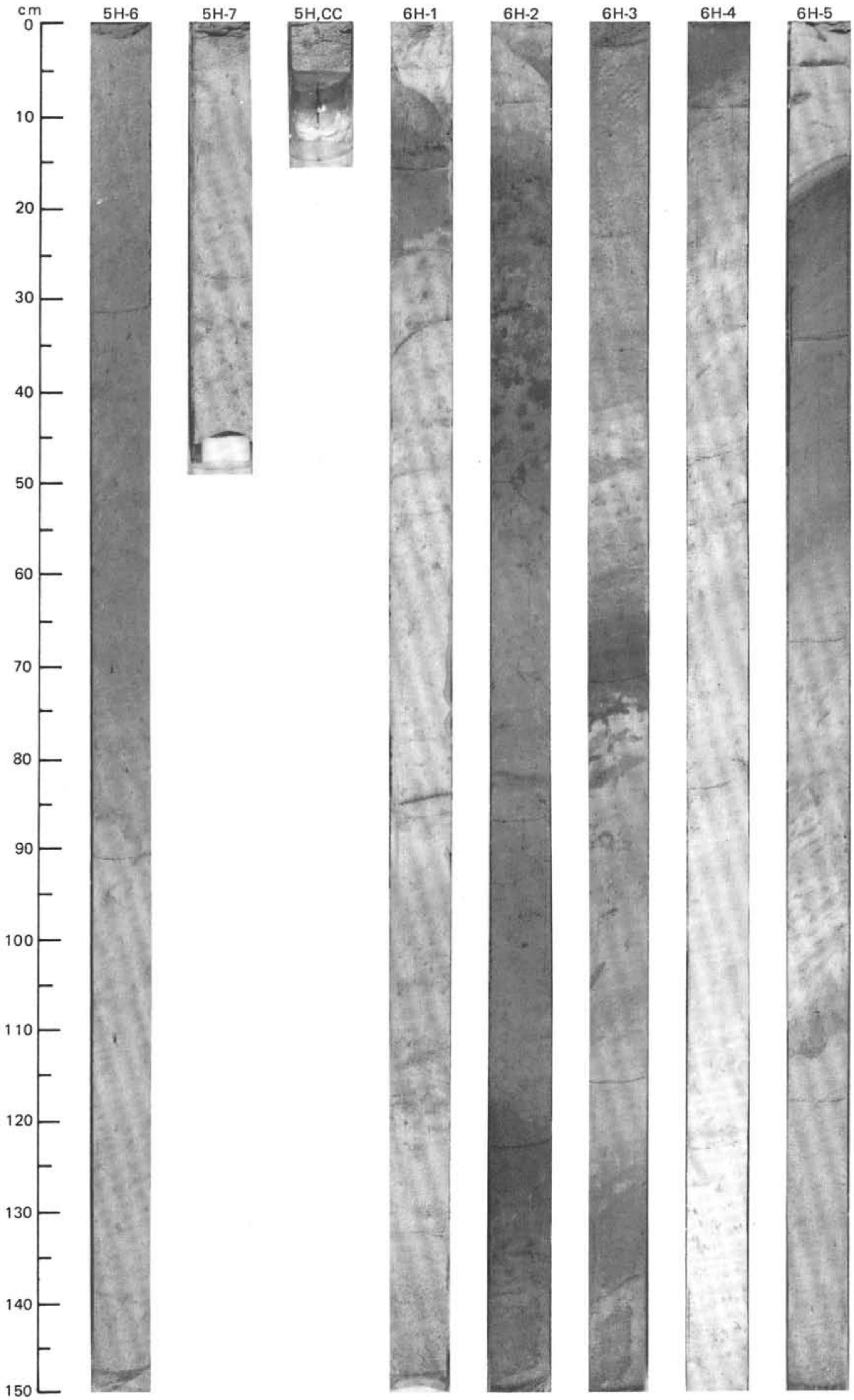
cm
0
10
20
30
40
50
60
70
80
90
100
110
120
130
140
150
5H-6
5H-7
5H,CC
6H-1
6H-2
6H-3
6H-4
6H-5

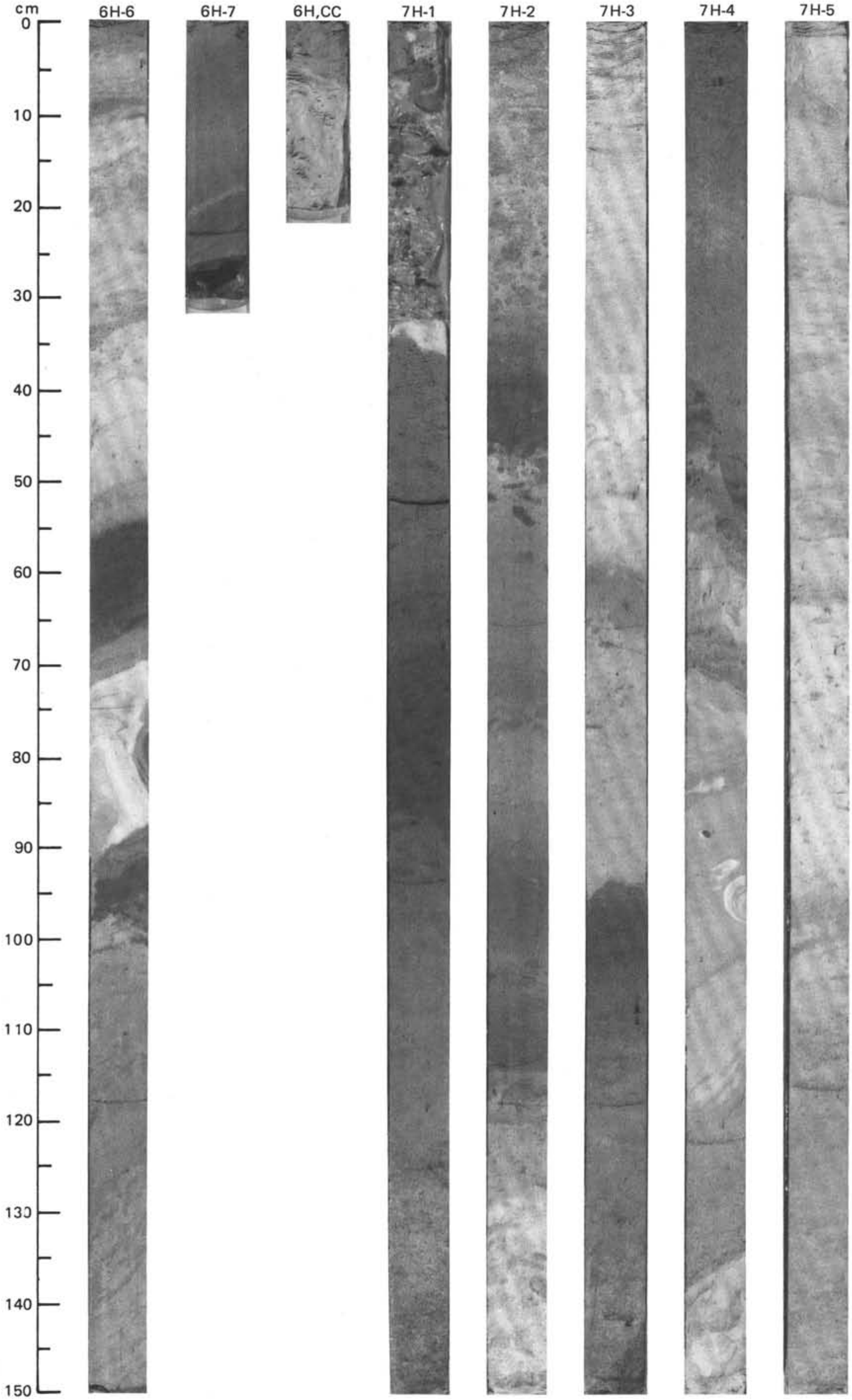
cm
0
10
20
30
40
50
60
70
80
90
100
110
120
130
140
150
6H-6
6H-7
6H,CC
7H-1
7H-2
7H-3
7H-4
7H-5

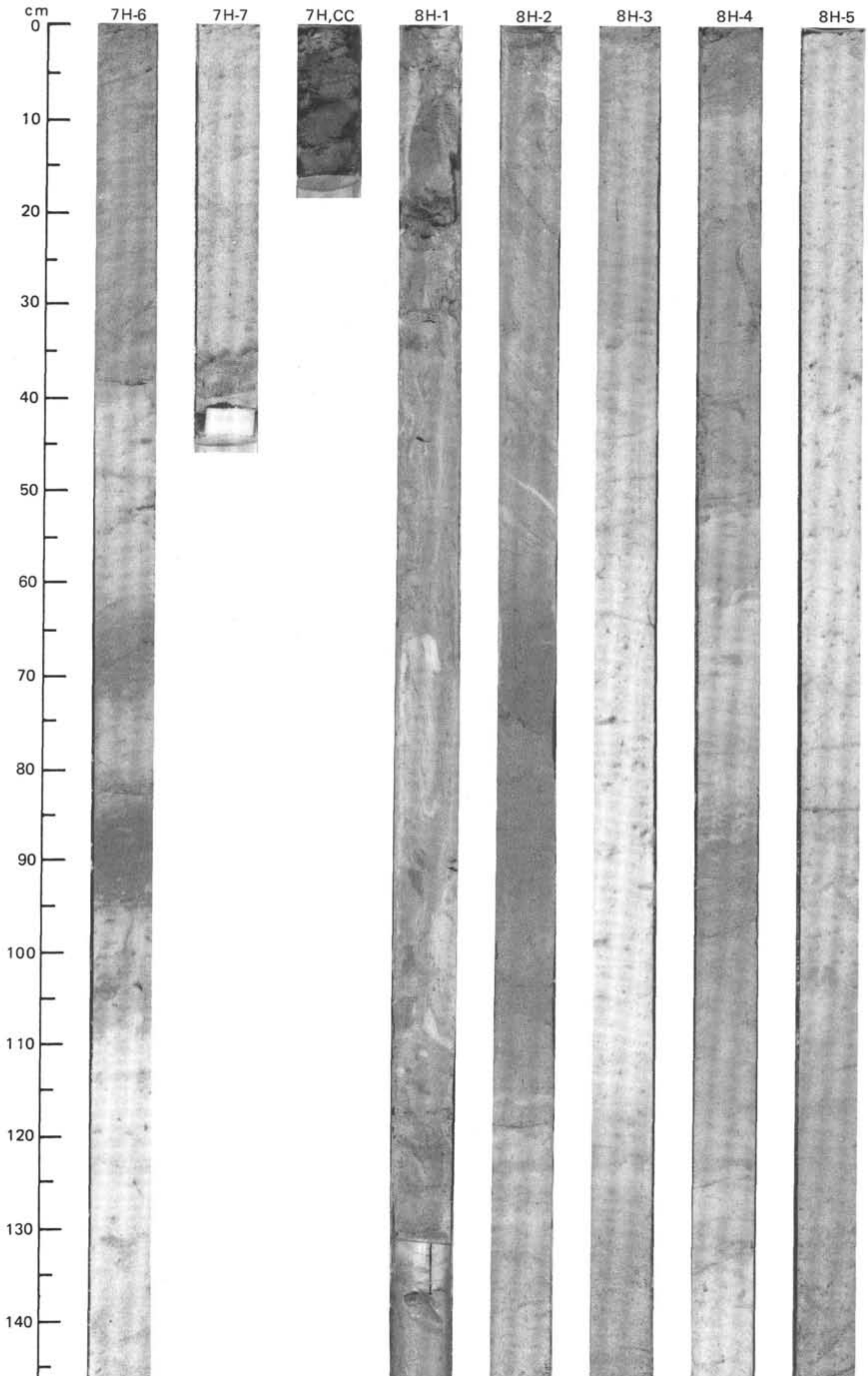
cm
0
10
20
30
40
50
60
70
80
90
100
110
120
130
140
150
7H-6
7H-7
7H,CC
8H-1
8H-2
8H-3
8H-4
8H-5

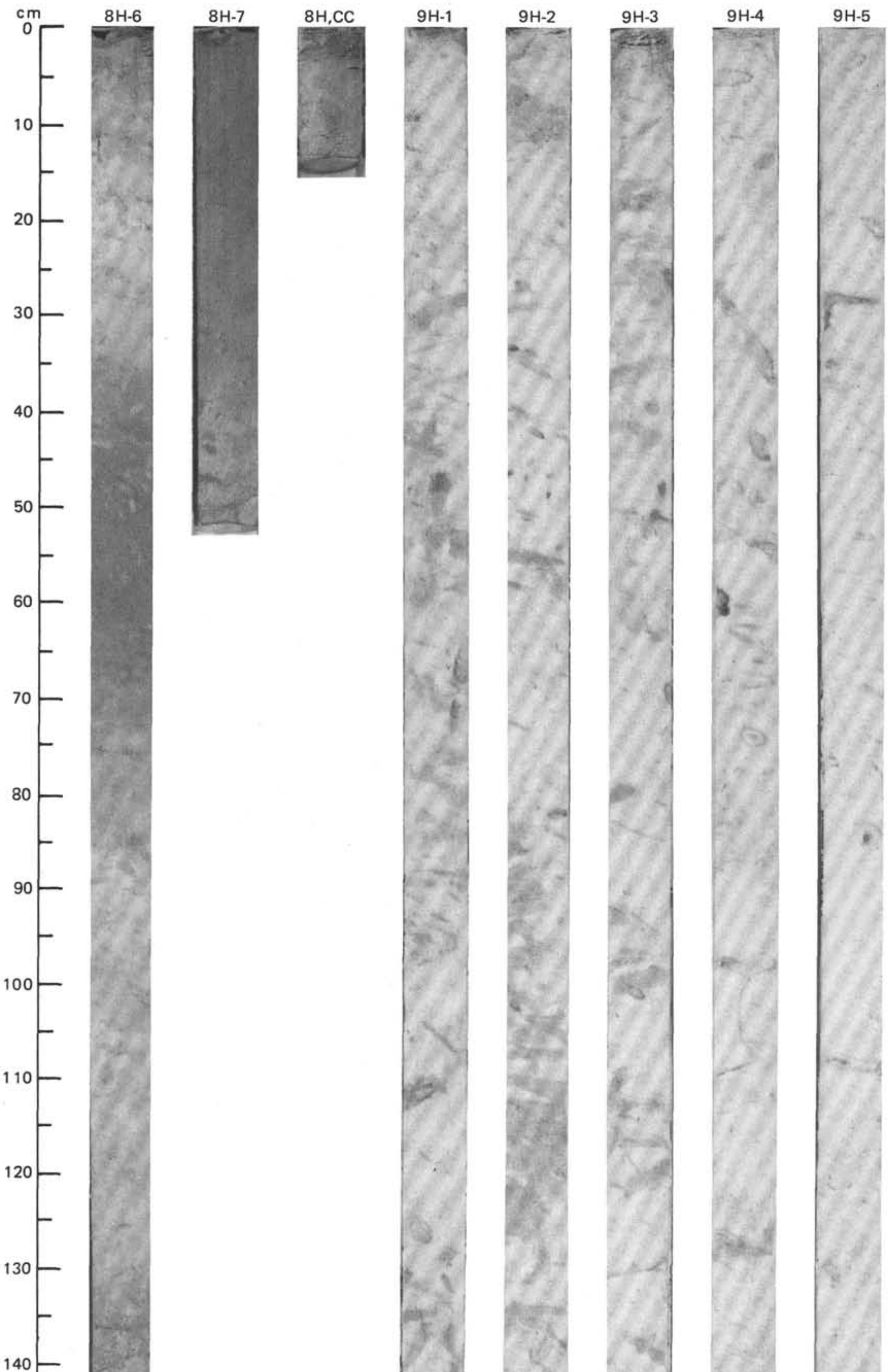
cm
0
10
20
30
40
50
60
70
80
90
100
110
120
130
140
150
8H-6
8H-7
8H,CC
9H-1
9H-2
9H-3
9H-4
9H-5

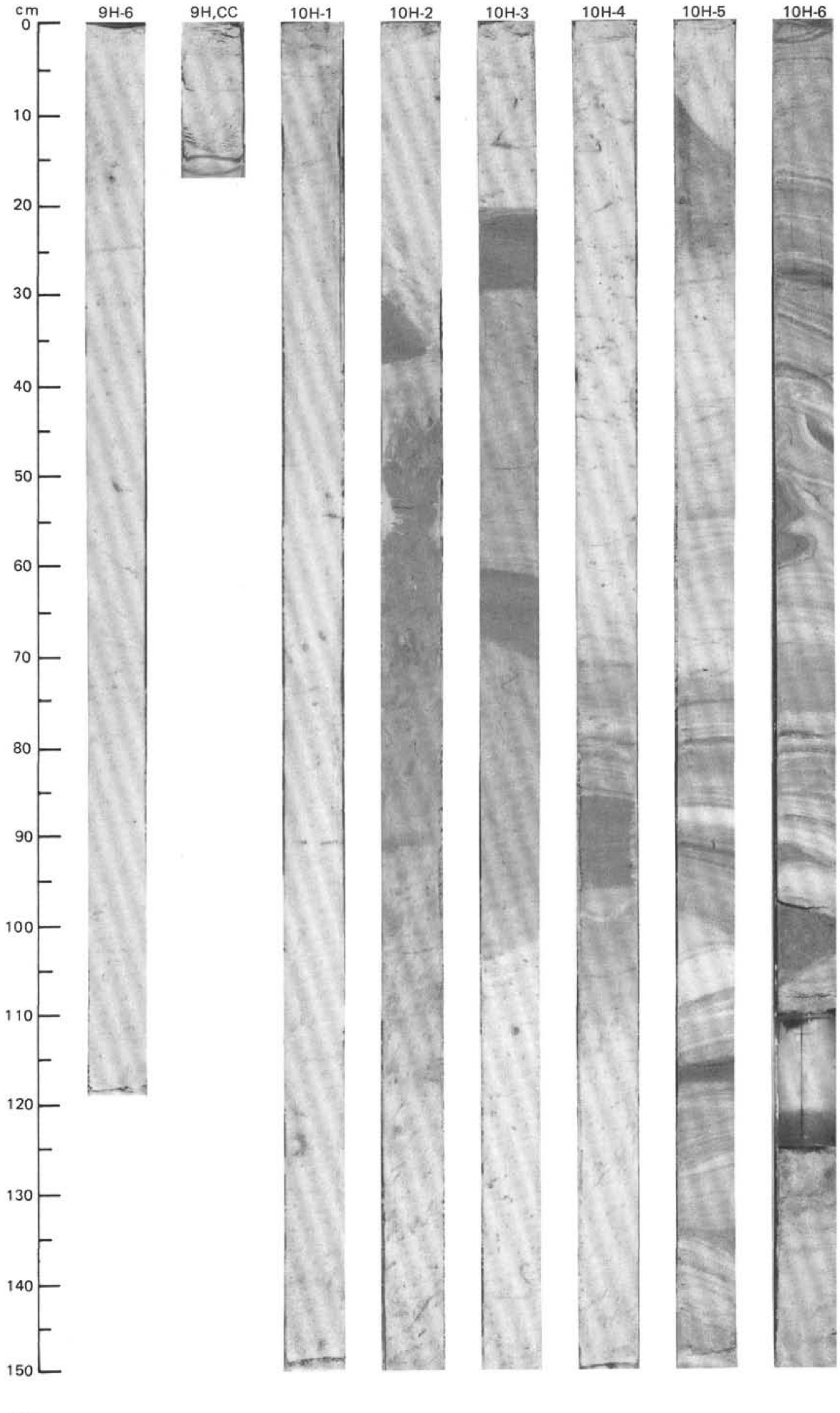
cm
0
10
20
30
40
50
60
70
80
90
100
110
120
130
140
150
9H-6
9H,CC
10H-1
10H-2
10H-3
10H-4
10H-5
10H-6

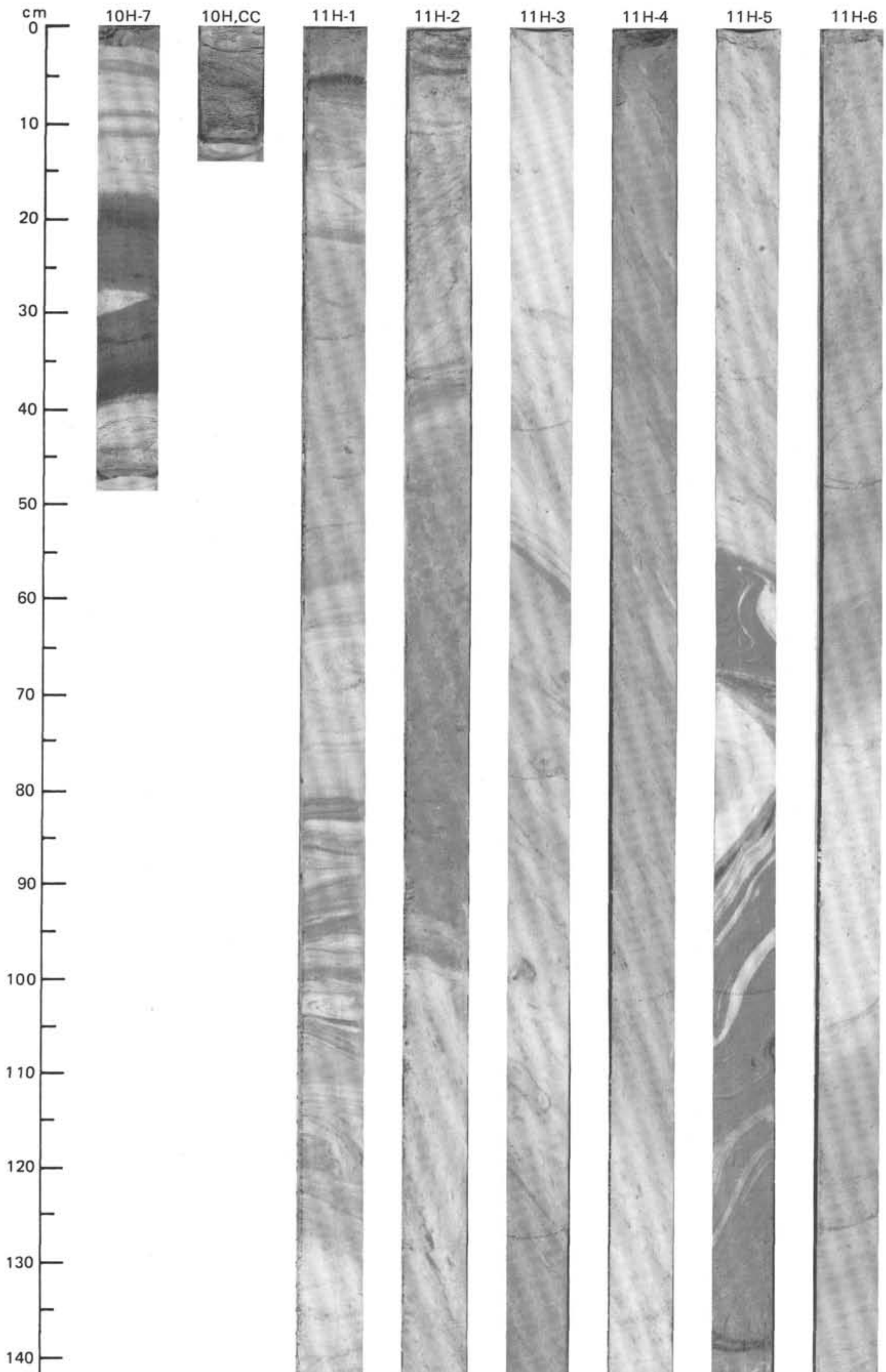
cm
0
10
20
30
40
50
60
70
80
90
100
110
120
130
140
150
10H-7
10H,CC
11H-1
11H-2
11H-3
11H-4
11H-5
11H-6

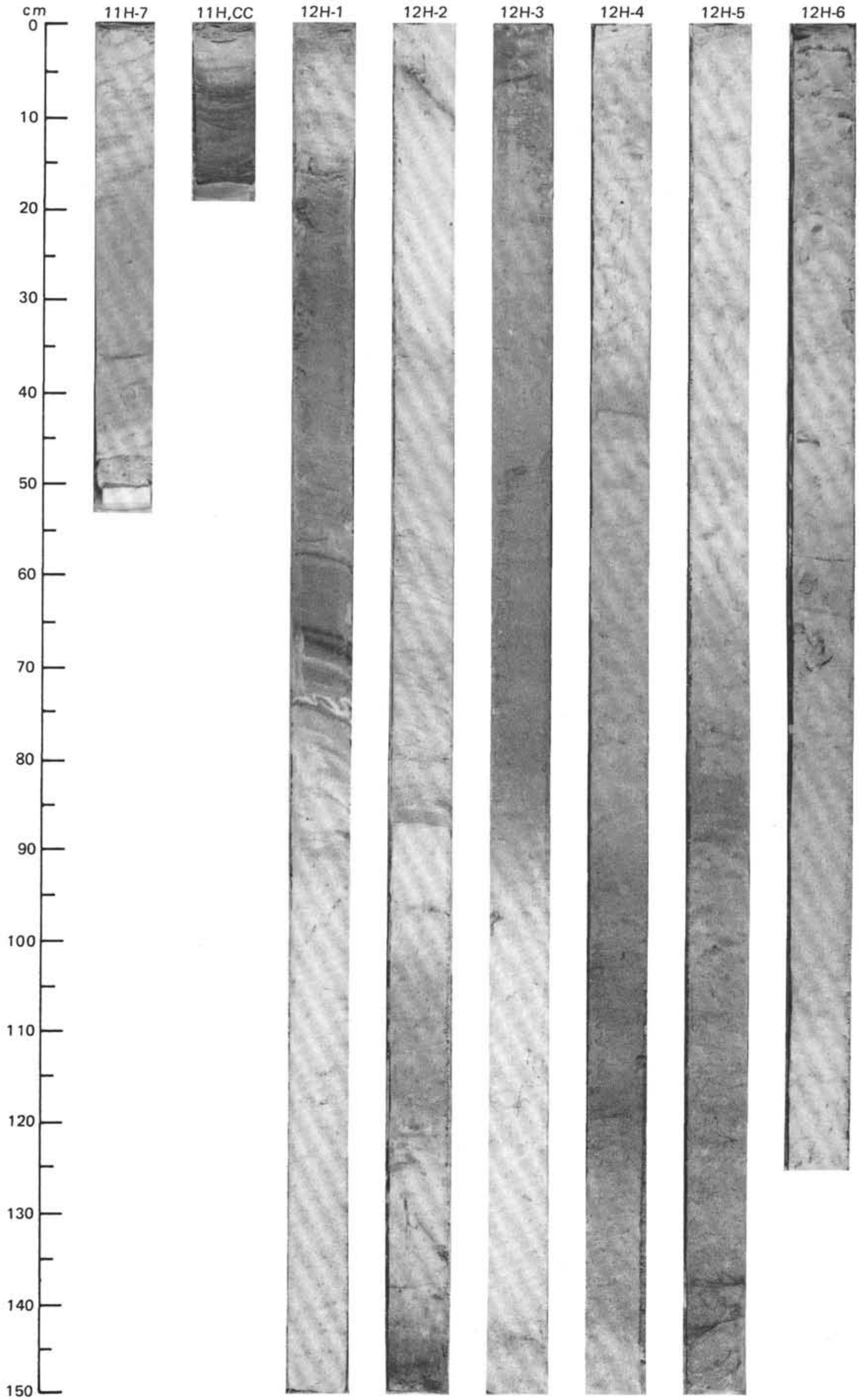
cm
0
10
20
30
40
50
60
70
80
90
100
110
120
130
140
150
11H-7
11H,CC
12H-1
12H-2
12H-3
12H-4
12H-5
12H-6

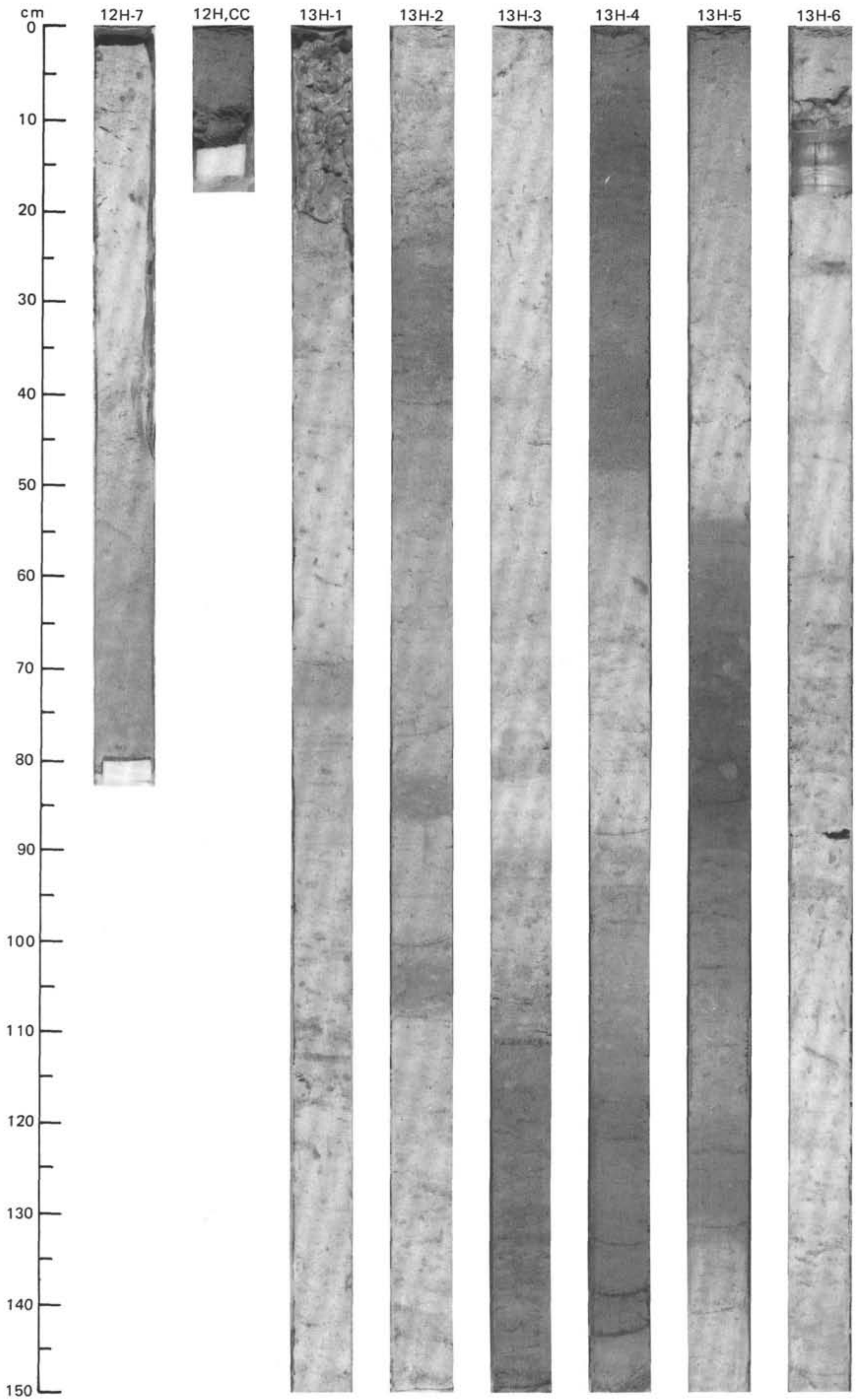
cm
0
10
20
30
40
50
60
70
80
90
100
110
120
130
140
150
12H-7
12H,CC
13H-1
13H-2
13H-3
13H-4
13H-5
13H-6

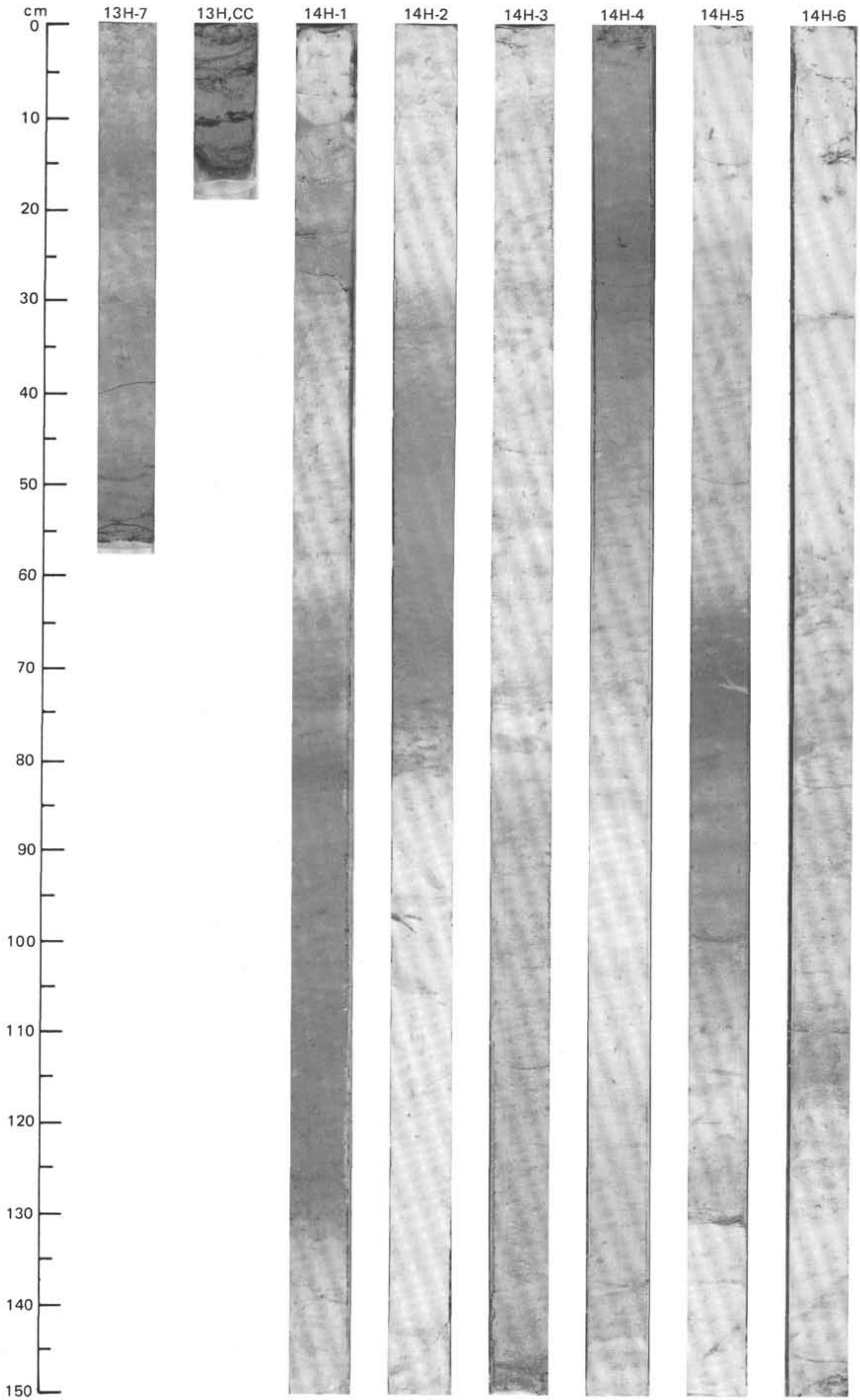
cm
0
10
20
30
40
50
60
70
80
90
100
110
120
130
140
150
13H-7
13H,CC
14H-1
14H-2
14H-3
14H-4
14H-5
14H-6

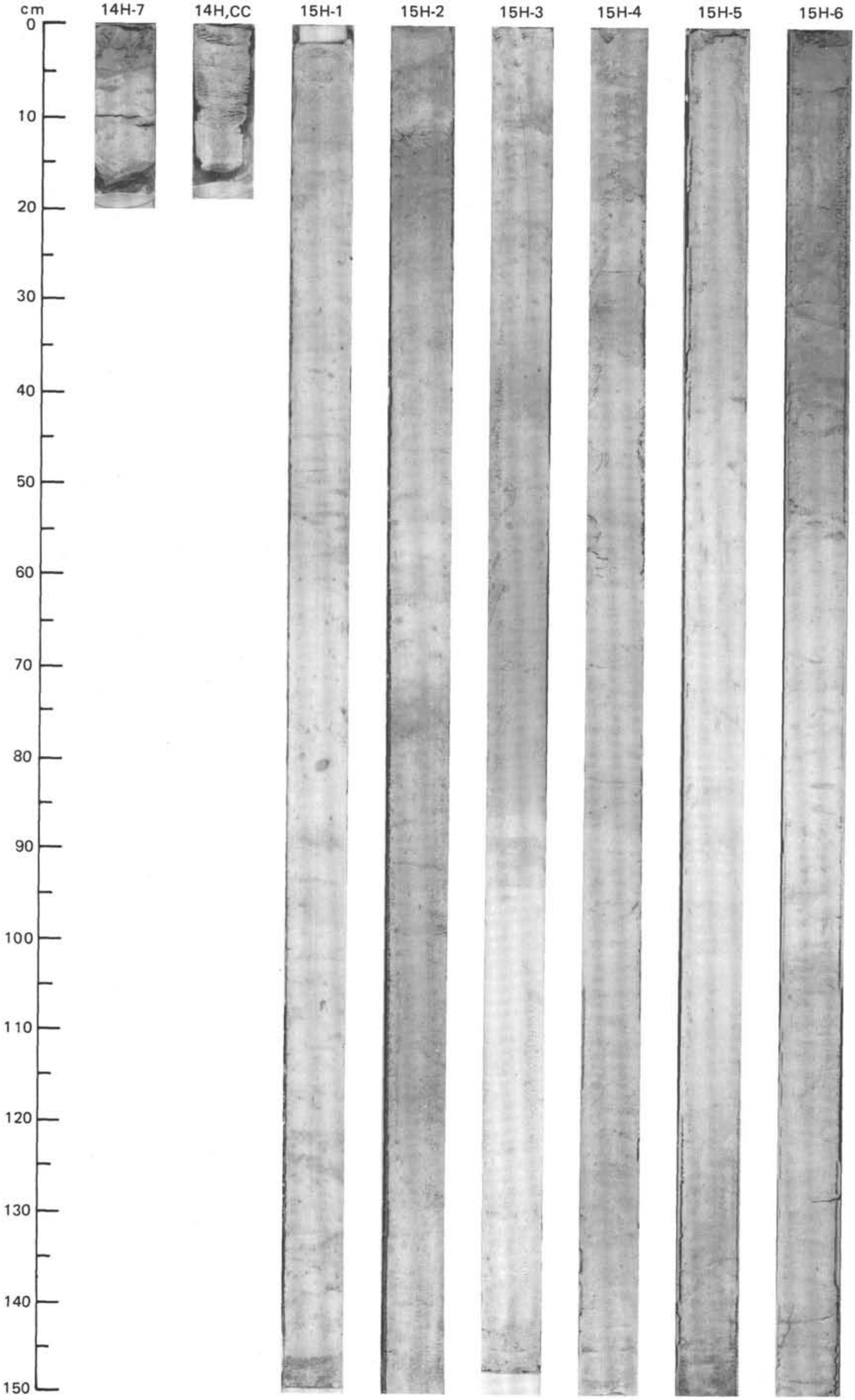
cm
14H-7
14H,CC
15H-1
15H-2
15H-3
15H-4
15H-5
15H-6
0
10
20
30
40
50
60
70
80
90
100
110
120
130
140
150

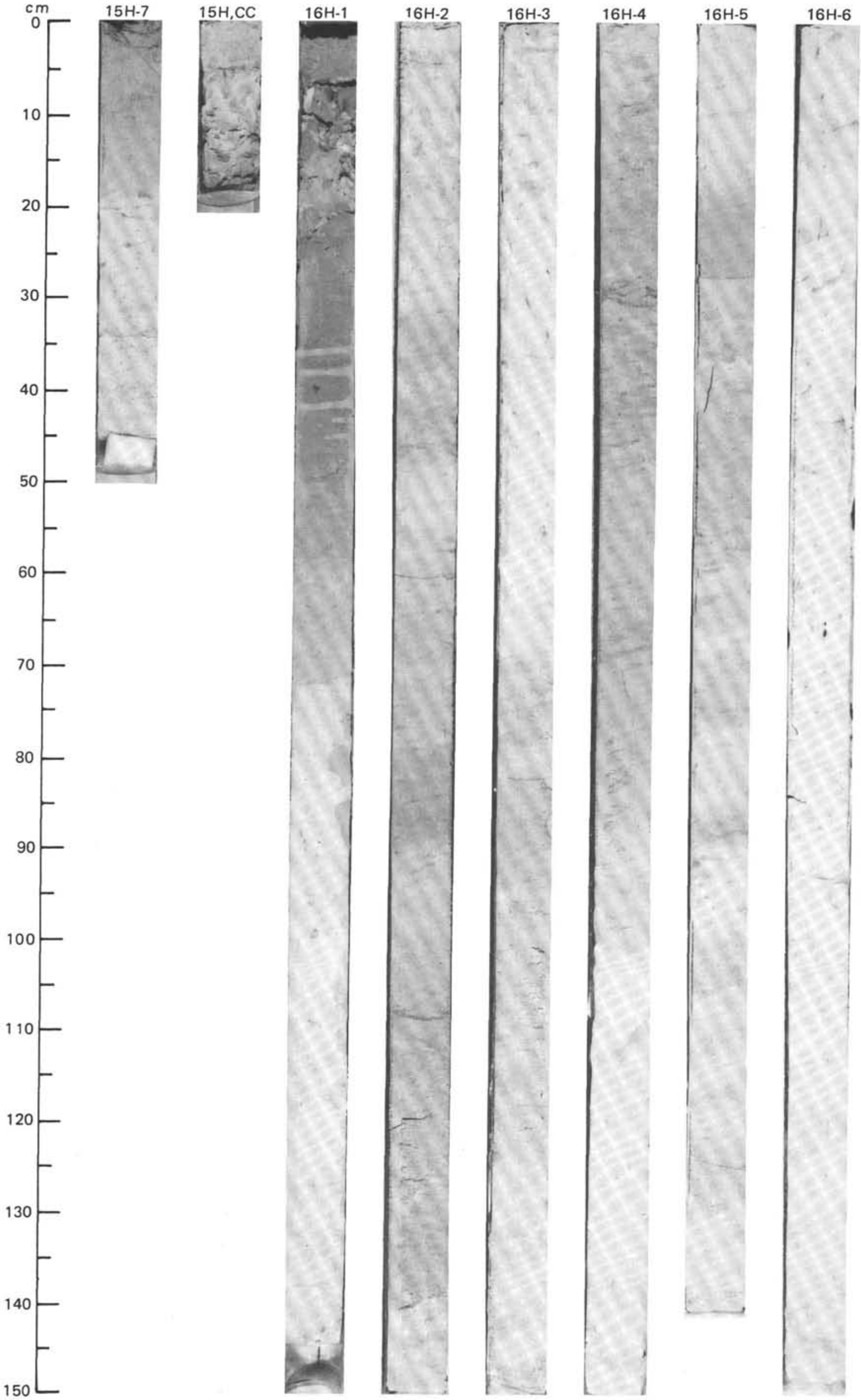
cm
0
10
20
30
40
50
60
70
80
90
100
110
120
130
140
150
15H-7
15H,CC
16H-1
16H-2
16H-3
16H-4
16H-5
16H-6

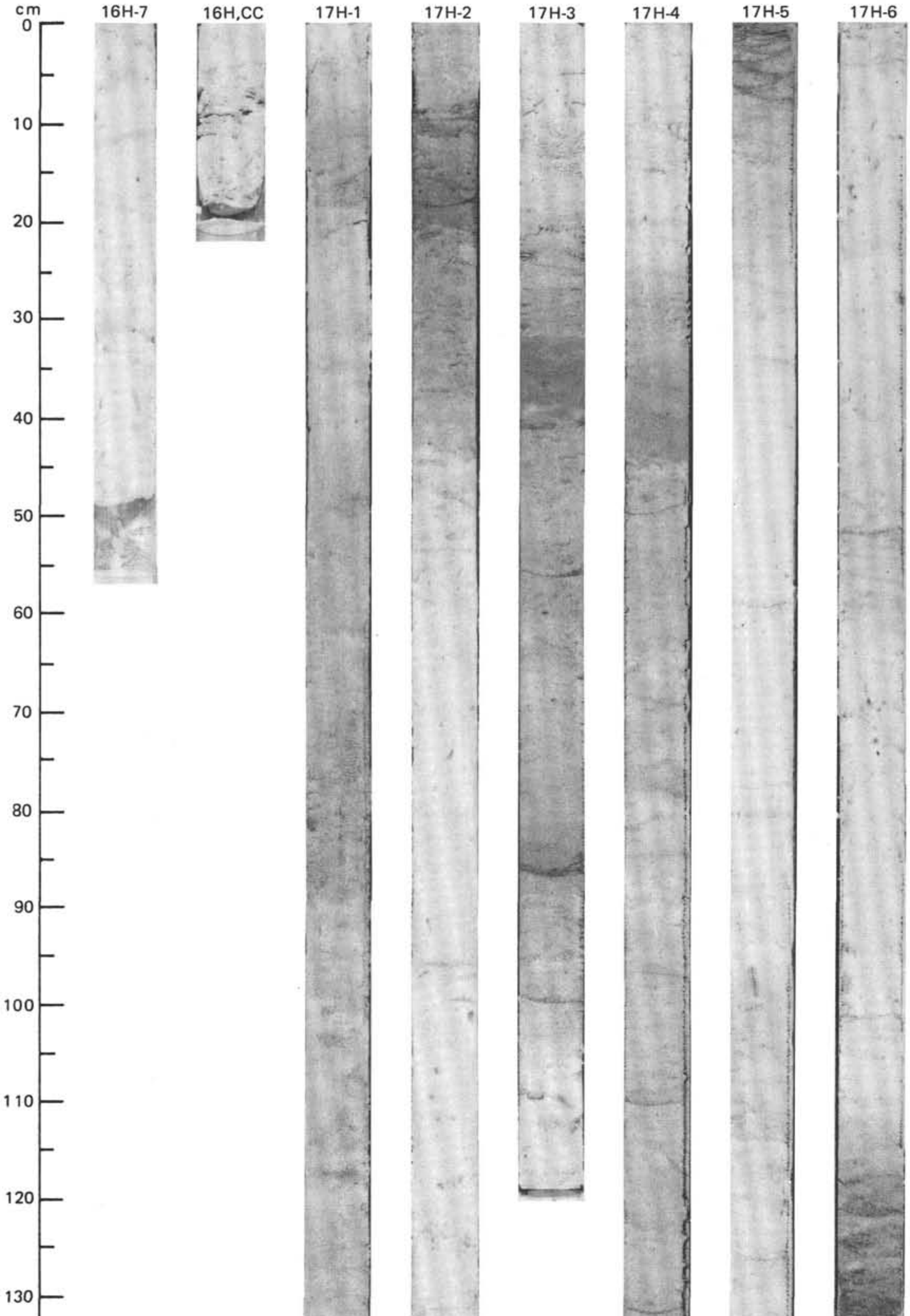
cm
0
10
20
30
40
50
60
70
80
90
100
110
120
130
140
150
16H-7
16H,CC
17H-1
17H-2
17H-3
17H-4
17H-5
17H-6

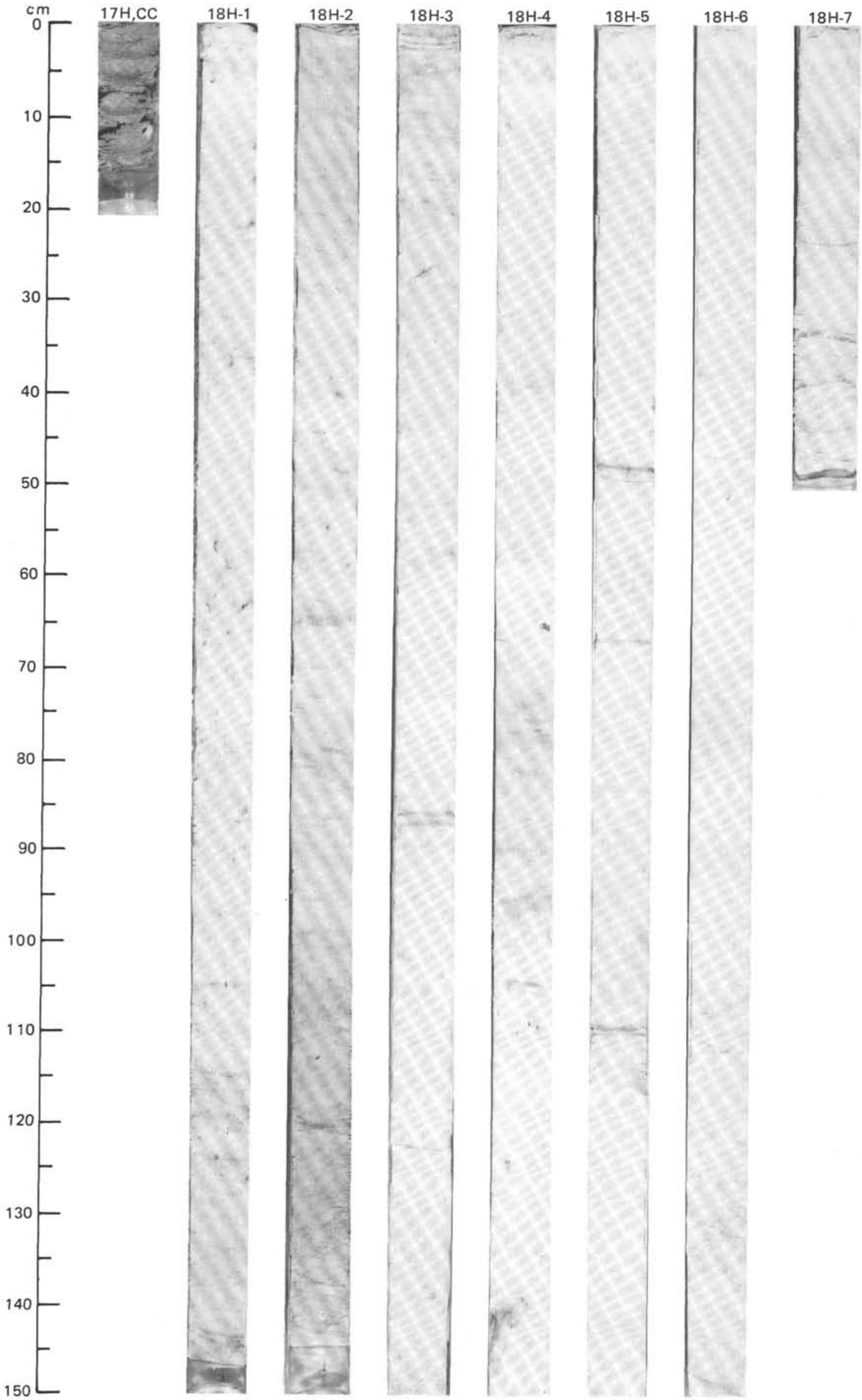
cm
0
10
20
30
40
50
60
70
80
90
100
110
120
130
140
150
17H,CC
18H-1
18H-2
18H-3
18H-4
18H-5
18H-6
18H-7

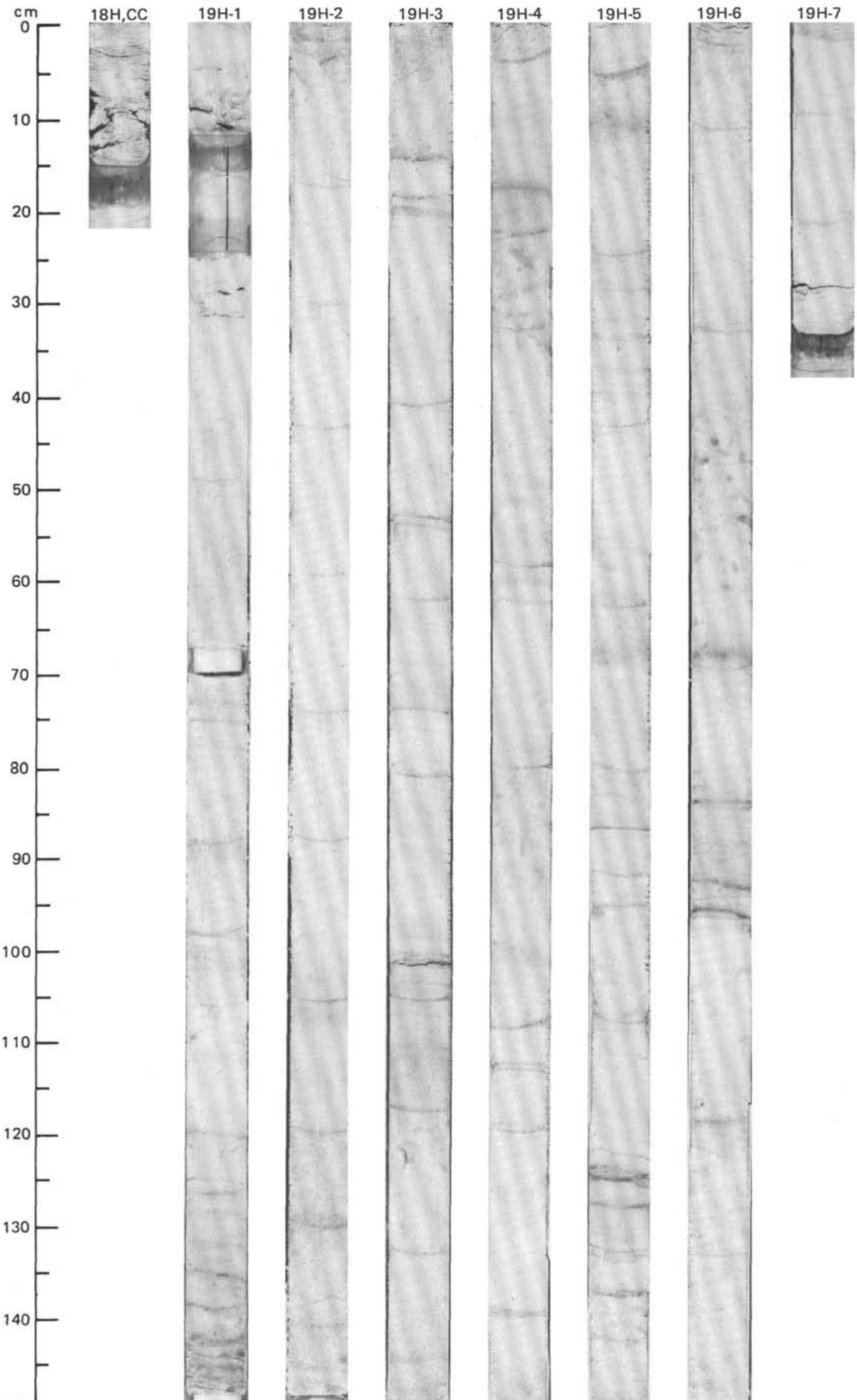
cm
0
10
20
30
40
50
60
70
80
90
100
110
120
130
140
150
18H,CC
19H-1
19H-2
19H-3
19H-4
19H-5
19H-6
19H-7

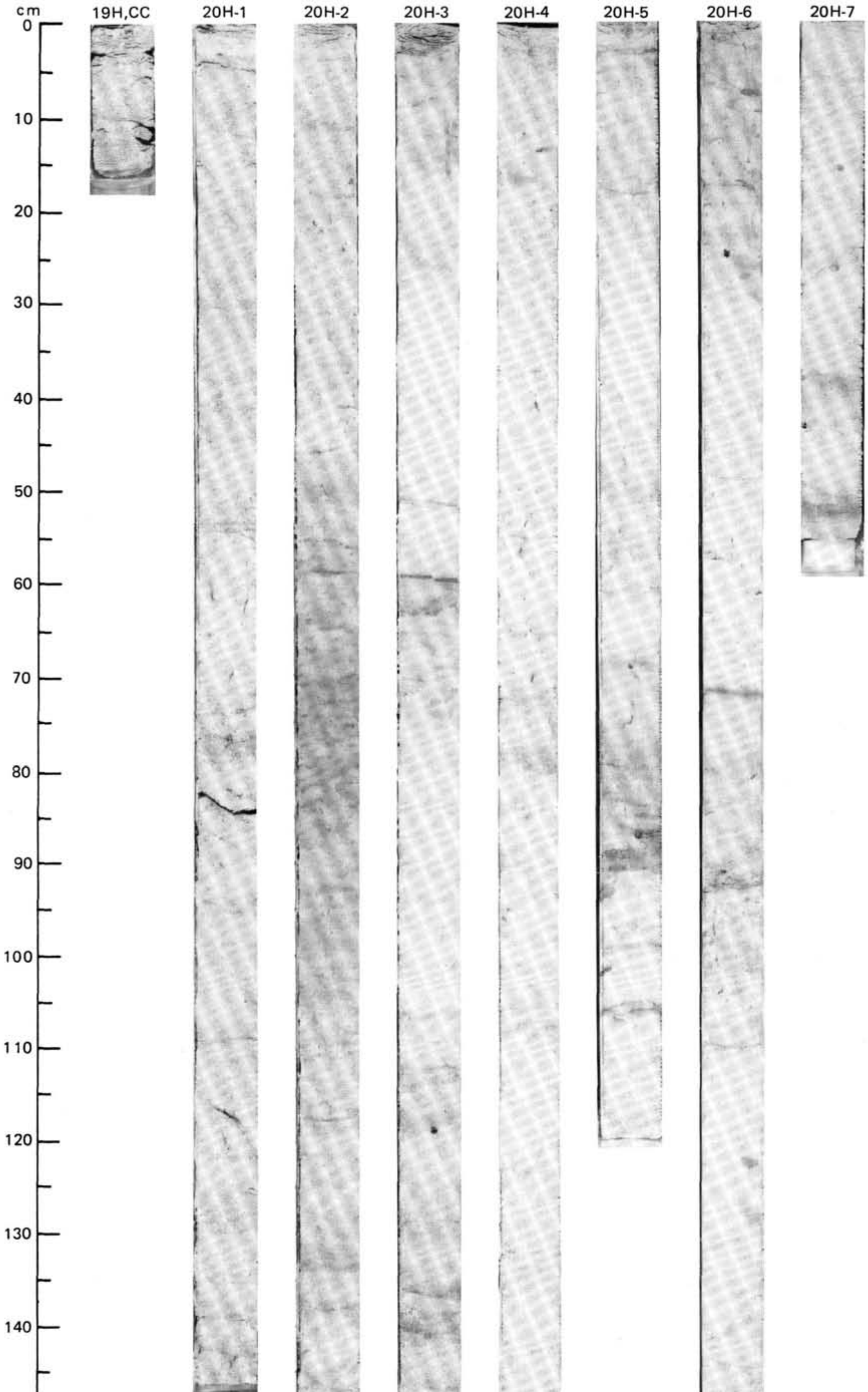
cm
0
10
20
30
40
50
60
70
80
90
100
110
120
130
140
150
19H,CC
20H-1
20H-2
20H-3
20H-4
20H-5
20H-6
20H-7

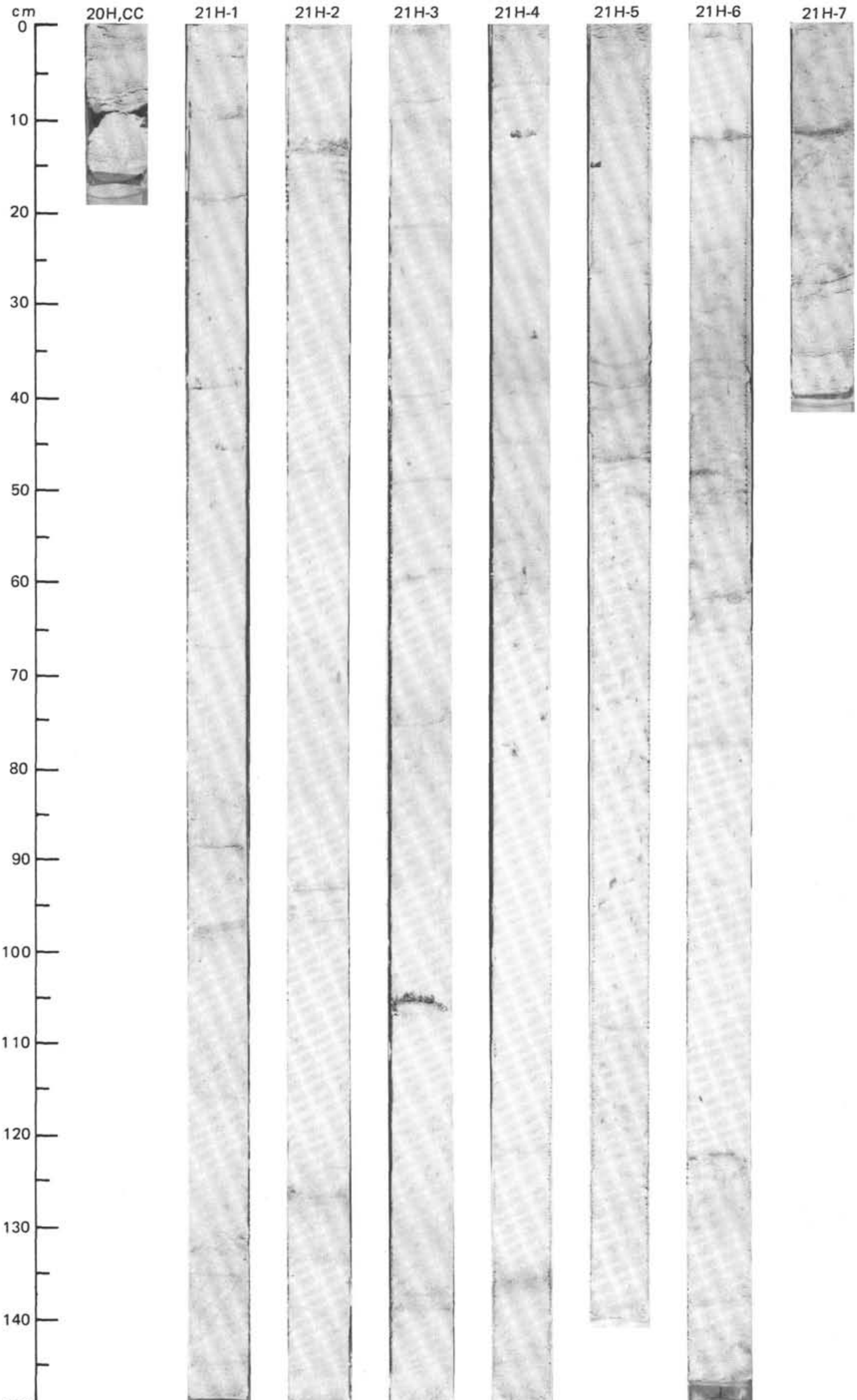
cm
0
10
20
30
40
50
60
70
80
90
100
110
120
130
140
150
20H,CC
21H-1
21H-2
21H-3
21H-4
21H-5
21H-6
21H-7

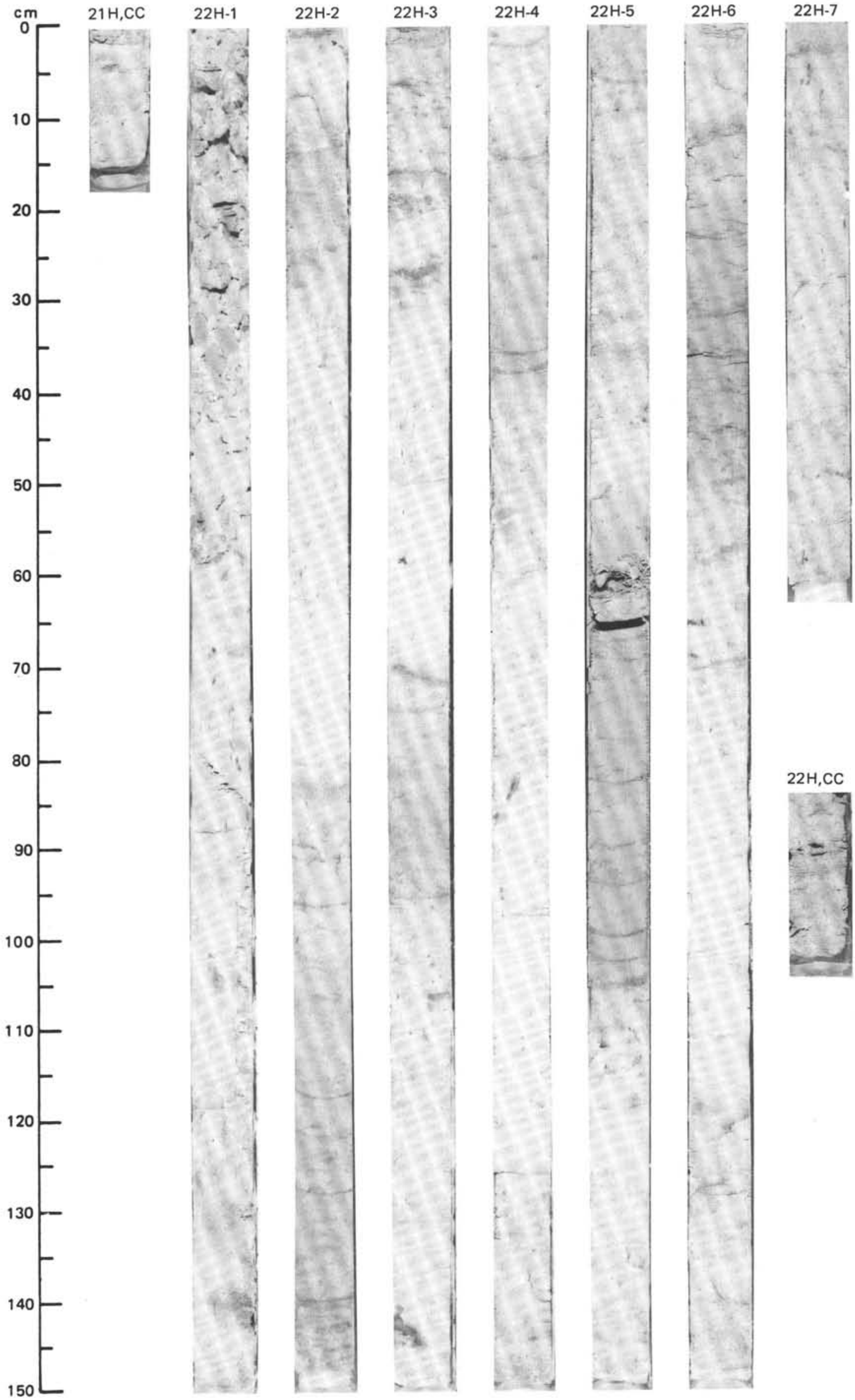
cm
0
10
20
30
40
50
60
70
80
90
100
110
120
130
140
150
21H,CC
22H-1
22H-2
22H-3
22H-4
22H-5
22H-6
22H-7
22H,CC

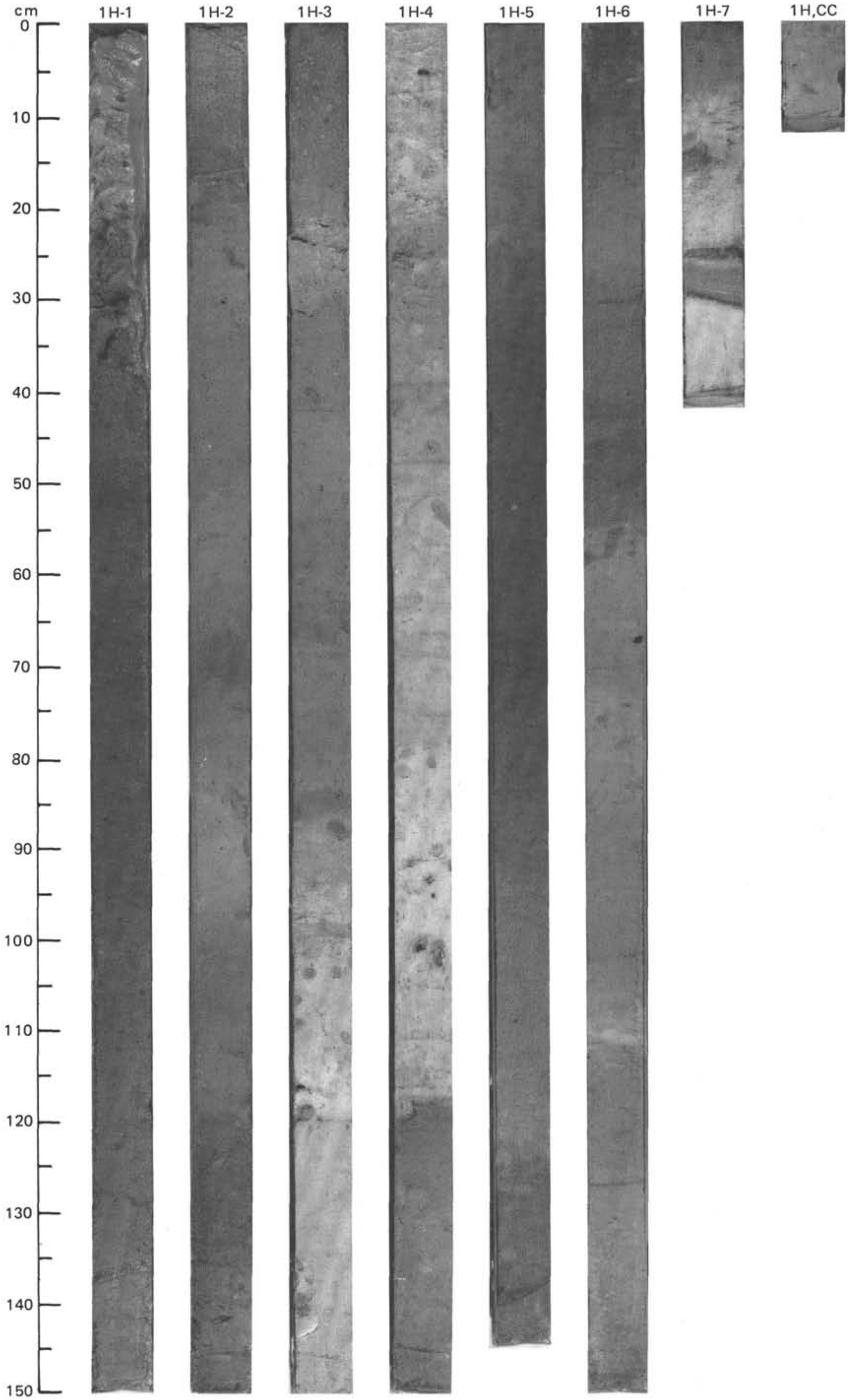
cm
0
10
20
30
40
50
60
70
80
90
100
110
120
130
140
150
1H-1
1H-2
1H-3
1H-4
1H-5
1H-6
1H-7
1H,CC

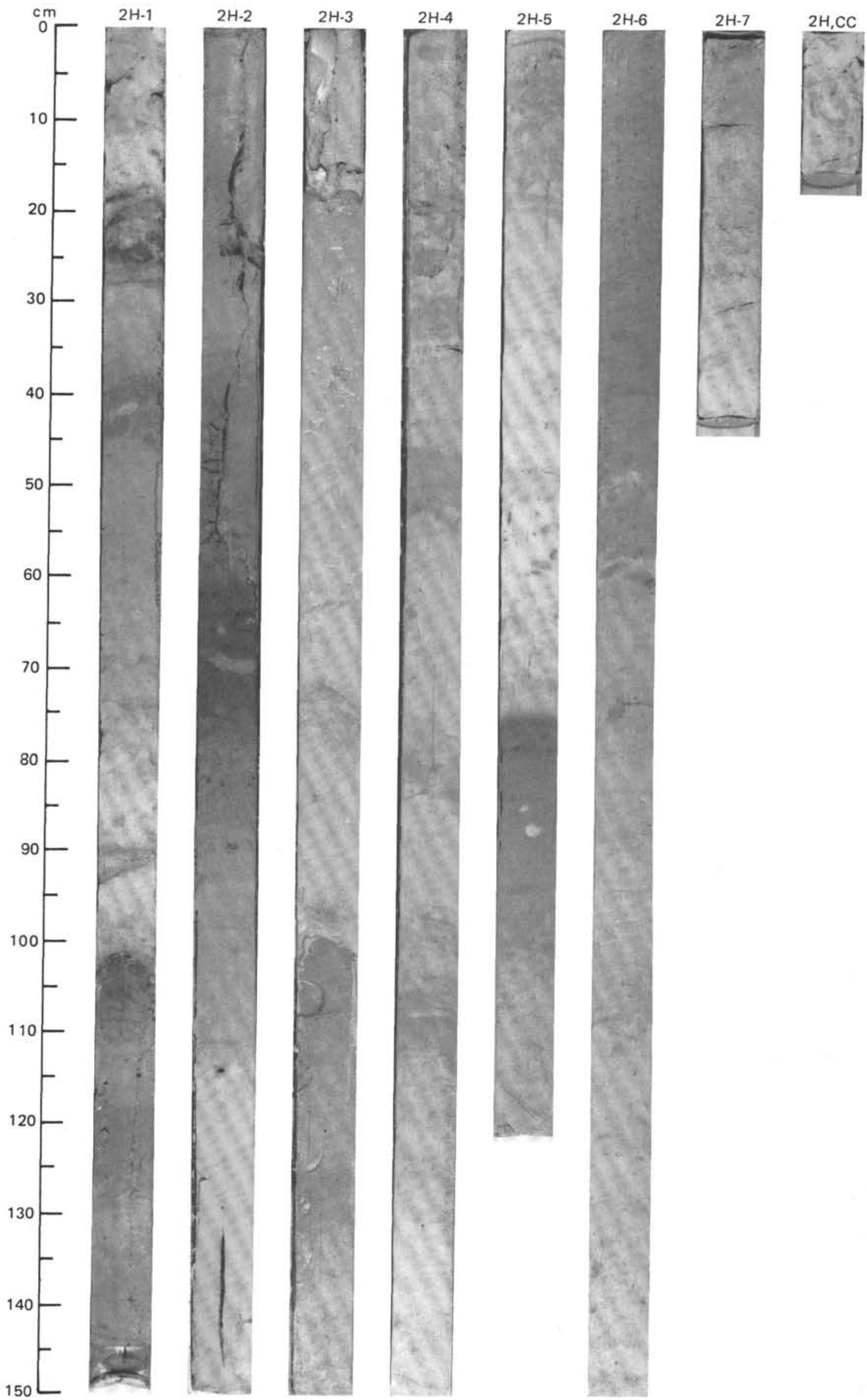
cm
0
10
20
30
40
50
60
70
80
90
100
110
120
130
140
150
2H-1
2H-2
2H-3
2H-4
2H-5
2H-6
2H-7
2H,CC

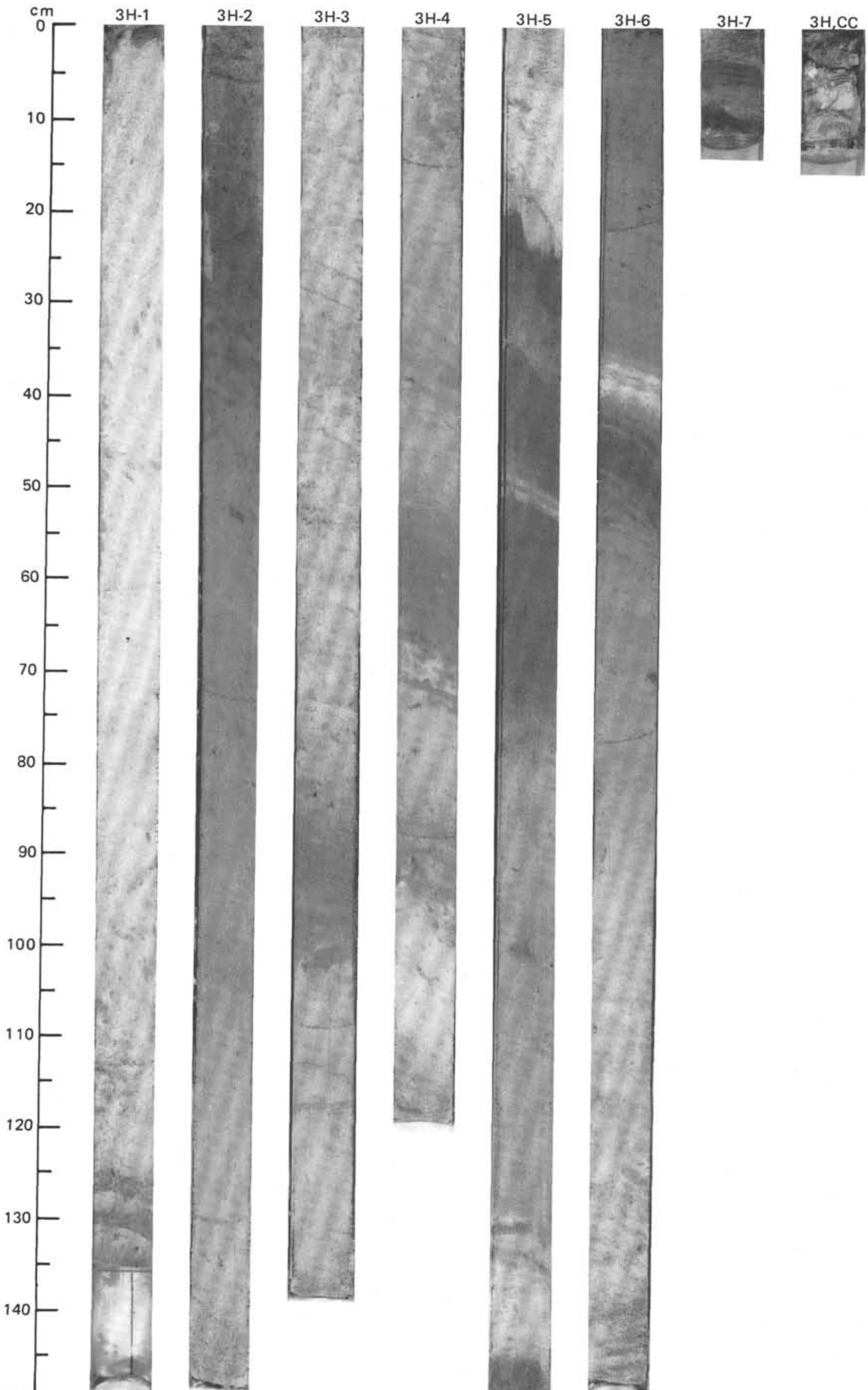
cm
0
10
20
30
40
50
60
70
80
90
100
110
120
130
140
150
3H-1
3H-2
3H-3
3H-4
3H-5
3H-6
3H-7
3H,CC

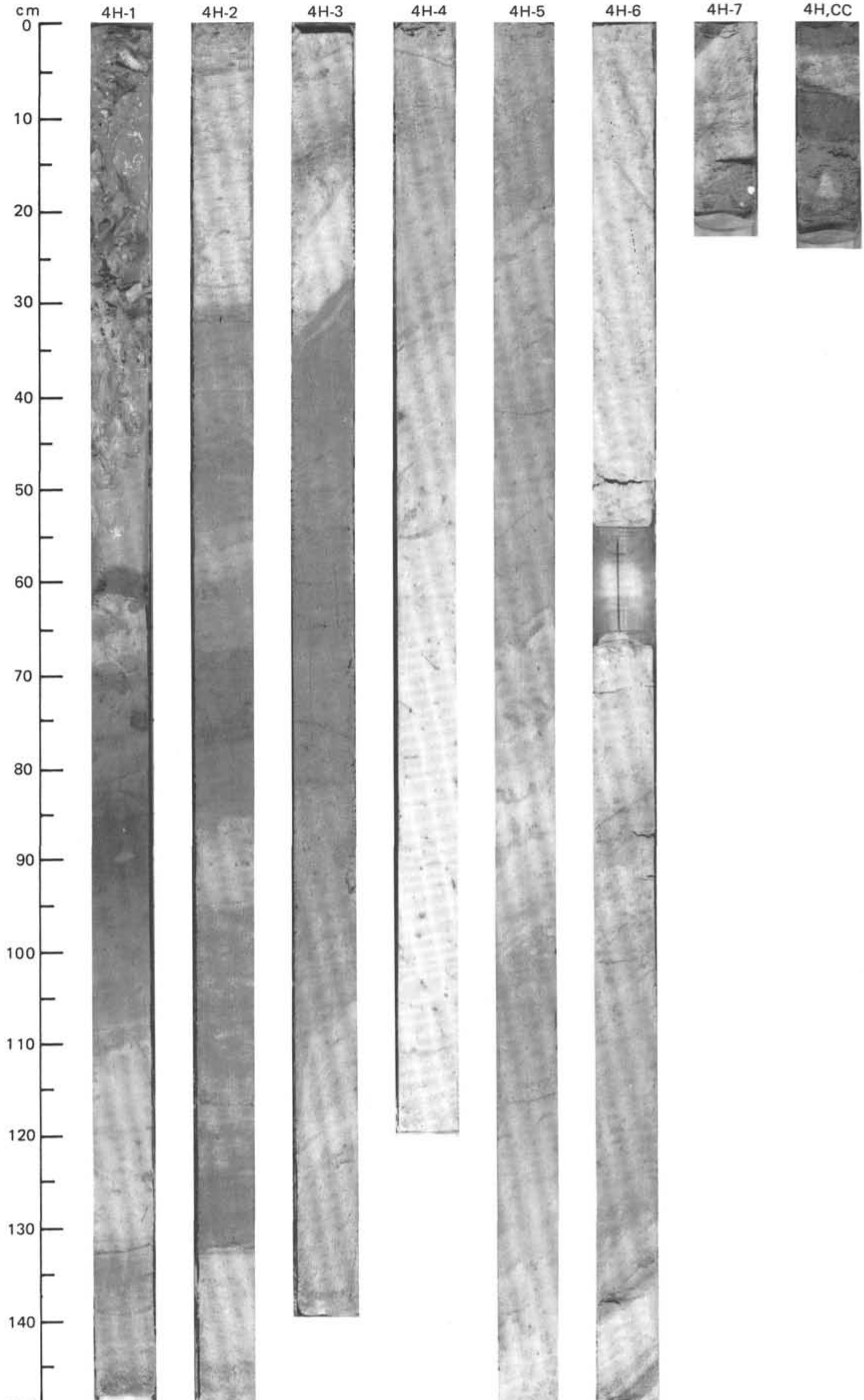
cm
0
10
20
30
40
50
60
70
80
90
100
110
120
130
140
150
4H-1
4H-2
4H-3
4H-4
4H-5
4H-6
4H-7
4H,CC

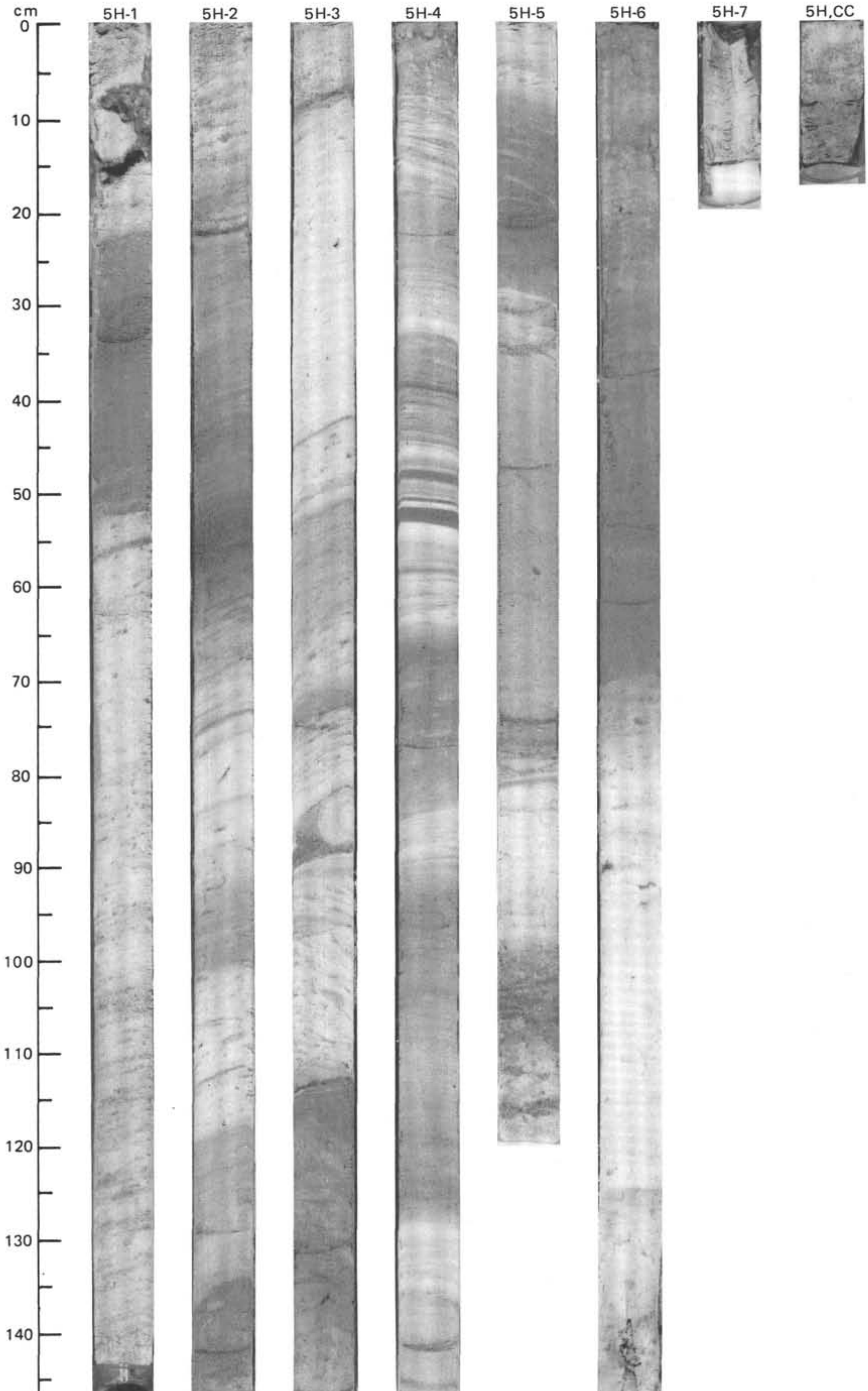
cm
0
10
20
30
40
50
60
70
80
90
100
110
120
130
140
150
5H-1
5H-2
5H-3
5H-4
5H-5
5H-6
5H-7
5H,CC

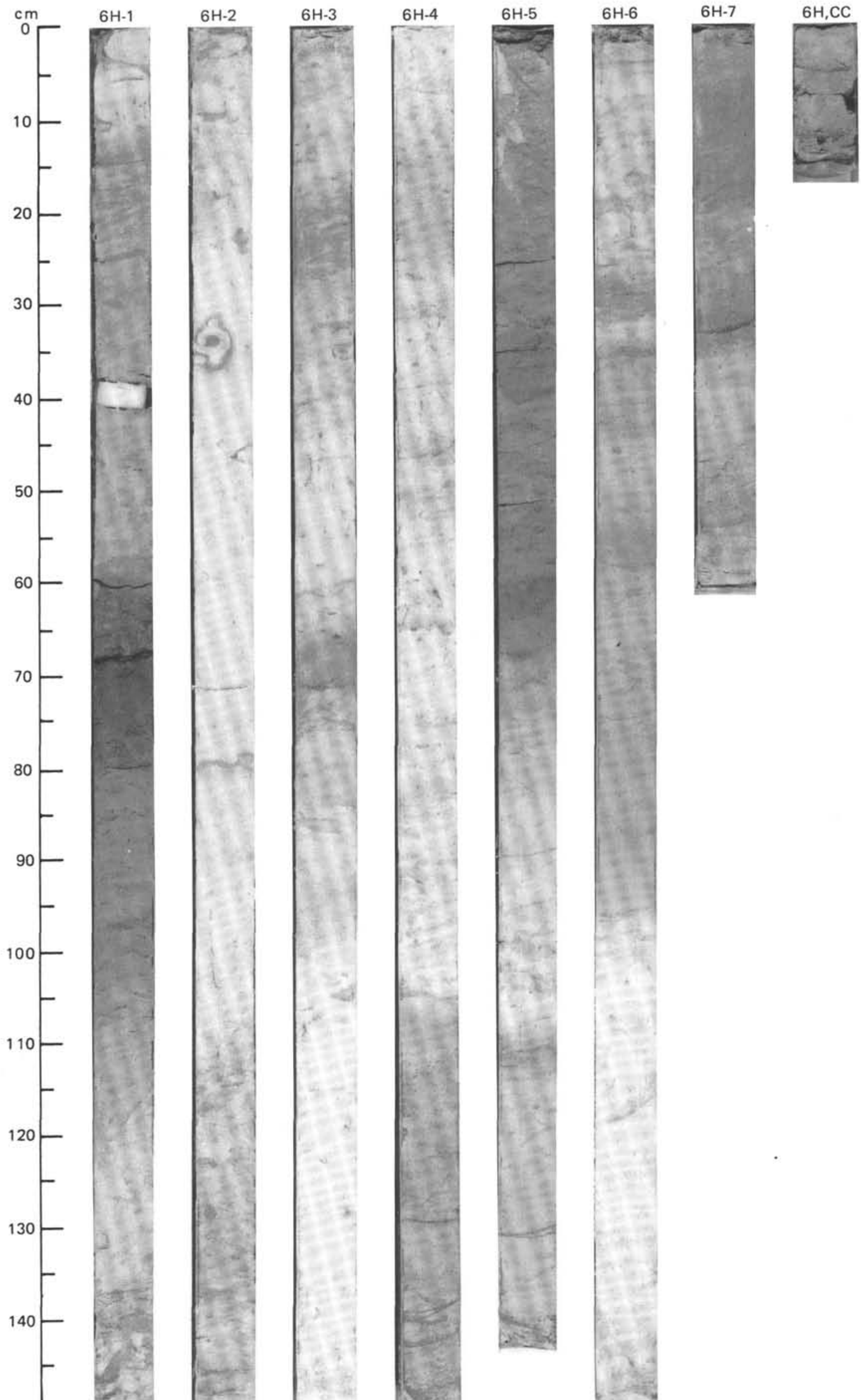
cm
0
10
20
30
40
50
60
70
80
90
100
110
120
130
140
150
6H-1
6H-2
6H-3
6H-4
6H-5
6H-6
6H-7
6H,CC

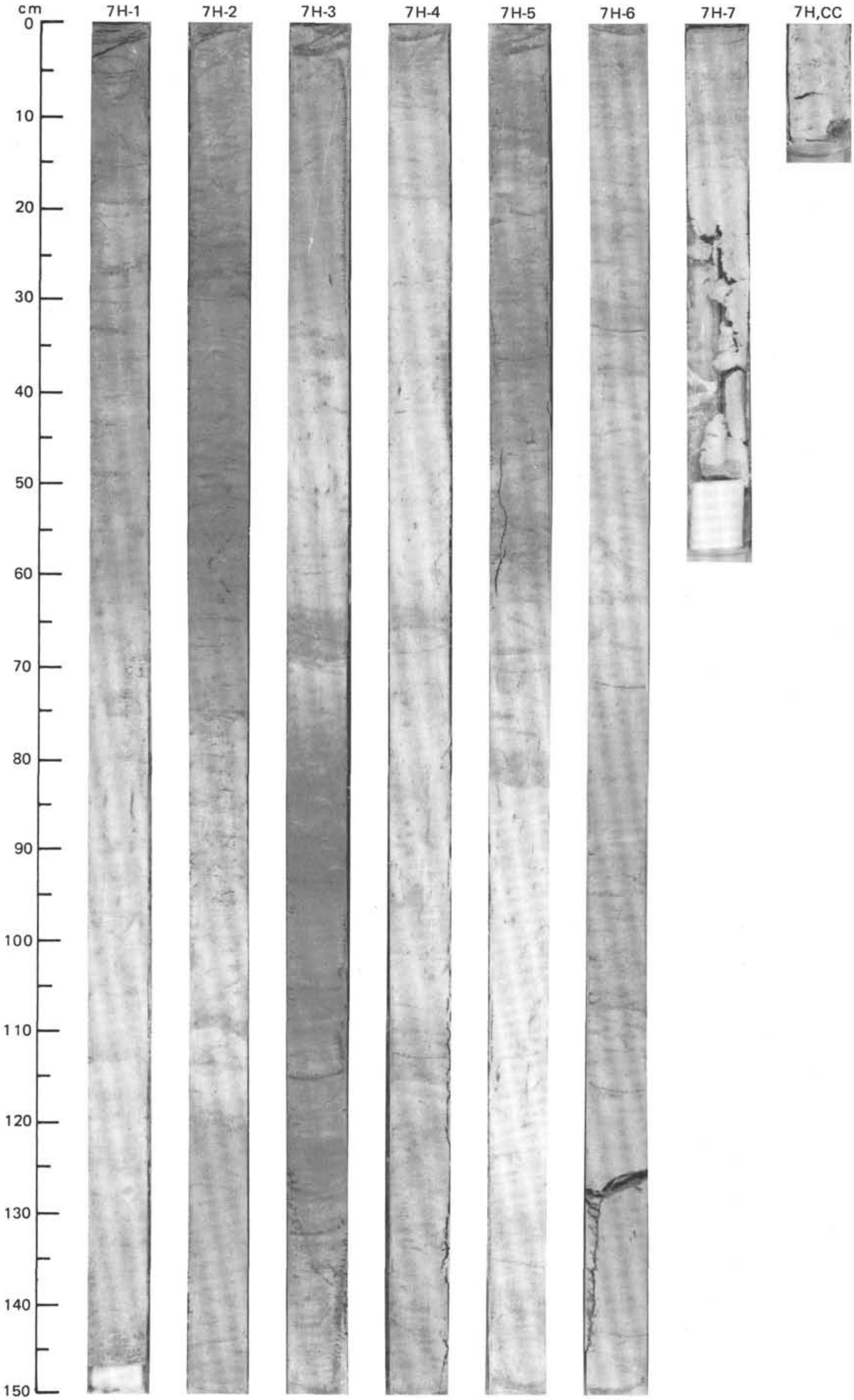
cm
0
10
20
30
40
50
60
70
80
90
100
110
120
130
140
150
7H-1
7H-2
7H-3
7H-4
7H-5
7H-6
7H-7
7H,CC

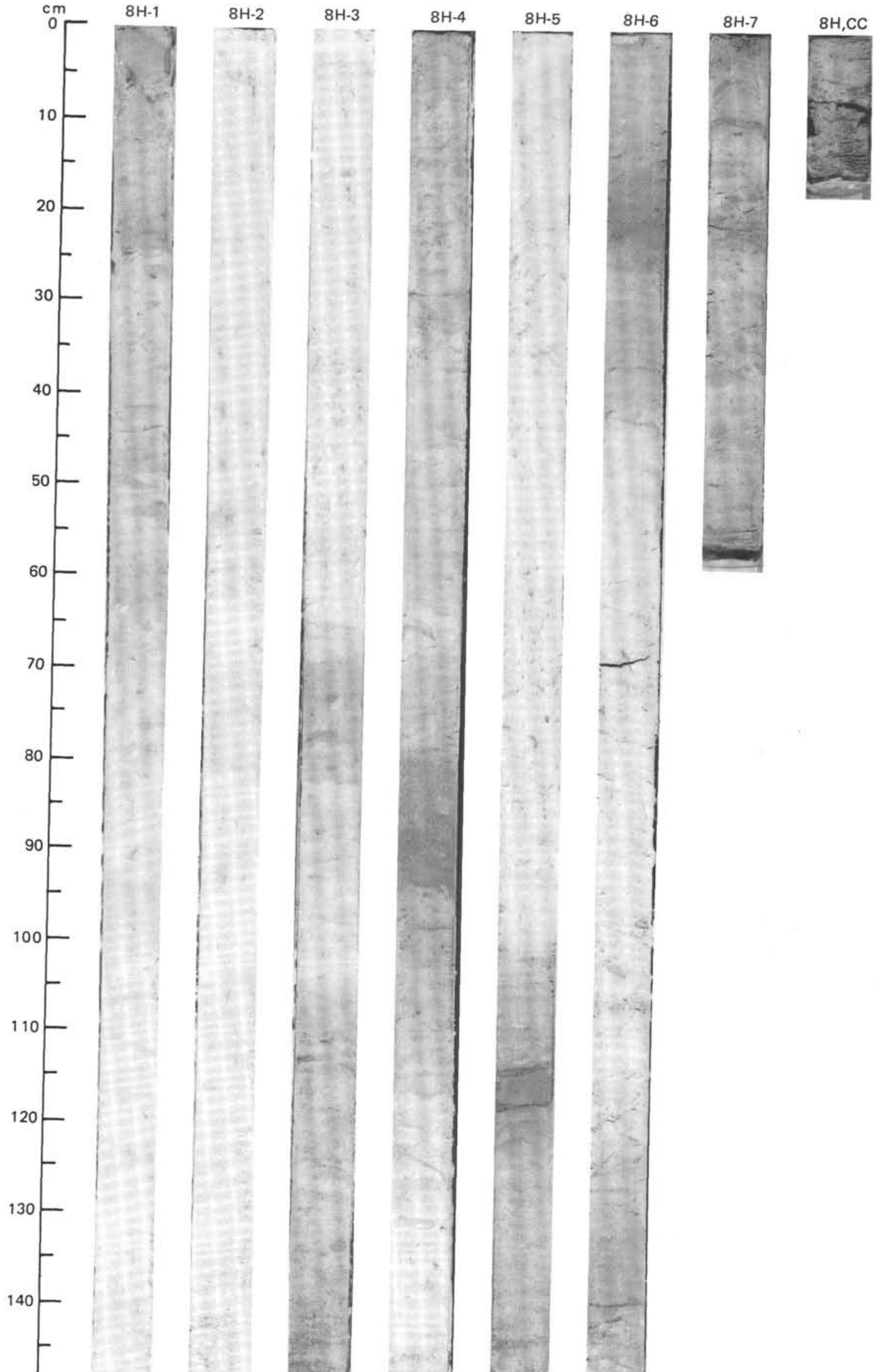
cm
0
10
20
30
40
50
60
70
80
90
100
110
120
130
140
150
8H-1
8H-2
8H-3
8H-4
8H-5
8H-6
8H-7
8H,CC

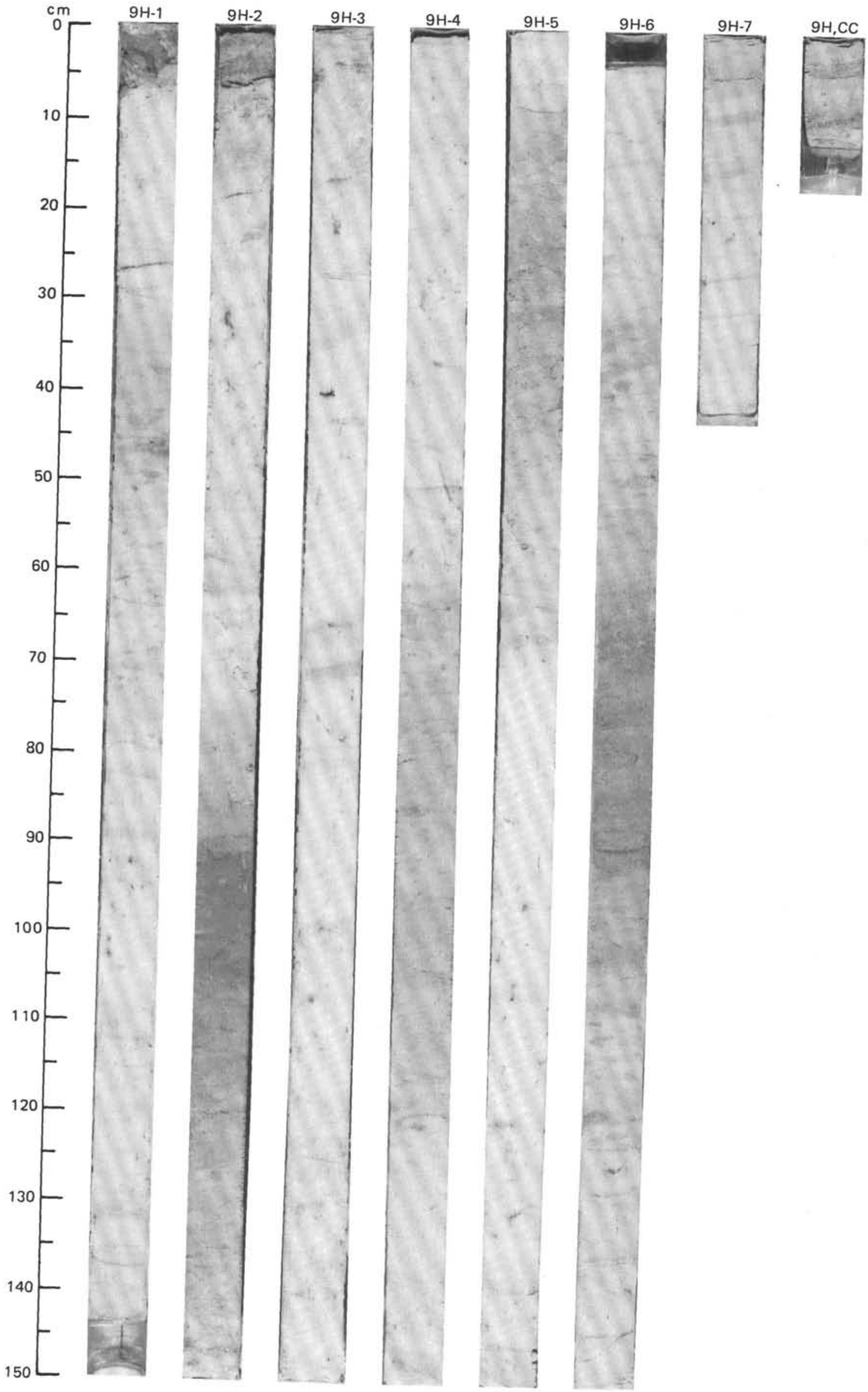
cm
0
10
20
30
40
50
60
70
80
90
100
110
120
130
140
150
9H-1
9H-2
9H-3
9H-4
9H-5
9H-6
9H-7
9H,CC

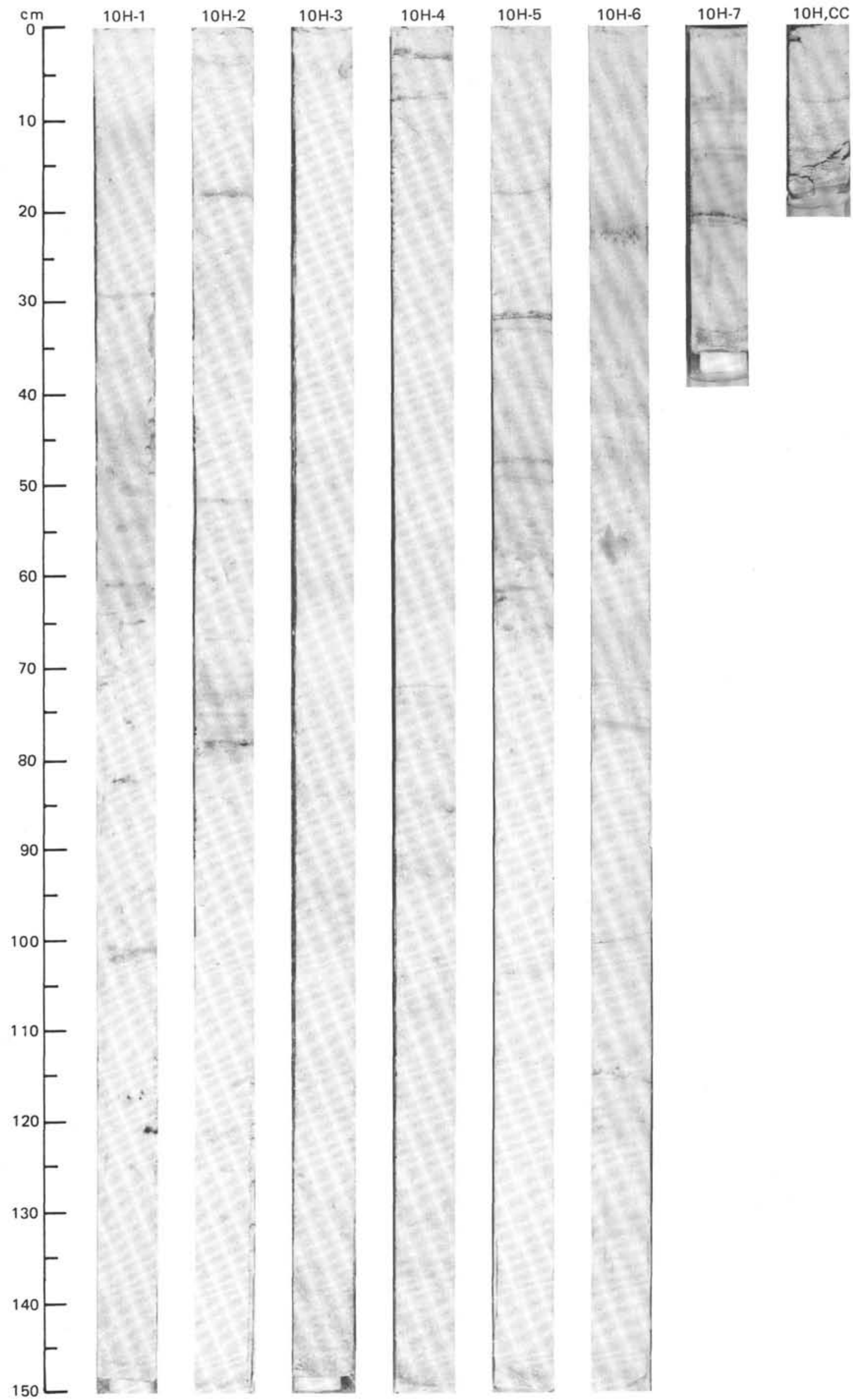
cm
0
10
20
30
40
50
60
70
80
90
100
110
120
130
140
150
10H-1
10H-2
10H-3
10H-4
10H-5
10H-6
10H-7
10H,CC

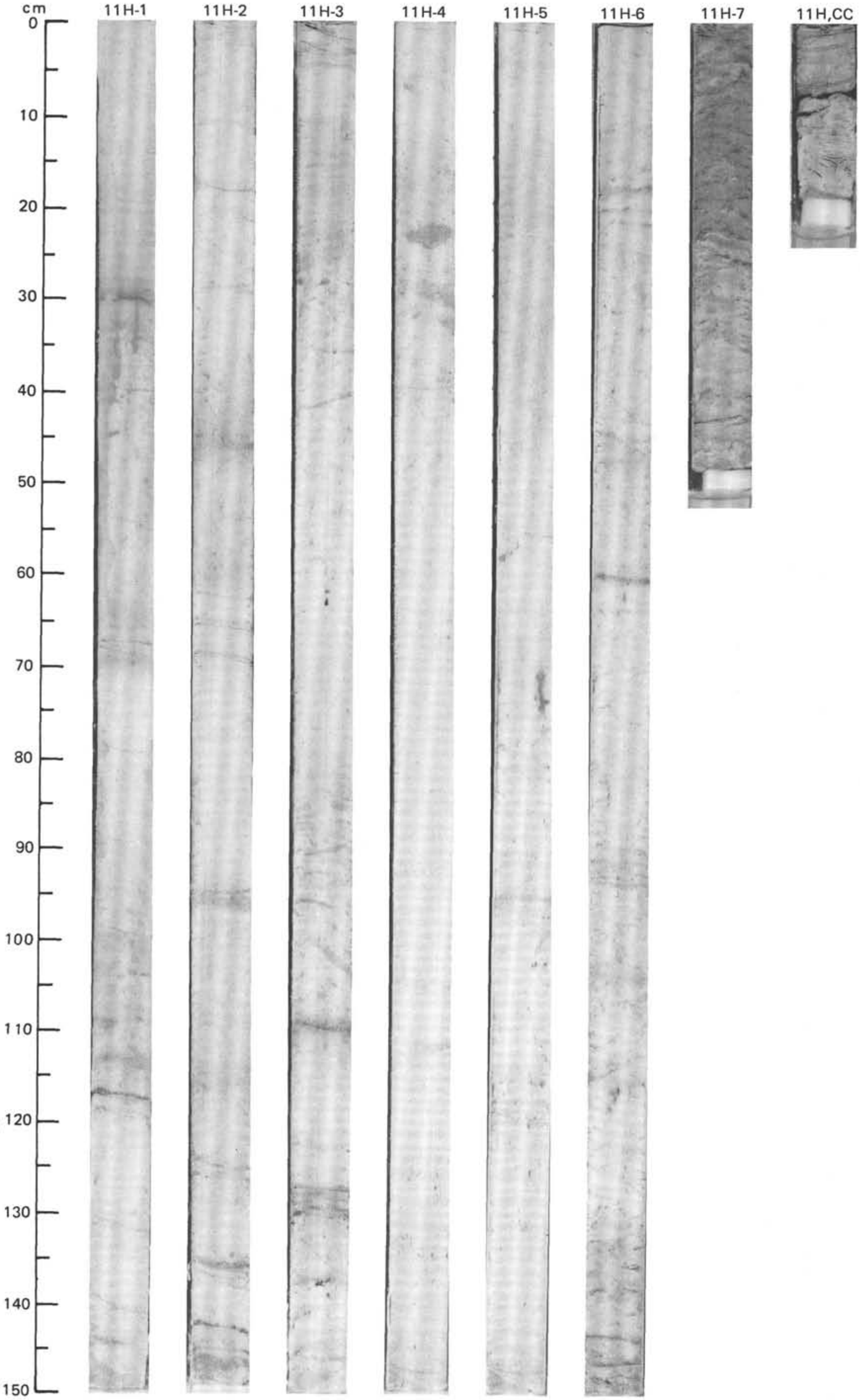
cm
0
10
20
30
40
50
60
70
80
90
100
110
120
130
140
150
11H-1
11H-2
11H-3
11H-4
11H-5
11H-6
11H-7
11H,CC

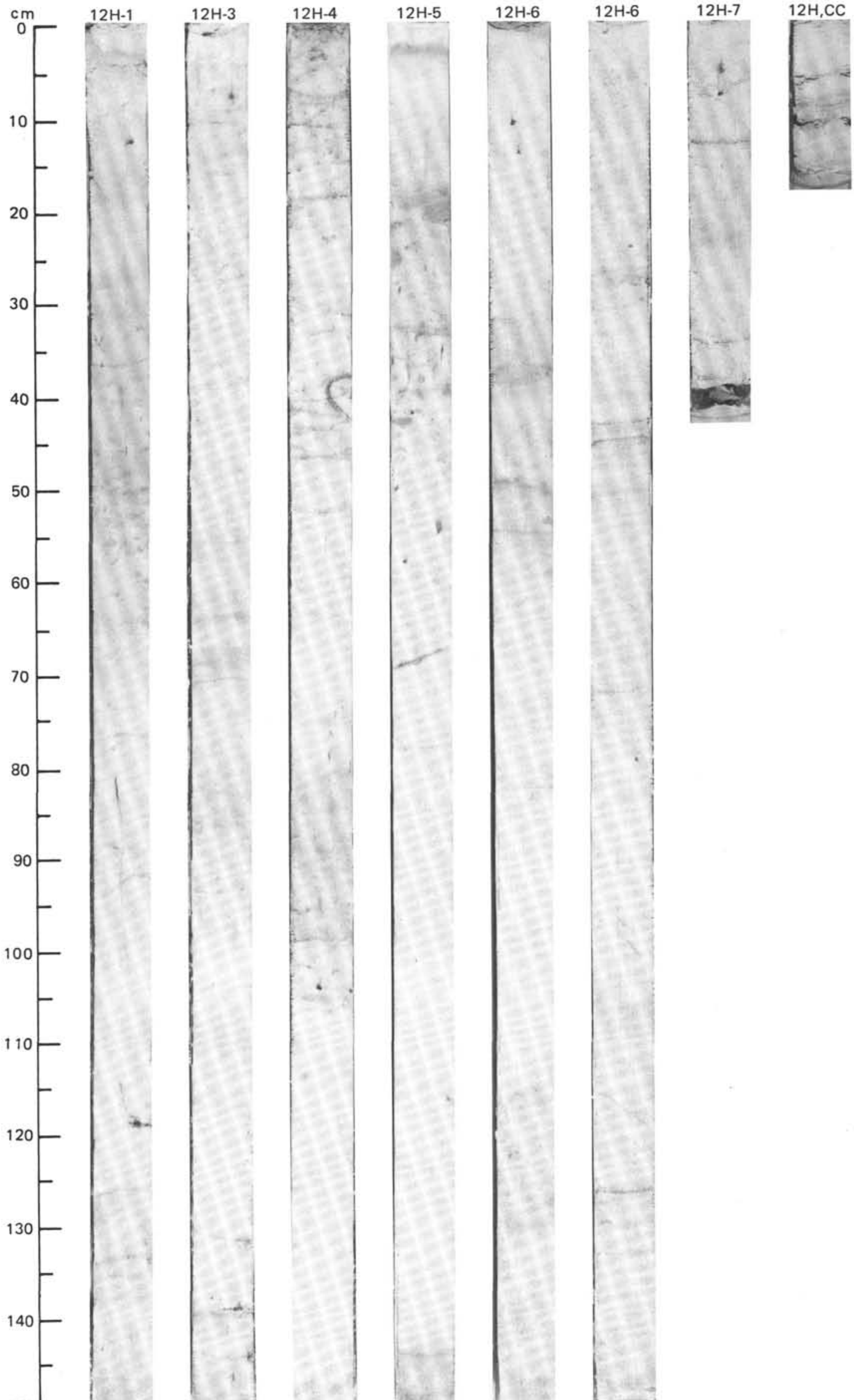
cm
0
10
20
30
40
50
60
70
80
90
100
110
120
130
140
150
12H-1
12H-3
12H-4
12H-5
12H-6
12H-6
12H-7
12H,CC